

Mechanisms of **epithelial**
homeostasis **in** adult
Drosophila midgut



INSTITUTO DE NEUROCIENCIAS

ZEUS ANDREA ANTONELLO

- 2014 -

Mechanisms of epithelial homeostasis in adult *Drosophila* midgut

PhD Thesis

Zeus Andrea Antonello

2014

Thesis Director

María Domínguez Castellano, PhD

Prof. Juan Lerma Gómez, Director del Instituto de Neurociencias, Centro Mixto de la Universidad Miguel Hernández de Elche y la Agencia Estatal Consejo Superior de Investigaciones Científicas,

CERTIFICA:

que la Tesis Doctoral titulada: “Mechanisms of epithelial homeostasis in *Drosophila* midgut”, ha sido realizada por D. Zeus Andrea Antonello, bajo la dirección de la Prof. María Domínguez Castellano, y da su conformidad para que sea presentada a la Comisión de Doctorado de la Universidad Miguel Hernández.

Para que así conste, y a los efectos oportunos, firma el presente Certificado en San Juan de Alicante, a 16 de Octubre de 2014.

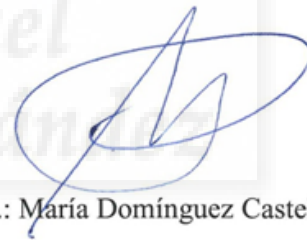

Fdo.: Prof. Juan Lerma Gómez
Director del Instituto de Neurociencias



María Domínguez Castellano, Profesora de Investigación del Consejo Superior de Investigaciones Científicas,

AUTORIZA la presentación de la Tesis Doctoral titulada: “Mechanisms of epithelial homeostasis in adult *Drosophila* midgut”, realizada por D. Zeus Andrea Antonello, bajo su inmediata dirección y supervisión en el Instituto de Neurociencias (CSIC-UMH) y que presenta para la obtención del grado de Doctor por la Universidad Miguel Hernández.

Para que así conste, y a los efectos oportunos, firma el presente Certificado en San Juan de Alicante, a 15 de Octubre de 2014.



Fdo.: María Domínguez Castellano



Index

<u>Abstract</u>	1
<u>Resumen</u>	3
<u>Introduction</u>	5
<i>Homeostatic mechanisms balance cell loss with cell division to ensure proper tissue integrity and function</i>	7
Tissue homeostasis versus regeneration	7
Control of stem cells behavior during homeostasis and regeneration	8
Imbalanced stem cell division, differentiation and cell death lead to tissue dysfunction, aging and cancer	13
<i>Drosophila midgut as a model for the study of adult stem cells behavior during homeostasis and regeneration</i>	15
General aspects of <i>Drosophila</i> as a model organism	15
The anatomy and cell composition of the <i>Drosophila</i> intestinal tract are similar to mammals	17
The adult <i>Drosophila</i> digestive system contains somatic stem cells which sustain homeostasis and regeneration.....	21
The dynamic control of <i>Drosophila</i> midgut stem cells in homeostasis and regeneration requires integration of several signals	22
<i>The role of Snail and miR-200 family genes in EMT, MET and homeostasis</i>	29
Epithelial-to-mesenchymal transition and its reverse counterpart.....	29
The <i>snail</i> family genes positively control EMT and are implicated in homeostasis	30
<i>escargot</i> is a marker of stem and progenitor cells of adult <i>Drosophila</i> midgut	31
The <i>mir-200</i> microRNA family negatively regulates EMT and is negatively regulated by EMT inducers	32

miR-8 is the sole homologue of the miR-200 family in <i>Drosophila</i>	34
<u>Hypotheses and objectives</u>	37
Hypotheses	39
Objectives	40
<u>Results</u>	41
<i><u>PART 1 - ReDDM: A novel method to follow stem cell and tissue replenishment simultaneously</u></i>	43
<i>escargot</i> is a midgut stem cells and progenitor marker	43
Design and proof of a dual differential marking system	47
<i>escargot</i> expression pattern by “Dual Differential Marker” system	51
Generation of “Repressible Dual Differential Marker” fly stocks to monitor intestinal epithelium homeostasis	54
<i><u>PART 2 - Global monitoring unveils unexpected dynamics of midgut turnover during homeostasis</u></i>	60
Replenishment dynamics by global monitoring indicates a slow and non-homogenous turnover	60
Heat shock induces tissue replenishment	63
Stem cells proliferation rate correlates with replenishment degree and fluctuates locally	65
Jak/Stat pathway is locally activated to initiate replenishment	69
Progenitors have plastic differentiation behavior in space and time	72
<i><u>PART 3 – A delayed progenitors differentiation strategy mediates adaptive responses to homeostatic demand</u></i>	75
Progenitor cells have mesenchymal traits	75
<i>escargot</i> is required for mesenchymal traits of enteroblasts and sufficient to retain their undifferentiated state	79
<i>escargot</i> is required for stem cells division and long term maintenance.	82
<i>mir-8</i> is expressed in late enteroblasts	88
<i>mir-8</i> is induced during tissue replenishment	92

Adult <i>mir-8</i> mutants have impaired homeostasis and regeneration.....	97
miR-8 is required and sufficient for EBs differentiation and resemble escargot phenotypes.....	100
Antagonistic activity of Escargot and miR-8 modulate enteroblasts mesenchymal to epithelial transition	104
<i>escargot</i> is a direct target of miR-8 <i>in silico</i> and <i>in vitro</i>	106
Escargot represses <i>mir-8</i> locus expression <i>in vivo</i>	110
<u>Discussion</u>	115
How homeostasis and regeneration resemble each other? A “spot the differences game” with a novel method	117
Which are the intrinsic mechanisms controlling stem and progenitor cells? The co-option of a metastatic mechanism.....	122
How slow cycling stem cells can elicit rapid responses to unpredictable demand? Ask their daughters	125
<u>Conclusions</u>	127
<u>Materials and methods</u>	135
<i>Drosophila melanogaster genetics</i>	135
Stocks, maintenance and crosses.....	135
Establishment of recombinant lines	137
<i>Induction of midgut regeneration</i>	139
Mechanical damage.....	139
Paraquat exposure	139
Survival curves.....	139
<i>Immunohistochemistry</i>	140
Dissection of adult fly intestines	141
Standard immunohistochemistry protocol.....	142
<i>Relative quantification of gene expression levels</i>	143

Dissection of adult flies intestines for RNA extraction	143
RNA extraction from intestines	143
cDNA preparation	143
Real Time PCR.....	144
<i>Evaluation of cell death by TUNEL.....</i>	145
<i>Luciferase assay to test microRNA targets</i>	145
S2 cells preparation and transfection.....	145
<i>mir-8 mutagenesis</i>	146
<i>Image acquisition, processing and data analysis</i>	146
Confocal microscopy.....	147
<i>GFP signal intensity measuraments for STAT-GFP reporter and miR8-GAL4 flies.....</i>	147
<i>Ex-vivo time lapse imaging</i>	147
<u>Bibliography</u>	149
<u>Glossary</u>	173
Acronyms and abbreviations	175
Definitions.....	176
<u>Acknowledgments</u>	179

List of Figures

Introduction

Fig. 1 – A comparison of tissue homeostasis and regeneration	11
Fig. 2 - Anatomy of the adult <i>Drosophila</i> digestive tract	20
Fig. 3 - Intestinal stem cells proliferation depend on the integration of several signals	28

Results

PART I

Fig. 1.1 – The <i>escargot</i> GeneTrap P01986 (“ <i>esg</i> -GFP”) labels cells basally located and scattered along the midgut epithelium	45
Fig. 1.2 – The <i>escargot</i> -Gal4 enhancer trap drive expression of membrane GFP in ISCs and EBs without leaky expression in EC or ee cells	46
Fig 1.3 – The Dual Differential Marker (DDM) concept for cell lineage in <i>Drosophila</i> midgut	49
Fig. 1.4 – Dynamic report of <i>escargot</i> activity in the midgut epithelium by Dual Differential Marking (DDM)	50
Fig. 1.5 – <i>escargot</i> -Gal4 adult expression pattern by Dual Differential Marking system	52
Fig 1.6 – <i>escargot</i> expression profiling by microarray indicate strong expression in midgut and testis	54
Fig 1.7 – The temperature sensitive GAL80 ^{ts} allows temporal and regional gene expression targeting (TARGET)	55
Fig 1.8 – The <i>escargot</i> -Repressible Dual Differential Marker (<i>esg</i> -ReDDM) allows to temporally monitor cell turnover at the single cell and whole tissue level	56

PART 2

Fig 2.1 – <i>escargot</i> -ReDDM allows to follow midgut tissue replenishment over time in a quantitative manner and indicates a slow and “patchy” turnover rate	62
Fig 2.2 – Heat Shock induces tissue replenishment	65
Fig 2.3 – Stem cells proliferation rate correlate with replenishment degree and fluctuates locally	68
Fig 2.4 – Jak/Stat signaling is basally active in all ISCs/EBs and is locally increased to initiate replenishment	71
Fig. 2.5 – Progenitors have plastic differentiation behavior in space and time	74

PART 3

Fig 3.1 – <i>Drosophila</i> midgut progenitor cells have mesenchymal traits	78
Fig 3.2 – <i>escargot</i> is required for mesenchymal traits of EBs and is sufficient to retain undifferentiated state	81
Fig 3.3 – <i>escargot</i> is required for ISCs proliferation and is sufficient to retain ISCs/EBs undifferentiated state in regenerative condition	85
Fig 3.4 – <i>escargot</i> is required for stem cells maintenance replenishment	86
Fig 3.5 – <i>escargot</i> is required but not sufficient for ISCs proliferation but required and sufficient to retain undifferentiated state	87
Fig 3.6 – <i>mir-8</i> is a marker of progenitor cells	90
Fig 3.7 – <i>mir-8</i> is a marker of late progenitor cells	91
Fig 3.8 – <i>mir-8</i> is induced upon epithelial damage and its expression correlate with cell size increase	94
Fig 3.9 – <i>mir-8</i> is activated in progenitors cells to replenish the epithelium upon damage	96
Fig 3.10 – Adult <i>mir-8</i> mutant flies have impaired homeostasis and regeneration	99
Fig 3.11 – miR-8 is required and sufficient for tissue replenishment	102
Fig 3.12 – miR-8 gain and loss of function resemble <i>escargot</i> phenotypes	103

Fig 3.13 – Antagonistic activity of <i>escargot</i> and miR-8 modulates enteroblast mesenchymal to epithelial transition	105
Fig 3.14 – <i>escargot</i> mRNA levels are higher in <i>mir-8</i> mutants and it is predicted as a direct miR-8 target	109
Fig 3.15 – <i>escargot</i> overexpression represses <i>mir-8</i> locus <i>in vivo</i>	112

Conclusions

Fig. 1 – <i>Escargot</i> and miR-8 control midgut epithelial homeostasis	131
--	-----



List of Tables

Introduction

Table 1 – Key differences between adult tissue homeostasis and regeneration	12
Table 2 – Similarities and differences between <i>Drosophila</i> midgut and mammalian small intestine	19
Table 3 – The microRNA miR-8 is the sole fly homologue of the mammalian miR-200 family	35

Results

Table 1 – <i>escargot</i> -Gal4 adult expression pattern by Dual Differential Marking system	53
Table 2 – ReDDM stocks generated and summary of adult expression pattern	59

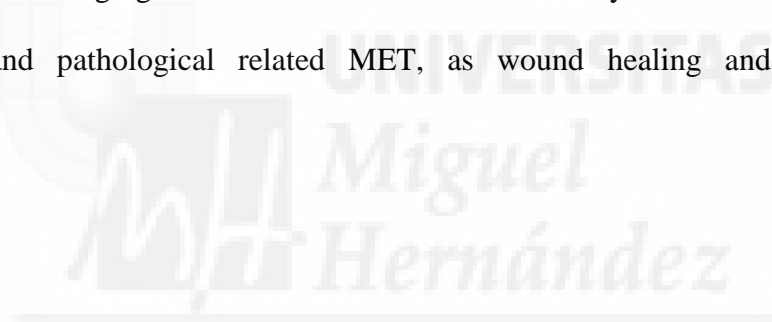
Materials and methods

Table 1. Fly stocks used	135
Table 2. Recombinant flies and stocks generated	138
Table 3. Primer pairs used for genotyping	139
Table 4. Primary antibodies	140
Table 5. Primer pairs used for qPCRs	144
Table 6. Primer pairs used for <i>mir-8</i> mutagenesis and sequencing	146

Abstract

Stem cells confer to adult tissues the capacity to maintain morphology and function counterbalancing intrinsic wear and tear (homeostasis) and environmental damages (regeneration). Stem cells are undifferentiated multipotent cells that perpetuate themselves indefinitely. To sustain cell demand from the tissue, they generate progenitors which are able to differentiate to substitute old and/or damaged cells. In the process of cell replacement, feedback mechanisms from the tissue to stem cells ensure adequate proliferation rate and exact lineage specification. Unfortunately, cell turnover is difficult to monitor and regeneration paradigms have been widely used to infer molecular mechanisms behind homeostatic cell turnover. But actually, very little is known about how mechanisms of regeneration resemble or differ from homeostatic tissue maintenance. In this work, using *Drosophila* midgut as a model, we investigated directly the basic mechanisms of epithelial homeostasis, in unchallenged conditions. To this end, we devised an original method which allowed detecting tissue turnover in a precise and temporally controllable manner in midguts. We found that in normal homeostatic conditions, midgut turnover follows unexpected asynchronous dynamics and that, surprisingly, progenitor cells sense where exactly to differentiate independently of birth time. We have identified *Escargot*, a Snail family gene, and the miR-200-related microRNA miR-8, as key intrinsic elements controlling this progenitor behavior during homeostasis. The *escargot* gene hold progenitors in undifferentiated state repressing *mir-8* locus and conferring them marked mesenchymal traits that we found to be a prerequisite for proper intercalation into the epithelium. Conversely, miR-

8 controls through direct targeting of *escargot* mRNA, the transition from undifferentiated toward differentiated state by repressing mesenchymal characteristics. The break of this reciprocal regulation impacts on homeostasis by altering the spatial and timing control of progenitors differentiation. Altogether, these results indicated that progenitors are not simple transient and passive entities but active players in homeostasis. Possibly, progenitors are able to integrate local feed-back signals to regulate their cellular state via the antagonistic Escargot/miR-8 action. Given the striking analogies between Escargot/miR-8 “undifferentiated to differentiated transition” and the Snail/miR-200 mesenchymal to epithelial transition (MET), we think the future identification of the signals and molecular mechanisms controlling Escargot and miR-8 would be of wide-ranging relevance to understand not only homeostasis but also physiological and pathological related MET, as wound healing and metastasis establishment.



Resumen

Las células madre confieren a los tejidos adultos la capacidad de mantener su morfología y función contrarrestando el desgaste intrínseco (homeostasis) y los daños ambientales (regeneración). Las células madre son células no diferenciadas multipotentes que se pueden perpetuar indefinidamente. Para sustentar la demanda celular de los tejidos, generan células progenitoras que son capaces de diferenciar para substituir las células viejas y/o dañadas. En el procesos de recambio celular, mecanismos moleculares de retroalimentación (feedbacks) procedentes del tejido hacia las células madre aseguran una adecuada tasa de proliferación y precisa especificación celular. Desafortunadamente, el recambio celular es difícil de supervisar, y frecuentemente se han usado paradigmas de regeneración para inferir los mecanismos moleculares que respaldan el recambio celular en homeostasis. Pero en realidad se conoce muy poco sobre cuanto los mecanismos de regeneración se parecen o diferencian de los homeostáticos. En este trabajo de investigación, utilizando el intestino medio de *Drosophila* como modelo, hemos investigado directamente los mecanismos base de la homeostasis epitelial, sin inducir regeneración. Para este fin, hemos diseñado un nuevo método que ha permitido detectar el recambio celular de manera precisa y temporalmente controlable. Hemos encontrado que en condiciones de homeostasis, el recambio celular del intestino medio sigue un inesperado patrón asincrónico y que, sorprendentemente, las células progenitoras pueden decidir donde diferenciar exactamente, independientemente del momento de su nacimiento. Hemos identificado *escargot*, un gen de la familia *snail*, y el microRNA miR-8, homólogo de los miR-200 de mamíferos, como elementos intrínsecos clave que intervienen en el

comportamiento de los progenitores durante la homeostasis. El gen *escargot* retiene los progenitores en un estado no diferenciado reprimiendo el locus de *mir-8* y otorgando evidentes características mesénquimales que hemos encontrado ser un prerrequisito para la adecuada intercalación en el epitelio. Recíprocamente, miR-8 controla a través de la sub-regulación directa del mRNA de *escargot*, la transición desde un estado no diferenciado a diferenciado reprimiendo las características mesénquimales. La ruptura de esta regulación recíproca afecta la homeostasis alterando el control espacial y temporal de los progenitores. En conjunto, estos resultados indican que los progenitores no son simplemente entidades transitorias y pasivas sino más bien elementos activos en la homeostasis. Posiblemente, los progenitores son capaces de integrar señales de retroalimentación para regular su estado celular a través de la acción antagónica entre Escargot y miR-8. Considerada la llamativa analogía entre la “transición indiferenciado-diferenciado” mediada por Escargot/miR-8 y la transición mesénquima a epitelio (mesenchymal to epithelial transition, MET) mediada por Snail/miR-200, creemos que la futura identificación de las señales y mecanismos moleculares que controlan Escargot y miR-8 serán de amplia relevancia para el entendimiento no solo de la homeostasis sino también de la transición mesénquima-epitelio en contextos fisiológico y patológico, como la cicatrización de heridas o el establecimiento de la metástasis.

Introduction

“Reality is the leading cause of stress amongst those in touch with it”

Jane Wagner, *The Search for Signs of Intelligent Life in the Universe*, 1985



Homeostatic mechanisms balance cell loss with cell division to ensure proper tissue integrity and function

Tissue homeostasis *versus* regeneration

Homeostasis was originally defined as the ability of living organisms to maintain their internal conditions despite environmental changes (*homeo* = "the same" and *stasis* = "standing") (Cannon, 1941). This concept was born in the field of organism's physiology, but has extended to cells, tissues and organs to describe their ability to preserve integrity and function regardless of environmental changes (Leopold and Perrimon, 2007). During tissues homeostatic equilibrium, subfunctional differentiated cells are continuously replaced with new cells (cell turnover). It has been proposed that homeostatic cell turnover occurs when there is (I) continual or periodic elimination of choice differentiated cells from the tissue; (II) eliminated cells are replaced by cell division, typically involving adult stem cells and their direct descendants, termed progenitor cells; and (III) the newly generated cells differentiate and become functionally integrated with the pre-existing tissue (Pellettieri and Sanchez Alvarado, 2007). Homeostatic cell turnover is working as a dynamic equilibrium which is vital to organisms and is indeed genetically encoded and tightly regulated in every aspect (cell loss, stem cell division and maturation/integration of new progeny). Deregulation of this dynamic equilibrium occurs temporally during regeneration (fig. 1) but if sustained can lead to tissue dysfunction (e.g. atrophy or cancer) as will be introduced later.

Regeneration is a response to an acute injury that results in extensive cell loss within the tissue (fig. 1), often triggered by an exogenous stimulus (e.g. infection,

mechanical injury or other stresses). Importantly, also regeneration is dedicated to the maintenance of integrity and function of tissues but it is a departure from homeostasis since it occurs when the cell turnover is temporarily unbalanced due to fast tissue loss.

In summary, homeostatic cell replacement can be seen as a “wear and tear process” in which during normal function cells become inefficient by intrinsic mechanisms of aging and/or usage, while regeneration can be seen as sudden rupture of tissue homeostasis. Clearly, cell replacement in homeostatic conditions (continuous or periodic replacement of “selected” sub-optimal cells) or during regeneration (sudden replacement of acutely damaged cells) must have critical differences (*Table 1*), although might share common pathways and mechanisms. Since cell turnover is often difficult to detect, regeneration paradigms have been widely used to infer molecular mechanisms behind homeostatic cell turnover. However, very little is known about how mechanisms of regeneration resembles or differs from homeostatic tissue maintenance (Pellettieri and Sanchez Alvarado, 2007; Rando, 2006).

Control of stem cells behavior during homeostasis and regeneration

Adult organism’s homeostasis and regeneration rely on a population of undifferentiated cells termed adult stem cells or somatic stem cells, which have (I) self-renewal capacity and (II) pluripotency.

Self-renewal is the process by which stem cells divide to make identical siblings, perpetuating the stem cell pool throughout life (He et al., 2009; Morrison and Spradling, 2008). Self-renewal requires division with maintenance of the undifferentiated state. Referring to adult stem cells, pluripotency means the ability to generate the entire specialized, post-mitotic cell types of the tissue where they reside (He et al., 2009;

Leedham et al., 2005; Potten and Loeffler, 1990; Simons and Clevers, 2011a). Altogether, the properties of stem cells are referred as “stemness”. Adult stem cells generate committed progeny (named progenitor or precursor cells) which lose self-renewal capacity (fig. 1B) and can either directly differentiate or proliferate for a limited number of cycles before terminal differentiation (Blanpain and Fuchs, 2009; Fuchs, 2009; Simons and Clevers, 2011b).

Adult stem cells reside in specific locations termed niches, which provide the structural and functional signals necessary to stem cell during homeostatic and regenerative processes (Li and Xie, 2005; Morrison and Spradling, 2008; Nystul and Spradling, 2006; Sahai-Hernandez et al., 2012). Extrinsic signals coming from the niche and/or the post-mitotic cells of tissues that need to be substituted are integrated to intrinsic mechanisms to control the behavior of adult stem cells and their progeny. Extrinsic signals include diffusible signals such as wingless, epidermal growth factor receptor (EGFR) ligands and cytokines (Jiang et al., 2011; Jiang et al., 2009; Lin and Xi, 2008; Lin et al., 2008, 2010; Xu et al., 2011). Intrinsic signals are those mechanisms not directly dependent on a described extracellular signaling, i.e. fate decisions regulated by the Delta-Notch signaling (Fre et al., 2011; Micchelli and Perrimon, 2006; Ohlstein and Spradling, 2006; Wilson and Kotton, 2008) and/or asymmetric distribution of genetic determinants (Goulas et al., 2012; Morrison and Kimble, 2006; Takashima et al., 2013). Proper integration of extrinsic and intrinsic mechanisms is necessary to regulate correctly stem cells division and differentiation to ensure homeostasis and regeneration (Biteau et al., 2011) and to prevent stem cell proliferation exhaustion that might diminish the prospect of future tissue repair (Fuchs, 2009).

Adult stem cells are critical drivers of both homeostasis and regeneration (Barker, 2014). However, as described in the previous chapter, regeneration and homeostasis have fundamental differences and stem cells indeed behave differently in the two conditions. During homeostasis stem cells divide infrequently and slowly (fig.1B) (Cotsarelis et al., 1990; Foudi et al., 2009; Fuchs, 2009; Micchelli and Perrimon, 2006; Ohlstein and Spradling, 2006; Tumbar et al., 2004; Wilson et al., 2008). The low division rate of homeostatic stem cells is believed to preserve their long-term proliferation potential and to minimize the acquisition of errors through numerous rounds of DNA replication (Cairns, 1975a, b). Homeostatic stem cells have been proposed to divide continually or basally in the adult fly mid-intestine (Micchelli and Perrimon, 2006), in the mice small intestine and epidermis (Blanpain and Fuchs, 2009; Simons and Clevers, 2011a). During regeneration stem cells have high proliferation rate and increased rate of symmetric cell divisions to meet the increased demand (fig.1B) of the injured tissue (Blanpain and Fuchs, 2009; Fuchs, 2009; Jiang and Edgar, 2012; Micchelli and Perrimon, 2006; Ohlstein and Spradling, 2006). This cellular plasticity relies on an intricate and complex crosstalk between multiple positive feed-back signaling pathways produced by the “dying” cells and the niche. In *Drosophila* adult intestinal regeneration, in example, positive feed-back signaling include the Wingless/Wnt, Epidermal Growth Factor Receptor (EGFR) and JAK/STAT families. However, while individual genetic inactivation of each of these pathways compromise regenerative intestinal stem cell proliferation, none of them could completely impede “basal” division of stem cells (Ren et al., 2010; Xu et al., 2011).

Overall, is largely accepted that most adult stem cells have the capacity to both sustain homeostasis and regeneration adapting dynamically their behavior (i.e. their

division kinetics). Positive feedback responsible for this adaptation have been identified, however, the exact nature and the existence of positive feed-back loops in normal tissue homeostasis remains still unproven.

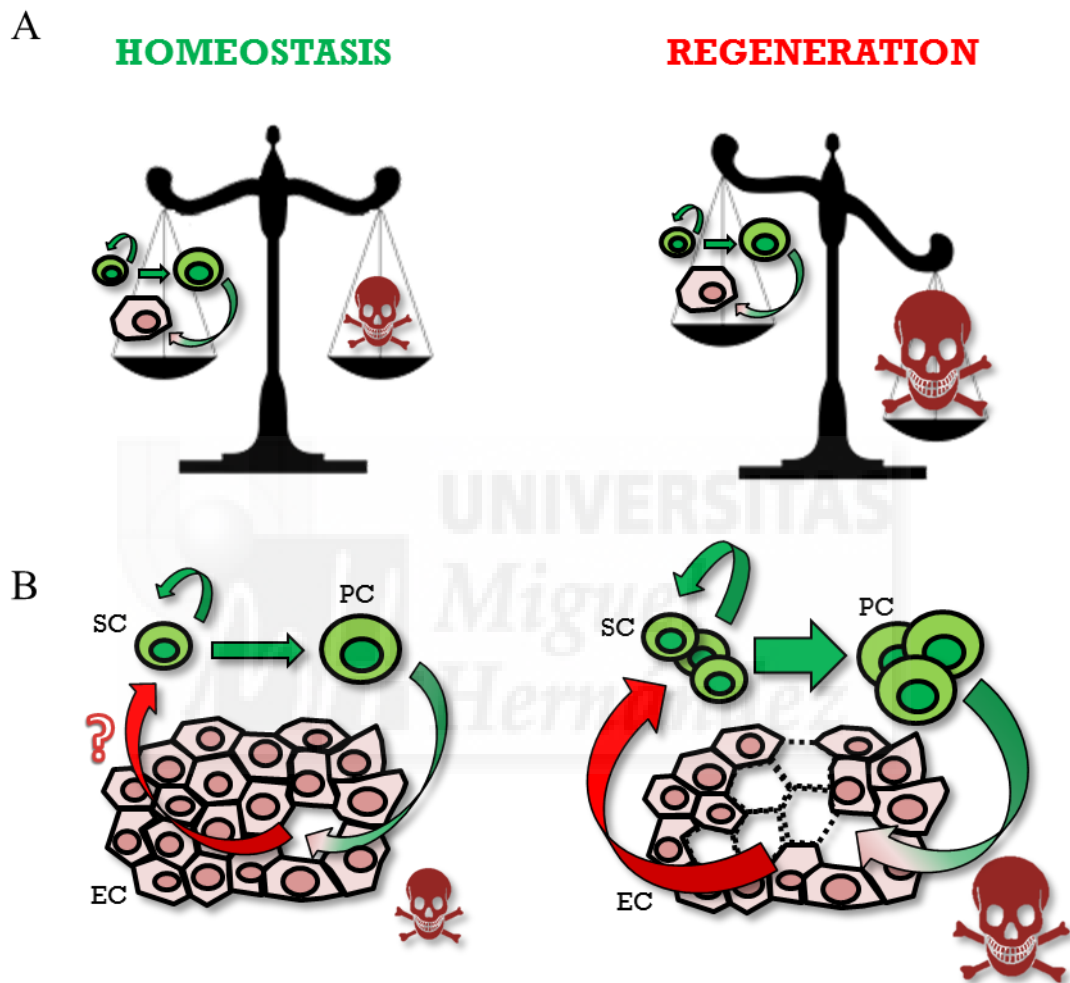


Fig. 1 – A comparison of tissue homeostasis and regeneration. A) During homeostasis there is a perfect balance of stem cells (SC) proliferation, progenitor cells (PC) differentiation and epithelial cells (EC) death, while during regeneration the normal tissue turnover rate cannot balance the cell loss. B) In homeostatic conditions, sub-functional ECs are eliminated by apoptosis and are readily replaced by a differentiating PC originated by SC division. The existence of feed-back mechanisms during homeostasis is unclear. During regeneration, external insults lead massive cell loss that feedbacks to SCs which

increase their proliferation rate to produce the adequate number of PCs and re-establish the tissue structure and the homeostatic balance.

Table 1 – Key differences between adult tissue homeostasis and regeneration.

Homeostasis	Regeneration
Cell loss due to age or wear and tear	Sudden and massive cell loss due to external insult or disease
Prevents physiological dysfunction	Prevent pathological dysfunction and damage
Tissue size and cell density are preserved	Tissue size reduction and/or decrease in cell density followed by recovery
Aged or worn out cells are eliminated by genetically programmed cell death (PCD)	Damaged cells are eliminated by PCD and necrosis
Does not induce an inflammatory response	Associated with an inflammatory response
Stem cell number is constant	Stem cell number increases by symmetric cell division
Stem cells divide infrequently	Stem cells divide rapidly
Cell turnover is problematic to detect	Regeneration is easy to monitor

Imbalanced stem cell division, differentiation and cell death lead to tissue dysfunction, aging and cancer

Organism's epithelia serve several vital functions, including protection against pathogens and environmental stressors, secretion and absorption. Damages in tissues like the intestinal epithelium can be highly deleterious to the organism. Epithelial tissues are protected from physio-pathological dysfunction by robust mechanisms balancing proliferation of stem cells, differentiation of progenitors and elimination of damaged cells, as described in previous sections. Aging, adult-onset diseases and cancer largely involve the deregulation of this fine balance. Conditions that exacerbate the rate of cell loss or impede the restorative action of adult stem cell populations underlie degenerative disorders and contribute to aging (Sharpless and DePinho, 2004). Conversely, situations that unbalance tissue homeostasis toward a net increase in cell number i.e. by increased proliferation and/or reduced apoptosis have been proposed to create a platform that is both necessary and sufficient for tumor formation (Evan and Vousden, 2001; Green and Evan, 2002). Nevertheless, this is a cell autonomous perspective which misses regards environmental influences that work through feedback loops between different cell populations. In fact, also conditions that exacerbate cell loss and produce inflammation, like bacterial infection, can lead to dysplasia if on a genetically predisposed background. In particular it has been shown that mutations which are silent during homeostatic conditions, i.e. gain of function of Ras1, synergize with regenerative feedback signals induced by sustained stress, like inflammation induced by bacterial infection (Apidianakis et al., 2009).

Although parallels have long been drawn between somatic stem cells and tumor cells to explain tumor heterogeneity (Pardal et al., 2003) only recently two independent

research works (Barker et al., 2009; Zhu et al., 2009) demonstrated that deregulation of somatic stem cells behavior in homeostatic conditions is sufficient to produce neoplasia. These works indicated that crypt stem cells are the cells of origin of colon cancer (Fodde, 2009). In particular they showed that stem-cell-specific activation of Wnt/ β -catenin pathway by loss of adenomatous proliferating coli gene (Apc) (Barker et al., 2009) or nuclear β -catenin expression (Zhu et al., 2009) resulted in rapidly and progressively growing neoplasia while the same genetic manipulations in transient amplifying progenitor cells did not resulted in a tumoral phenotype. These works importantly demonstrated that the tumorigenic potential of Wnt/ β -catenin pathway, which is critical for normal intestinal homeostasis, is confined to stem cells. As previously mentioned, the failure to engage cell death mechanisms in response to oncogenes activity is also thought to contribute to tumoral phenotypes (Evan and Vousden, 2001; Green and Evan, 2002; Hanahan and Weinberg, 2011). Indeed, oncogenic mutations inducing pathological cell proliferation also induce mechanism of senescence and cell death (Elgandy et al., 2011; Overmeyer et al., 2008; Sarkisian et al., 2007; Serrano et al., 1997). In fact, pro-apoptotic genes have a clear tumor suppressor role (McCurrach et al., 1997; Soengas et al., 1999; Yin et al., 1997) and is only when their action is overcome that tumors progress (Hanahan and Weinberg, 2011). Indeed, altered expression of Bcl-2 family proteins occurs commonly in human cancers (Reed, 1998). Also, mutations, amplifications and chromosomal translocations of IAP genes are associated with various malignancies and are proposed as possible targets for therapy (Fulda and Vucic, 2012). Given these considerations, there is significant interest in developing clinical treatments that might restore the normal balance between cell death and stem cell division in pathological contexts.

***Drosophila* midgut as a model system for the study of adult stem cells behavior during homeostasis and regeneration**

General aspects of *Drosophila* as a model organism

Drosophila melanogaster has more than a 100 years of history in research (Castle, 1906) and in the last decades has been widely used as a model organism for human diseases, including cancer (Bier, 2005; Brumby and Richardson, 2005; Vidal and Cagan, 2006). Its rapid life cycle, the relative ease with which it can be handled and the multitude of genetic tools that are available makes of it an amenable model organism for research (Greenspan, 2004).

Common genetic tools available for research with *Drosophila* include mutations made by P-elements insertion/imprecise excision (Spradling et al., 1999) and engineered transposons or site specific transgenics to allow controlled miss-expression of genes (Bellen et al., 2004; Bellen et al., 1989; Rorth et al., 1998; Venken et al., 2011), RNA interference (Dietzl et al., 2007; Ni et al., 2009; Ni et al., 2008) or reporters such as β -galactosidase (Bellen et al., 1989; Bier et al., 1989) or green fluorescent protein (GFP) (Clyne et al., 2003; Morin et al., 2001). Reporter lines can be “Enhancer traps”, which allow expression pattern studies and provide information about locus expression levels, or “protein trap” transgenic lines which inform about protein subcellular localization (Clyne et al., 2003; Morin et al., 2001). *Drosophila* transgenic genes expression systems allow tissue specific gene manipulations using the binary expression components GAL4/UAS (Brand and Perrimon, 1993) or the more recent

QF/QUAS (Potter et al., 2010). Genes expression systems can also be temporally controlled using the “temporal and regional gene expression targeting” (TARGET) system, which is based on the temperature sensitive allele of the GAL80 repressor (McGuire et al., 2003) or the “Gene Switch” system, which uses a GAL4-progesterone receptor chimera that is hormone-inducible (McGuire et al., 2004). Site specific recombinases, like the flippase (FLP), are used to generate knock-in lines and for mosaic analysis. “Mosaic” approaches allow the analysis, on a wild-type background, of mutant or gain of function (GOF) discrete patches of tissue (Golic and Lindquist, 1989; Struhl and Basler, 1993). Mutant clones are normally negatively marked while GOF clones (Flip-out technique) are positively marked. Conversely, the mosaic analysis with a repressible cell marker (MARCM) is a FLP/FRT-based genetic mosaic system which allow the positive marking of generated mutant patches of cells (Lee and Luo, 1999, 2001; Wu and Luo, 2006). This system is particularly useful to mark and follow single cell gain or loss of function lineages in *Drosophila* brain and intestine, where clones can be too small to be detected by negative marking.

Finally, is not only the great handiness and richness of genetic tools just resumed in the previous paragraph that makes *Drosophila* an unvaluable model system, but also the extensive conservation of pathways and genes (Edwards, 1999). Although *Drosophila* and human physiology might be considerably different, pathways controlling fundamental cell-biological processes, like proliferation, cell specification / differentiation and programmed cell death, are highly conserved and seminal discoveries made using *Drosophila* as a model system have greatly contributed also to the cancer field (Edwards, 1999). Indeed, a systematic analysis available online (Chien et al., 2002) of human disease-associated gene sequences conserved in *Drosophila*

revealed that about 75% of known human disease genes have a recognizable match in the genome of fruit flies (Reiter et al., 2001). Overall, *Drosophila* can be considered the most advanced model system and its historical importance for research is still actual and projected to the most novel approaches.

The anatomy and cell composition of the *Drosophila* intestinal tract are similar to mammals

The whole gastro-intestinal tract of adult *Drosophila* (fig. 2A) is approximately one centimeter long but contains cell types that resemble those in mammals. *Drosophila* intestine can be divided into three main portions: foregut, midgut and hindgut (Fig.2B). The foregut includes the pharynx and esophagus. The midgut starts from cardia (also termed proventriculus) and extends to the hindgut junction where malpighian tubules arise. Malpighian tubules are the fly homologue organ of the mammalian kidneys. The hindgut extends from this junction to the anal plate (also termed ampulla) (fig. 2B).

The three main portions of *Drosophila* gut are independently formed from different embryonic layers but linked together during embryonic development: foregut and hindgut are a neuroectodermic derivative while the midgut is endodermic. Malpighian tubules have mesodermic and neuroectodermic components, stellate and principal cells respectively. The whole *Drosophila* gut is lined by transversal and longitudinal muscles of mesodermic origin (Nakagoshi, 2005).

The midgut portion of the *Drosophila* intestine, and in particular the posterior midgut, is widely used as a model for the understanding of stem cells behavior during tissue homeostasis, regeneration and disease, including inflammation (Bonney et al.,

2013; Chatterjee and Ip, 2009; Christofi and Apidianakis, 2013) and cancer (Cordero et al., 2012a; Lee et al., 2009; Wang et al., 2013). Anatomy and cell renewal in the *Drosophila* midgut are similar to those in mammalian small intestine (Casali and Batlle, 2009; Jiang and Edgar, 2012; Wang and Hou, 2010): in both systems is a tube composed of epithelial cells with absorptive and secretory functions; the Notch signaling controls absorptive versus secretory fate decisions; cell renewal in both systems starts from stem cells in the basal cell layer, and the differentiating cells move toward the lumen. Still, the two systems have also clear differences. Homeostatic turnover in the mammalian intestinal epithelium is achieved through the proliferation of both intestinal stem cells (ISCs) and progenitor cells (EBs). Slowly cycling ISCs first generate the rapidly cycling transient amplifying (TA) progenitor cells, which then become terminally differentiated cell types (Crosnier et al., 2006); in the *Drosophila* midgut, ISCs are the only proliferating cells, and rapidly cycling TA cells do not exist. The stem cell progeny is not dividing anymore and is just differentiating, according to Notch signaling, in absorptive epithelial cells (enterocyte fate, EC) or secretory cells (enteroendocrine fate, ee). In this respect, the *Drosophila* hindgut is more similar to the mammalian small intestine than is the midgut. In the *Drosophila* hindgut, the slowly proliferating stem cells are immediately followed by rapidly cycling TA daughter cells, and the TA cells then produce the terminally differentiated cell types. However, the cell renewal in *Drosophila* hindgut occurs along the anterior–posterior axis, which is different from the basal-to-lumen direction of cell renewal in the mammalian small intestine. Moreover it seems that hindgut stem cells are not constitutively active for continue tissue turnover, rather they are quiescent, but able to respond to severe tissue damage. In this sense, drosophila hindgut doesn't conform to the crypt model (Fox and Spradling, 2009). Another difference is that in mammals ISCs are located at the base of

each intestinal crypt in a specific niche (Barker et al., 2007) while in *Drosophila* are scattered all along the basement membrane. Finally, despite loss of function of Notch drives enteroendocrine fate both in mammals and *Drosophila*, Notch gain of function has opposite outcomes: in *Drosophila* it leads to enterocytes specification and cell cycle exit while in mammals causes increased cell proliferation. This difference rather than species related is dependent on a specific tissue difference. In fact, in other *Drosophila* tissues, like larval neuroblasts (Bowman et al., 2008) or imaginal discs, Notch activity can drive proliferation and inhibit differentiation, similarly to mammals.

Table 2 - Similarities and differences between *Drosophila* midgut and mammalian small intestine

<i>Similarities</i>	<i>Differences</i>	
<u>Drosophila and Mammals</u>	<u>Drosophila</u>	<u>Mammals</u>
Cellular composition (ISC, EB, EC, ee)	Progenitors are post-mitotic	Progenitors divide (transient amplifying cells)
Notch LOF leads to ee fate	The epithelium is not folded	The epithelium is organized in villi and crypts
Stem cells are basally located	Stem cells are scattered along the basal membrane	Stem cells are located in a niche, at the crypt bottom
Differentiating cells move toward the lumen	Notch GOF blocks proliferation and promotes differentiation	Notch GOF induces proliferation and blocks differentiation.
Remarkable regenerative capacity		
Functional conservation (absorption of nutrients)		

LOF = loss of function; GOF = gain of function; ISC = intestinal stem cell; EB = enteroblast; EC = enterocyte; ee = enteroendocrine cell

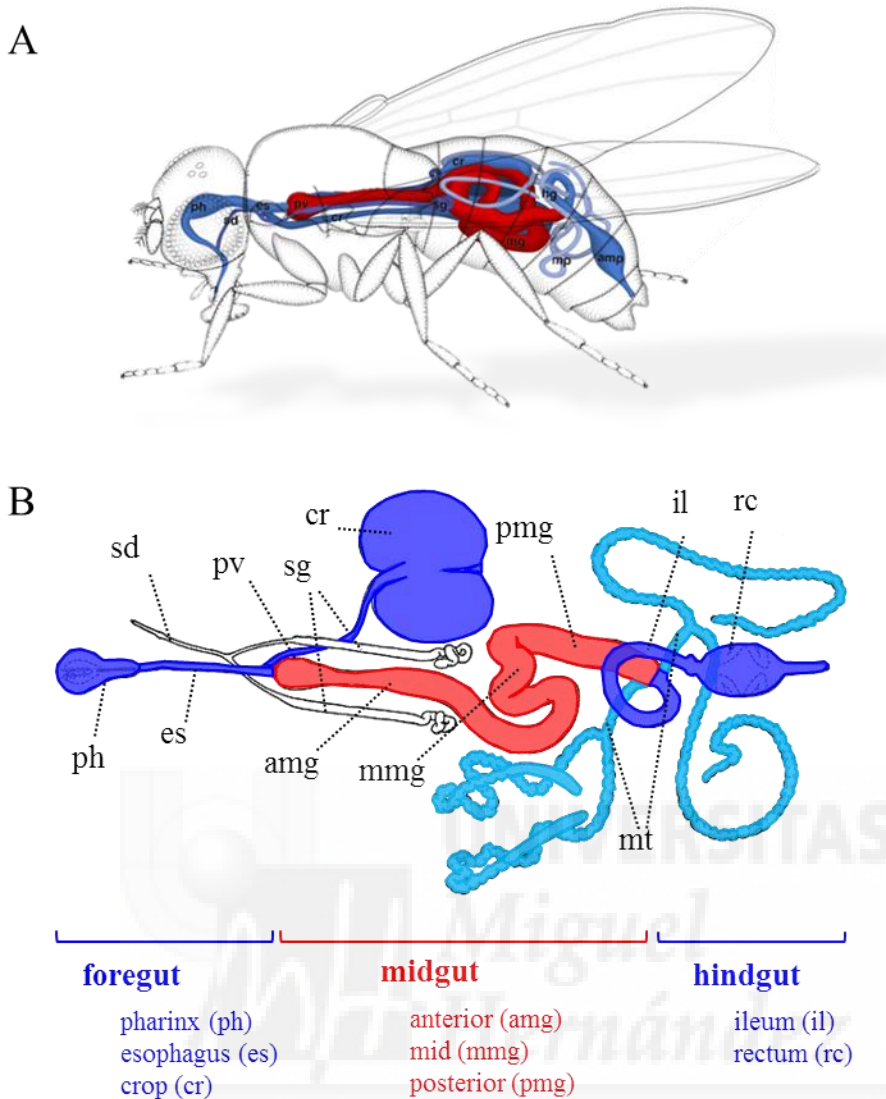


Fig. 2 - Anatomy of the adult *Drosophila* digestive tract. A) 3D cartoon showing adult *Drosophila* digestive tract. B) Cartoon displaying partition of the fly digestive tract. Foregut (blue) includes pharynx (ph) and esophagus (es), midgut (red) extends from proventriculus (pv) to the pylorus (not indicated), at the posterior midgut/hindgut boundary (pmg/hg), where malpighian tubules arise (mt - turquoise). The midgut is subdivided in three main portions along the longitudinal axe: anterior midgut (amg), mid-midgut (mmg) and posteriormidgut (pmg). The hindgut (hg, blue) starts from the pylorus and include the ileum (il) and the rectum (rc or also named ampulla). Salivary duct (sd) and salivary glands (sg) in white. Images are oriented anterior-left / posterior-right. Modified from “*Atlas of Drosophila Development*”, Volker Hartenstein, Cold Spring Harbor Laboratory Press, 1993.

The adult *Drosophila* digestive system contains somatic stem cells which sustain homeostasis and regeneration

First report of diploid cells in the *Drosophila* midgut dates 1950 (Miller A., 1950); another more recent histological analysis (Baumann, 2001) reported the presence of hypothetical regenerative cells that could also be distinguished from enterocytes by differences in their immuno-fluorescent staining for various proteins. However, formal demonstration of the existence of somatic stem cells in *Drosophila* came in 2006 from two independent works (Micchelli and Perrimon, 2006; Ohlstein and Spradling, 2006). Lineage tracing methods based on mitotic recombination (MARCM, see “General aspects of *Drosophila* as a model organism” section) were used to demonstrate that those cells previously reported were constitutively active stem cells able to self-renew and give rise, through differential Notch-Dl signaling, to the two major mature cell types of *Drosophila* midgut (pluripotency): absorptive octa-ploid cells (8n), termed enterocytes (EC) and secreting enteroendocrine cells (ee). Each of these cell types have different specialized subtypes, i.e. iron copper enterocytes or allatostatin versus tachykinin expressing enteroendocrine cells (Ohlstein and Spradling, 2006) however the mechanisms of their specification are unknown.

At present, five types of region and organ-specific multipotent adult stem cells have been characterized in the *Drosophila* digestive system: intestinal stem cells (ISCs) in the posterior midgut (Micchelli and Perrimon, 2006; Ohlstein and Spradling, 2006); hindgut intestinal stem cells (HISCs) at the midgut/hindgut junction (pylorus) (Takashima et al., 2008); renal and nephric stem cells (RNSCs) in the malpighian tubules (Singh and Hou, 2009); type I gastric stem cells (GaSCs) at foregut/midgut junction (Singh et al., 2011); and type II gastric stem cells (GSSCs) at the middle of the

midgut (Strand and Micchelli, 2011). Each type of stem cell is unique to a particular organ, however they share common molecular markers and regulatory signaling pathways (Zeng et al., 2013).

It was commonly accepted that the adult fly was post-mitotic and the only stem cells present in the organism were the germline stem cells (GSCs) and the three kinds of stem cells involved in follicle development (follicle stem cell, escort stem cell and cyst progenitor). However, the discovery of adult somatic stem cells in *Drosophila* has pushed the fly genetics research to the study of the mechanisms regulating stem cells behavior during homeostasis, regeneration and disease.

The dynamic control of *Drosophila* midgut stem cells in homeostasis and regeneration requires integration of several signals

Drosophila midgut intestinal stem cells (ISCs) maintenance and proliferation are modulated by systemic and local signals coming from insulin producing tissues (systemic), epithelial cells (local feedback), visceral muscles (niche) and their own progeny (fig. 3A). Intestinal stem cells integrate these signals to adapt their proliferation rate to tissue demand during homeostasis and regeneration (fig. 3B).

Stem cells maintenance typically depend on the local tissue microenvironment which constitutes a “niche” that provide paracrine signals (Morrison and Spradling, 2008; Ohlstein et al., 2004). ISCs in the *Drosophila* midgut are scattered along the basement membrane and are not associated with any obvious cellular niches. The ligand of the conserved Wnt / β -catenin pathway Wingless (Wg) is specifically expressed in the circular muscles next to ISCs, and has been shown to regulate ISCs self-renewal

(Lin and Xi, 2008; Lin et al., 2008). Reduced function of *wg* diminished ISC proliferation rate and differentiation, whereas *wg* overexpression produced excessive ISC-like cells expressing high levels of the Notch ligand, Delta. Clonal analysis showed that the main downstream components of the wingless pathway, including Frizzled, Dishevelled and Armadillo, are autonomously required for ISC self-renewal. Furthermore, epistasis analysis suggested that Notch acts downstream of the Wingless pathway and a hierarchy of Wg/Notch signalling pathways controls the balance between self-renewal and differentiation (Lin and Xi, 2008; Lin et al., 2008). However, loss of Wg from the whole intestine or loss of function clones of components of the Wg signaling pathway from the intestinal epithelium showed a rather mild, progressive decrease in homeostatic ISC proliferation (Lin and Xi, 2008; Lin et al., 2008). Indeed, later work from the same laboratory has shown that the niche provide further signals which act redundantly to maintain stem cells (Xu et al., 2011). This work showed that the EGFR ligand Vein is specifically expressed in muscle cells similarly to Wg and is important for ISC maintenance and proliferation. Also two additional EGFR ligands, Spitz and Keren, were shown to function redundantly as possible autocrine signals to promote ISC maintenance and proliferation. In fact, over-activated EGFR signaling could partially replace Wg or JAK/STAT signaling for ISC maintenance and division, and vice versa (Xu et al., 2011). Taken together, these data indicated that *Drosophila* midgut ISCs are maintained cooperatively by multiple signaling pathway.

Similarly to ISCs maintenance mechanism, ISCs basal homeostatic proliferation requires the activity of several growth factor signaling pathways. Using MARCM analysis, it was shown that the growth factor response pathways activated by EGF Receptor (EGFR) and the Insulin Receptor (InR) are essential for ISC proliferation

under normal conditions since mutant clones were mostly of single or few cells (Biteau and Jasper, 2011; Biteau et al., 2010; Jiang et al., 2011; Xu et al., 2011). Downstream mediators of these pathways include the InR substrates, PI3Kinase, Akt, Ras, and ERK, and all of these molecules have also been shown to be essential for ISC proliferation. Consistent with a general permissive role for these signaling pathways, activated ERK (dpERK) was detected in all ISCs under normal conditions (Biteau et al., 2011; Jiang et al., 2011; Xu et al., 2011). Importantly, the constitutive activation of EGFR/InR signaling components increase ISCs proliferation rates, indicating that the level of RTK signaling activity modulates the proliferative state of ISCs (Biteau et al., 2011; Jiang et al., 2011; Xu et al., 2011). In addition, the MAPK p38 was shown to be required for ISC proliferation under homeostatic conditions (Park et al., 2009) and it was suggested that it acts as a mediator of the effect of the PDGF/VEGF-like receptor signaling pathway (composed of Pvf ligands and the Pvr receptor) on ISC proliferation (Choi et al., 2008a; Park et al., 2009). Indeed, it was later demonstrated that mutant ISCs in the Pvf/Pvr pathway are defective in homeostatic proliferation and differentiation, resulting in a failure to generate mature cell types (Bond and Foley, 2012).

Pathways active in stem cells during homeostasis are up-regulated during infection with pathogenic bacteria. EGF-like ligand expression in the gut are secreted by both epithelial cells (including ISCs and ECs), and the surrounding visceral muscle, displaying a remarkable redundancy (Buchon et al., 2009a; Buchon et al., 2009b; Jiang et al., 2011; Xu et al., 2011). Nevertheless, regenerative mechanisms involve also other mechanisms which are essential for flies to survive to stresses. Upon stress or injury, ISCs respond by dramatically increasing their proliferative activity to replenish the epithelium with new cells. This activation occurs in response to infection (Apidianakis

et al., 2009; Buchon et al., 2009a; Buchon et al., 2009b; Cronin et al., 2009; Chatterjee and Ip, 2009; Jiang et al., 2011), oxidative stress (Biteau et al., 2008; Buchon et al., 2009a; Choi et al., 2008a; Choi et al., 2008b) and DNA damage (Amcheslavsky et al., 2009). Stem cells respond to changes in tissue integrity through the Hippo/Yorkie pathway (Karpowicz et al., 2010; Ren et al., 2010; Shaw et al., 2010; Staley and Irvine, 2010). JAK/Stat signaling is activated in ISCs by locally derived interleukin-6-like cytokines named Unpaired 1–3 (Upd1–3). These cytokines are secreted from damaged and dying ECs in response to infection (Buchon et al., 2009a; Cronin et al., 2009; Jiang et al., 2009; Osman et al., 2012). Artificial induction of JNK in ECs is sufficient to induce Upd expression (Jiang et al., 2009), potentially through the activation of the Yorkie transcription factor (Staley and Irvine, 2010). However, JNK is not required in ECs for the proliferative response upon infection (Buchon et al., 2009a; Jiang et al., 2009). Yorkie also induces Upd expression in ISCs themselves, activating proliferation in an autocrine manner (Karpowicz et al., 2010). In addition, JAK/Stat signaling acts indirectly to promote ISC proliferation by increasing the expression of the EGF-like ligand Vein in the visceral muscle (Buchon et al., 2010). Through secreted Upd cytokines, injured or dying ECs thus initiate and promote regenerative activity in the epithelium by directly activating cell cycle progression in ISCs, while at the same time triggering increased growth factor secretion from the muscle. In addition to its potential role in dying ECs, the JNK pathway also autonomously activates ISC proliferation by phosphorylating the AP-1 transcription factor Fos (Biteau and Jasper, 2011).

Oxidative stress and the redox state of the stem cells are also critical regulators of their behavior. A low intracellular concentration of reactive oxygen species (ROS) is increasingly recognized as a critical condition for stemness, self-renewal, and

pluripotency in both mammals and *Drosophila*. Increased ROS concentration promotes ISC proliferation in the adult *Drosophila* gut (Biteau et al., 2008; Buchon et al., 2009a; Choi et al., 2008a; Hochmuth et al., 2011). A central regulator of the intracellular redox state in vertebrates and invertebrates is Nrf2, a member of the “cap-and-collar” (Cnc) family of transcription factors. By influencing the redox state, the *Drosophila* homolog of Nrf2, CncC, and its negative regulator Keap1, control ISC proliferation rates, and this regulation is required to limit ISC hyperproliferation and intestinal degeneration in aging flies (Hochmuth et al., 2011).

Systemic signals represent another layer of regulation of stem cells behavior during homeostasis. Nutritional state can significantly affect insulin-like peptide (Dilp) expression, while oxidative stress or DNA damage results in repression of *dilp* expression (Geminard et al., 2009; Karpac et al., 2011; Slaidina et al., 2009; Wang et al., 2005). This systemic regulation may thus allow the adjustment of ISCs proliferation to nutritional state but also to stress levels (Amcheslavsky et al., 2009; McLeod et al., 2010). Nutrition also influences the activity of the TSC/Tor signaling pathway, and excessive Tor activation seems to have deleterious consequences for ISCs activity, reducing their proliferative capacity (Amcheslavsky et al., 2011). Importantly, ISCs have been shown to indirectly sense changes in nutrient and insulin levels through contact with their daughters. Nutrient deprivation and reduced insulin signaling result in production of growth-delayed enterocytes and prolonged contact between ISCs and EBs. Premature disruption of cell contact between ISCs and their progeny leads to increased proliferation and can rescue proliferation defects in insulin receptor mutants and nutrient-deprived animals indicating that a negative feedback loop between newly formed EBs and ISCs coordinate proliferation and differentiation (Choi et al., 2011).

In summary, intestinal stem cells proliferation is modulated by systemic and local signals coming from insulin producing tissues, epithelial cells, visceral muscles and their own progeny. Signaling pathways required for homeostatic proliferation and pathways required for stress- and injury- proliferation are integrated to dynamically modulate division rate of intestinal stem cells to cope with tissue demand. Importantly, regenerative pathways are redundant for stem cell maintenance and basal proliferation, and still remain poorly explored the intrinsic factors autonomously required to maintain stemness. It is known that stem cells within diverse tissues share the need for a chromatin configuration that promotes self-renewal and maintain undifferentiated state (Buszczak et al., 2009) however gene networks actively maintaining the “undifferentiated” epigenetic state and the mechanisms that allow differentiation remain elusive.



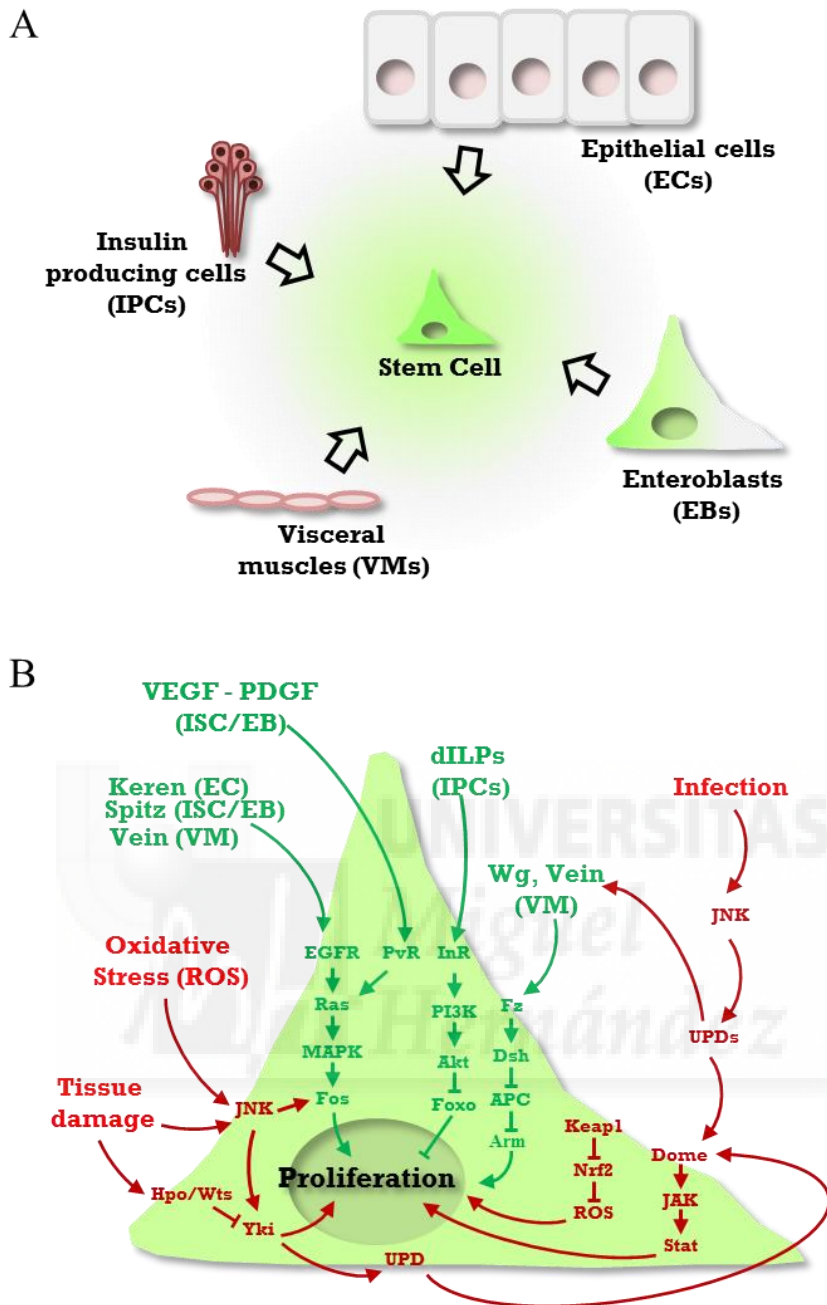


Fig. 3 – Intestinal stem cells proliferation depend on the integration of several signals. A) Intestinal stem cells proliferation is modulated by systemic and local signals coming from insulin producing tissues, epithelial cells, visceral muscles and their own progeny. B) Signaling pathways required for homeostatic proliferation are represented in green, and pathways required for stress- and injury- proliferation are in red. These pathways are redundant for stem cells maintenance and basal proliferation. Adapted from fig. 2 of Biteau et al., 2011.

The role of *snail* and *mir-200* family genes in EMT, MET and homeostasis

Epithelial-to-mesenchymal transition and its reverse counterpart

Epithelial-to-mesenchymal transition (EMT) is a morphogenetic process that occurs at several stages of development, including gastrulation and organogenesis, and in physiological conditions such as wound healing, fibrosis and cancer (Nieto, 2009, 2011; Thiery et al., 2009). The EMT involves profound changes in the morphology and behavior of epithelial cells. Epithelial cells lose contact with neighboring cells and become motile, acquiring the capacity to break through the basement membrane. Once the cells that have undergone EMT have reached their destination, they reverse back to an epithelial phenotype through the mesenchymal to epithelial transition (MET) which is thought to occur, at least in part, through mirror-like molecular mechanisms. Indeed, also MET take place in development and disease, including implantation, kidney organogenesis, somitogenesis and cancer, where is thought to be responsible of metastasis establishment (Chaffer et al., 2007; Dykxhoorn et al., 2009; Hugo et al., 2007).

EMT and MET are tightly controlled mechanisms in which their inducers and repressors have several levels of superimposed regulation, including post-transcriptional, splicing, and epigenetic programs. In example, EMT regulators are tightly regulated at the posttranscriptional levels, including control of translation (Evdokimova et al.; Hussey et al., 2011), stability (Park et al., 2010; Peinado et al., 2005; Wu et al., 2009), and subcellular localization (Domínguez et al., 2003; Mingot et al., 2009; Yamashita et al., 2004). Of the several inducers/repressor of EMT/MET, the

Snail and the miR-200 families are the most widely and best characterized. *snail* genes, which encode transcription factors of the zinc-finger type, have proven to behave like master inducers of EMT, while the miR-200 microRNA family has been shown to act as strong EMT repressors, as will be introduced in detail in the following sections.

The *snail* family genes positively control EMT and are implicated in homeostasis

snail genes encode transcription factors of the zinc-finger type (Boulay et al., 1987; Nieto, 2002). In *Drosophila*, Snail acts as a repressor to inhibit the expression of neuroectodermal genes such as *single-minded* and *shotgun* (an E-cadherin homologue) (Alberga et al., 1991) and it is essential for the formation of the mesoderm during gastrulation (Oda et al., 1998). The first indication that *snail* genes were involved in triggering EMT came from studies in the early chick embryo (Nieto et al., 1994). Snail was the first discovered transcriptional repressor of E-cadherin which loss is a hallmark of EMT (Cano et al., 2000). Several other transcription factors have been implicated in the transcriptional repression of E-cadherin, including Twist (Yang et al., 2004), ZEB1, ZEB2 (Comijn et al., 2001), and the basic helix-loop-helix factor E12/E47 (Perez-Moreno et al., 2001).

snail factors are not just related to EMT but have a broad spectrum of biological functions, including the regulation of cell proliferation and survival (Vega et al., 2004). Several evidences indicate that *snail* genes are related to stem cells function and that their negative regulation is required for normal adult tissues homeostasis. In *Drosophila*, *snail* has been involved in neural stem cell self-renewal and multipotency (Southall and Brand, 2009) while in mammals in renal (Boutet et al., 2006) and bone

homeostasis (de Frutos et al., 2009). Although the *snail* role in homeostasis is inferred by overexpression studies, *snail* genes have been found to be up-regulated in several pathological situations that imply disruption of normal tissue homeostasis, such as fibrosis (Boutet et al., 2007) and carcinomas, including colon cancer, in which are negative prognosis markers (Keck et al., 2013; Kim et al., 2014a; Kim et al., 2014b; Yamada et al., 2014; Zhang et al., 2013). Recently, *snail* expression has been shown to be sufficient to drives skin cancer initiation and progression through enhanced cytoprotection, epidermal stem/progenitor cell expansion and enhanced metastatic potential (De Craene et al., 2014).

***escargot* is a marker of stem and progenitor cells of adult *Drosophila* midgut**

The *escargot* gene encodes a zinc finger motif found in *snail*-related genes (Barralho-Gimeno and Nieto, 2009; Boulay et al., 1987; Nieto, 2002; Whiteley et al., 1992). It shares common functional properties with *snail* such as regulation of cell motility and adhesion. However, Escargot has been described also as an activator of DE-cadherin expression during tracheal morphogenesis to promote tracheal tube fusion (Tanaka-Matakatsu et al., 1996) while in mammals has been described just has a repressor. Escargot maintains diploidy in imaginal cells by inhibiting the transcription of genes required for endoreplication (Fuse et al., 1994) and acts as intrinsic factor in several developmental processes, including central nervous system development (Ashraf et al., 1999), development of the genital disk and determination of the wing cell fate (Fuse et al., 1996). It is also expressed in adult midgut precursor (AMPs), the cells that will give rise to the adult midgut of *Drosophila* (Jiang and Edgar, 2009; Micchelli et al., 2011). In adult flies, Escargot somatic protein has been shown to be required for maintenance of

male germ cells (Streit et al., 2002) and is commonly used as a midgut stem and progenitor cells marker (Micchelli and Perrimon, 2006). Nevertheless, at present, Escargot function in adult *Drosophila* intestinal stem and progenitors cells remains unexplored.

The *mir-200* microRNA family negatively regulates EMT and is negatively regulated by EMT inducers

MicroRNAs (miRNAs) are a class of short non-coding RNA molecules with post-transcriptional regulatory capacity on gene expression (Ambros, 2001; Bartel, 2004). MicroRNA primary transcripts (pri-miRNA) are derived from genomic DNA and synthesized by RNA polymerase II or III into a hairpin structure which is processed to generate a precursor microRNA (pre-miRNA) which will be exported to the cytoplasm where will be further processed to give rise to mature microRNA (miRNA). miRNAs are then able to target mRNAs leading to their degradation or blocking transcript translation (Bartel, 2004; Bushati and Cohen, 2007; Valencia-Sanchez et al., 2006). The members of a miRNA family contain highly conservative sequences, termed seed, which are required for the function and specificity of the microRNA. As a matter of fact, miRNAs with the identical seed sequences share the same putative target gene profiles. For the miR-200 family, two types of seed sequences were identified, which only have a nucleotide difference.

In several contexts, miR-200 microRNAs have been described as a key inhibitor for epithelial-to-mesenchymal transition (EMT) and promoters of the epithelial state through direct targeting of EMT inducers, such as ZEB1 and ZEB2, being therefore classified as tumor suppressors (Bracken et al., 2008; Burk et al., 2008; Cano and Nieto,

2008; Gregory et al., 2008; Korpál et al., 2008; Park et al., 2008). miR-200 family members are downregulated in several tumors, however, it has also been shown in breast cancer cell lines that miR-200 might be involved in promotion of the last step of the metastatic cascade when establishing macroscopic metastatic masses at distant sites (Dykhhoorn et al., 2009). Indeed, in human colorectal carcinomas it has been shown that miR-200 is downregulated at the tumors invasive front that have destroyed and invaded beyond the basement membrane, but show strong expression at the regional lymph node metastases indicating that miR-200 is involved in the recapitulation of the primary tumor phenotype at metastatic sites.

Even though in a much less extensive and direct manner, also EMT suppressing genes have been linked to stem cells behavior. The first report linking miR-200 and stem cells came in 2009 from a study in which all five members of the miR-200 family were shown to be downregulated in human breast cancer stem cells as well as in normal human and murine mammary stem/progenitor cells (Shimono et al., 2009). Restoration of miR-200 expression could decrease stem cell -like properties while promoting a transition to an epithelial phenotype (Lim et al., 2013). Such results were consistent with previous findings in cancer cell lines establishing a reciprocal repression between ZEB1 and members of the miR-200 family. Within the putative promoter region and in spacers between the miR-200s genes, there are highly conserved binding motifs to which ZEB1 and ZEB2 can bind for suppression of this family's polycistronic transcription (Bracken et al., 2008; Burk et al., 2008; Wellner et al., 2009). Additionally, two other related transcription factors known to be associated with EMT, Snail and Slug, were shown to be able to negatively regulate transcription of miR-200 (Gill et al., 2011; Liu et al., 2013).

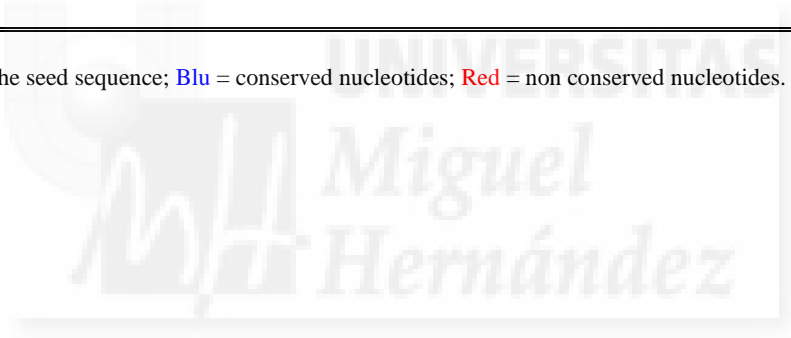
miR-8 is the sole homologue of the miR-200 family in *Drosophila*

Drosophila miR-8 (Dme-miR-8) is the sole homologue of the human miR-200 family sharing the same seed sequence and presenting high homology also in the rest of the mature microRNA sequence (table 3). This microRNA has over 250 conserved predicted targets (Grun et al., 2005; Stark et al., 2005) of which a certain number has been validated *in vivo*. At present, validated targets include *atrophin* (Karres et al., 2007), *wntless* (Kennell et al., 2008), *u-shaped* (Hyun et al., 2009), *serrate* (Vallejo et al., 2011) and *spitz* (Morante et al., 2013). This list of targets is representative of the importance of this microRNA which has been related to growth control (Hyun et al., 2009; Jin et al., 2012; Morante et al., 2013) and patterning (Kennell et al., 2008) but in other systems, including human cancer cell lines, has been implicated in suppression of mesenchymal phenotype and metastatic behaviour (Vallejo et al., 2011). In addition miR-8 has been characterized as a regulator of the actin cytoskeleton (Loya et al., 2014) and of cell adhesion proteins during synapse formation in the *Drosophila* neuromuscular junction, and of planar cell polarity in *Zebrafish* (Flynt and Patton, 2010).

Table 3. The microRNA miR-8 is the sole fly homologue of the mammalian miR-200 family

Organisms	Gene name	Sequence (5'→3')
<i>D. melanogaster</i>	dme-miR-8	UAAUACUGUCAGGUAAGAUGUC
<i>Homo sapiens</i>	hsa-miR-200b	UAAUACUGCCUGGUAAGAUGA
	hsa-miR-200c	UAAUACUGCCGGGUAAGAUGGA
	hsa-miR-429	UAAUACUGUCUGGUA AAAACCGU
	hsa-miR-200a	UAA <u>C</u> ACUGUCUGGUAACGAUGU
	hsa-miR-141	UAA <u>C</u> ACUGUCUGGUAAGAUGG

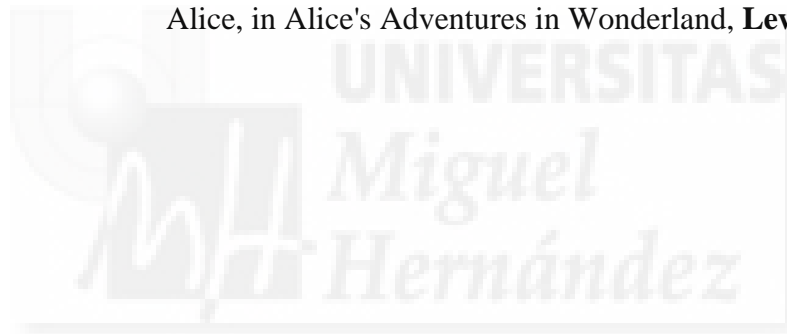
In color the seed sequence; **Blu** = conserved nucleotides; **Red** = non conserved nucleotides.



Hypotheses & Objectives

“... at least I know who I was when I got up this morning, but I think I must have been changed several times since then”

Alice, in Alice's Adventures in Wonderland, **Lewis Carroll**, 1865



The comprehensive purpose of this experimental work was to understand basic mechanisms of adult *Drosophila* midgut epithelial homeostasis in unchallenged conditions by direct and simultaneous observation of the behavior of intestinal stem cells (ISCs) / progenitors (EBs) and epithelial cell replenishment (enterocytes, ECs). In detail, we have delineated the following two hypotheses from which we conveyed three specific objectives of the work, which include the generation of a novel method.

Hypotheses

- (I) **ISCs possibly behave differently between them and tissue replenishment might not be homogeneous during homeostasis** – Current knowledge on regulation of ISCs proliferation and their progeny (EBs) differentiation during homeostasis were mainly gained through regenerative studies, however tissue homeostasis and tissue regeneration are only partially overlapping. In addition, ISCs division dynamics were primarily inferred by clonal analysis which requires the assumption that all stem cells are equal in division and differentiation potential and that midgut turnover occurs in an homogenous fashion. So far evidences for these expectations are lacking;

- (II) ***escargot* could play a role in controlling ISCs/EBs behavior during tissue replenishment, process which may also have analogies with a MET process** – Not only niche signals and tissue feedback mechanisms control ISCs proliferation and EBs differentiation but possibly also still unknown intrinsic cell autonomous factors. Epithelial to mesenchymal transition (EMT) and its reverse counterpart mesenchymal to epithelial transition

(MET) are genetic programs autonomously controlled by genes of the *snail* family and its repressors, among them the miR-200 family of non-coding genes. *escargot* is the *snail* family gene ancestor and is a specific midgut ISCs/EBs marker.

Objectives

- (I) Design and generation of a novel *in vivo* system to monitor tissue turnover during homeostasis (unchallenged conditions);
- (II) Analyze dynamics of midgut epithelial cells turnover during tissue homeostasis by monitoring stem/progenitors cells distribution, stem cells division and new cells distribution;
- (III) Test *escargot* as putative intrinsic factors involved in ISCs proliferation and/or maintenance and/or EBs maturations and explore for genetic and cellular analogies between ISCs/EBs behavior during tissue replenishment and MET.

Following the three delineated objectives, results have been divided in three corresponding parts.

RESULTS

“Enough research will tend to support your theory”

Murphy's Law of Research



PART 1 - ReDDM, a novel method to monitor stem cells and tissue replenishment simultaneously

***escargot* is a midgut stem cells and progenitors marker**

escargot (*esg*) gene expression was reported in the midgut imaginal islands during *Drosophila* development (Jiang and Edgar, 2009) and in the stem cell/progenitor compartment during its adult life (Micchelli and Perrimon, 2006). It has previously been shown to be expressed in imaginal discs and abdominal histoblast nests (Hayashi et al., 1993) and to be required there for maintaining cells in the diploid state during larval development (Fuse et al., 1994). *escargot* is the ancestor gene of the *snail* gene family which members are epithelial to mesenchymal (EMT) regulators (Barrallo-Gimeno and Nieto, 2009; Boulay et al., 1987; Manzanares et al., 2001; Nieto, 2002; Whiteley et al., 1992). In this first part of the result we will report *escargot* expression pattern and the genetic tools that were generated to investigate the mechanisms of *Drosophila* midgut homeostasis, including the role of *escargot* gene, which will be subject of the third part of the results.

We verified *escargot* expression pattern in the adult fly using a GFP reporter line, *esg*-GFP (fig. 1.1), and an *esg*-Gal4 (fig. 2.1) line available from our laboratory. Was also verified the expression of *esg*-Gal4 in the midgut imaginal islands, during midgut development to further confirm expression pattern (not shown). The *esg*-GFP is a Flytrap line (P01986) which has the green fluorescent protein (GFP) inserted into the *escargot* endogenous gene. Fluorescence is not particularly intense and of difficult detection by conventional microscopy, however detectable by confocal microscopy

without the need of GFP immunostaining. By position and morphology we initially assumed that these labeled cells were the described intestinal stem cells and/or progenitor cells (ISCs/EBs) (Micchelli and Perrimon, 2006; Ohlstein and Spradling, 2006). Indeed, the two lines available in our laboratory (*esg-GFP* and *esg-Gal4*) labelled non-cohesive cells scattered along the midgut (fig. 1.1 B) from just below the proventriculus to the midgut/hindgut junction, where is located the pylorus and malpighian tubules arise (see fig. 2 of the introduction for anatomical resume of *Drosophila* intestine). These cells are not arranged in a specific pattern or configuration and occupy interstitial space between visceral muscles (vm) and epithelial cells (ECs) (fig. 1.1 A, C). Approximately 40-50% of them are diploid and the rest have bigger nuclei which size ranges between a diploid cell and an enterocyte octaploid cell. *escargot* positive cells have all extensive contact with the basement membrane however the nucleus of the diploid cells have a more basal location with respect to the *escargot* polyploidy nuclei (not shown) as previously reported (Goulas et al., 2012; Ohlstein and Spradling, 2006, 2007). Initial tract of malpighian tubules (up to a bit further of their bifurcation) also present marked small diploid cells. We confirmed that these enhancer traps label ISCs and EBs by crossing it with the *SuH-LacZ* reporter (fig. 1.2 A-C), which is specifically active in the EBs, and staining for the ISC specific marker *Dl* and the enteroendocrine (ee) cell marker *prospero* (Micchelli and Perrimon, 2006; Ohlstein and Spradling, 2006) (fig. 1.2 D-F).

esg-GFP; anti DLG-1

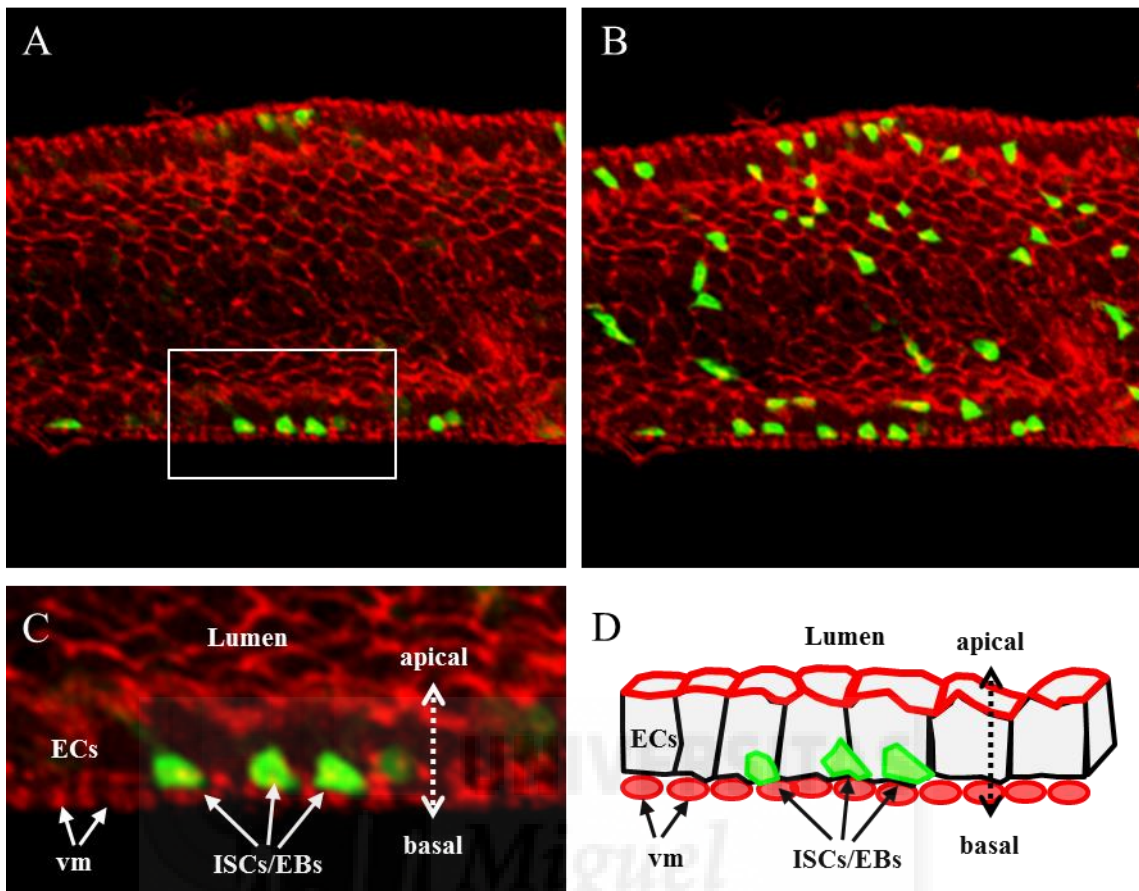


Fig. 1.1 - The *escargot* GeneTrap P01986 (“*esg-GFP*”) labels cells basally located and scattered along the midgut epithelium. A) 5 stacks max projection for red channel (anti- Disc Large -1, DLG-1), 1 stack for green channel (*esg-GFP*) to highlight 3D structure of the midgut; *esg* positive cells are basally located in the midgut epithelium, which is single-layered and not folded. B) Max projection of 5 stacks for red and green channel to show all the *esg*⁺ cells which are below the epithelial cells; *esg*⁺ cells appear evenly distributed along the tissue, however, are evident areas without *esg*⁺ cells. C) Inset from image (A) showing basal location of *esg*⁺ cells, just juxtaposed to visceral muscles (vm). D) Cartoon representing *Drosophila* midgut epithelium: absorptive cells, also named enterocytes (ECs), form a single layered and unfolded epithelium with marked apico-basal polarity, easily visualized by anti DLG-1 (red). DLG-1 is a septate junction protein that we found localized apico-laterally in the midgut. DLG-1 marks also visceral muscles. *esg*⁺ cells are putative intestinal stem cells (ISCs) and precursor cells (also named enteroblasts, EB) and are basally located in the epithelium, in strict contact with the visceral muscles.

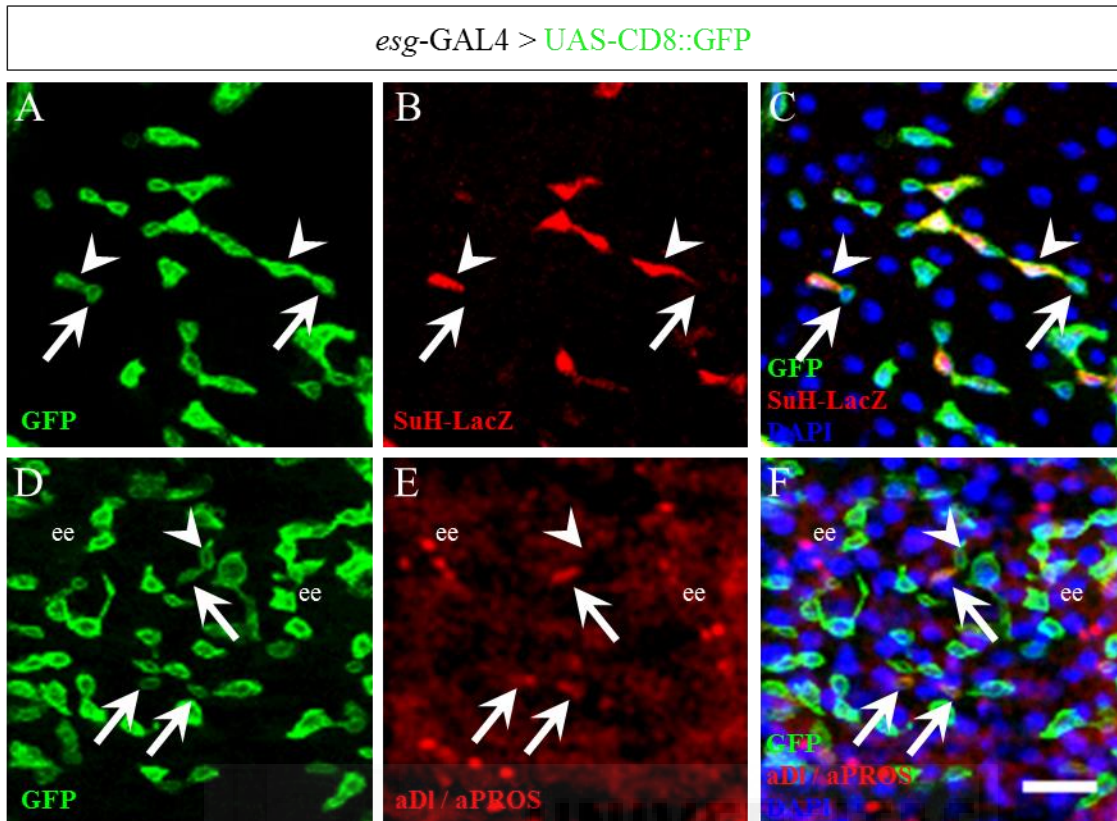


Fig. 1.2 - The *escargot*-Gal4 enhancer trap drives expression of membrane GFP in ISCs and EBs without leaky expression in EC or ee cells. A-C: EBs are identified by the *Su(H)*-lacZ reporter, ISCs by proximity with *Su(H)*-lacZ⁺ cells and diploid nucleus. D-F: ISCs are identified by anti-Delta, EBs by proximity with DI⁺ cells. Arrowheads indicate EBs; arrows indicate ISCs. ECs are identified by large polyploidy nucleus visible by DAPI. ISCs and ee cells are diploid and ee are identified by anti-Prospero staining (aPROS). ee cells are often in couples. Scale bar = 20 μ m.

Design and proof of a dual differential marking system

The binary Gal4/UAS system allows expression of one or more UAS transgenes by the yeast transcription factor Gal4 inserted under the control of endogenous or exogenous regulatory sequences of specific genes (Brand and Perrimon, 1993). The expression of reporter proteins unveils a promoter or enhancer intrinsic genetic activity, therefore giving information about the endogenous gene expression pattern. The combination of the binary Gal4/UAS system with reporter fusion proteins such as the membrane tethered human CD8 fused to GFP (hereafter CD8::GFP) or the histone-2B fused to i.e. RFP (hereafter H2B::RFP), provided great advances in the understanding of tissues morphogenesis (Lee and Luo, 1999) and subcellular dynamics (Langevin et al., 2005). These two reporters have different subcellular localization but also different turnover rate. Indeed, histones are highly stable and conserved proteins which half-life in mammals is estimated to be about 100 days in liver and more than 250 days in the brain, whereas common GFP has a turnover of near 24 hours.

We reasoned that the histone stability could be exploited in a cell lineage approach (fig 1.3). Membrane tethered CD8::GFP and nuclear localized H2B::RFP fusion proteins can be co-expressed *in vivo* with the Gal4/UAS system. If the driver is turning off, membrane GFP signal will be rapidly lost while histone-2B-fused RFP will persist (fig 1.3 A). On this basis, we named this approach Dual Differential Marker (DDM). The DDM approach can be used in hierarchical systems in which the driver is expressed in the parental cells (i.e. midgut ISC/EB cells) and then turned off in the descendant cells (midgut EC or ee cells) (fig. 1.3 B). Coupling DDM with a method to temporally control the driver expression, like temperature sensitive Gal80^{ts}, would be

possible to identify new descendants among older cells (present previously to the temperature shift) (fig. 1.3 B and C).

Expression of GFP in ISCs and EBs by the *escargot* enhancer trap and by *escargot*-Gal4 (which has a much higher expression of GFP than an endogenous enhancer trap) demonstrated that GFP has sufficiently rapid turnover to do not persist in their undifferentiated progeny (fig. 1.2 and fig. 1.3 C). We then assayed the expression pattern of *esg*-Gal4 driver line using simultaneously the membrane reporter CD8::GFP and the stable nuclear reporter H2B::RFP (fig 1.3 C and 1.4). We confirmed that the CD8::GFP reporter needs sustained expression to be detectable, while H2B::RFP has strong perdurance and labels also all the epithelial cells where the *escargot* driver is not active (fig 1.4). This pattern of labelling was independent of flies' age, indicating that the H2B::RFP trace was persisting from development. Indeed, has been reported and confirmed also for our *esg*-Gal4 line, that *escargot* is expressed in midgut imaginal islands, the larval precursors of the adult *Drosophila* midgut (not shown). Hence, this result formally demonstrated that all differentiated midgut cells originate from *escargot* expressing cells during development.

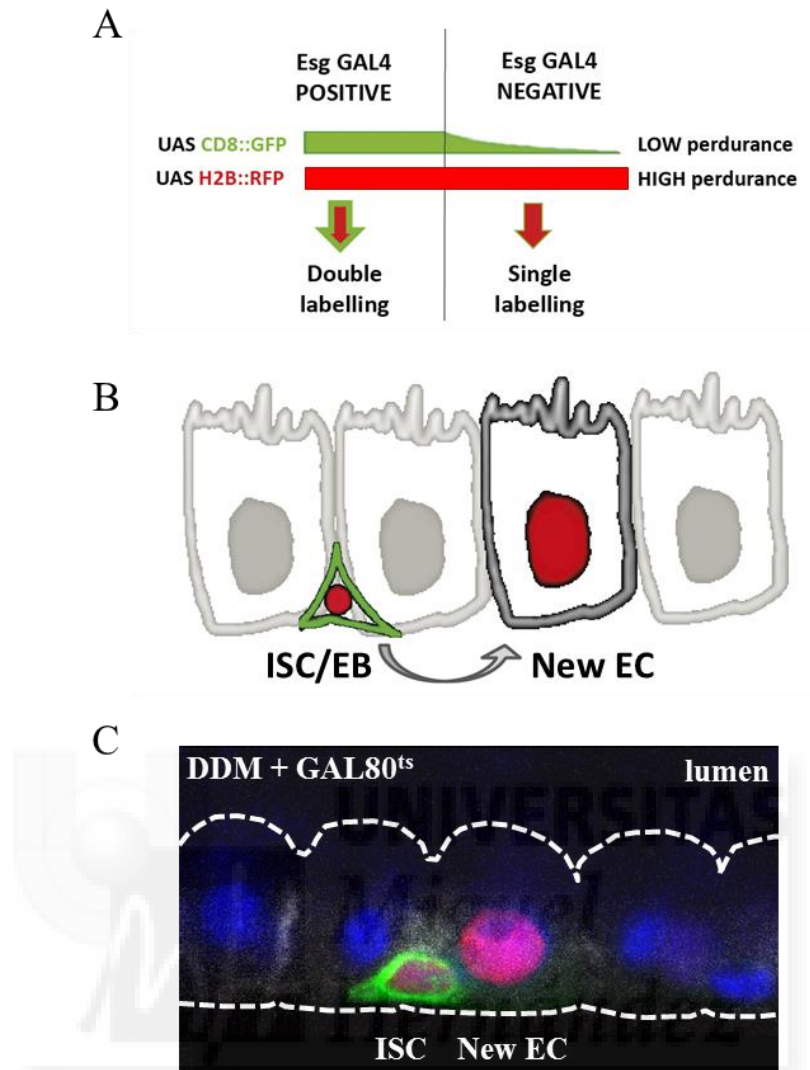


Fig 1.3 - The Dual Differential Marker (DDM) concept for cell lineage in *Drosophila* midgut. A) membrane tethered CD8::GFP and nuclear localized H2B::RFP fusion proteins can be co-expressed *in vivo* with the GAL4/UAS system. If the driver is turning off, membrane GFP signal will be rapidly lost while RFP-tagged histone-2B will persist. B) Cartoon showing how the DDM approach can be used in hierarchical systems in which a driver is expressed in the cells upstream (i.e. ISC/EB) and then turned off in the descendant cells (EC or ee). Coupling with a method to temporally control the driver expression, like temperature sensitive GAL80^{ts}, would be possible to identify new descendant. C) Confocal image of a transversal section of the intestinal epithelium in which the DDM is used with the ISC/EB specific driver *esg-Gal4* and the GAL80^{ts}. The *esg*⁺ double labelled cell is diploid and is basally located and is therefore an ISC while the single nuclear labelled cell is polyploidy and integrated in the epithelium is its new EC descendant. Old ECs are identified by DAPI staining.

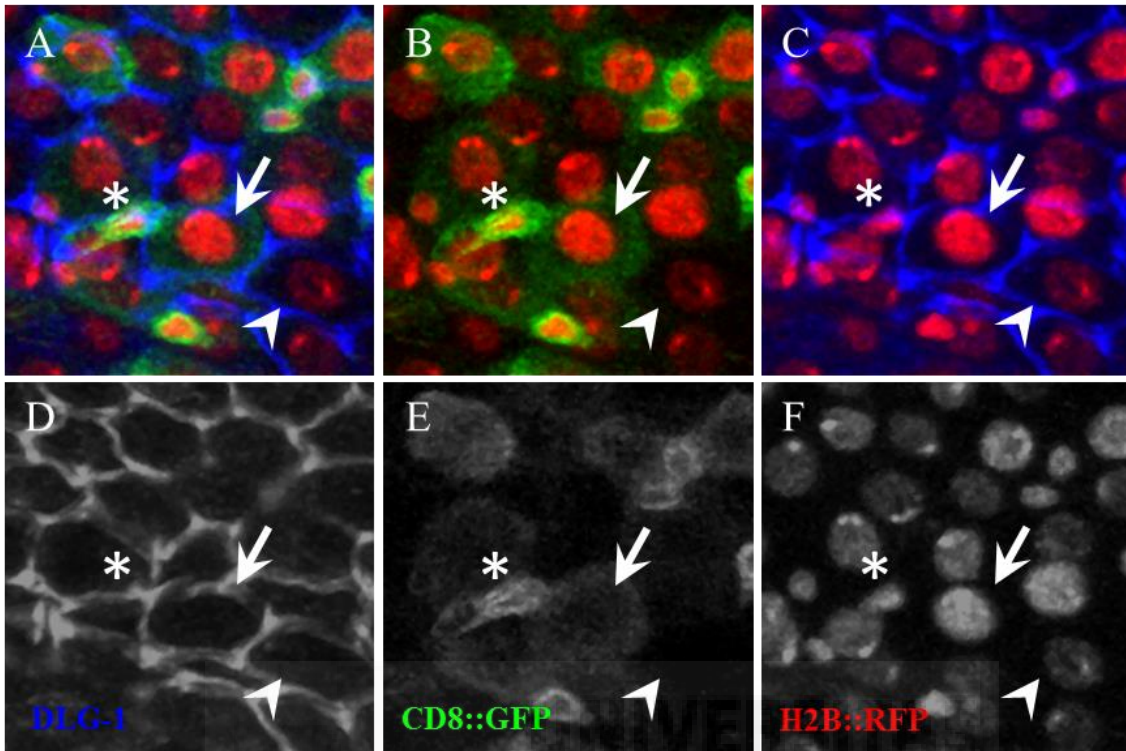


Fig. 1.4 - Dynamic report of *escargot* activity in the midgut epithelium by Dual Differential Marking (DDM). A-C) The DDM approach allows to identify undifferentiated and differentiated cells of the midgut epithelium in a dynamic manner. Stem and progenitor cells are double labeled by membrane GFP and nuclear RFP while the differentiated progeny marked by the epithelial marker DLG-1 retain only the stable H2B::RFP fusion protein. Enterocytes with very faint GFP and intense RFP (arrow) could be observed nearby ISCs (asterisk), suggesting that they are new enterocytes (compare to enterocytes with less RFP signal, arrowhead). D-F) single channels for DLG-1, CD8::GFP and H2B::RFP respectively. Note that the epithelial marker disc large (blue) marks enterocytes but not undifferentiated cells (*escargot*⁺ stem and progenitor cells).

***escargot* expression pattern by “Dual Differential Marker” system**

Adult expression pattern of the *esg*-Gal4 line was further characterized using DDM system to clearly define all the organs in which this driver was active (fig. 1.5) and summarized in *table 1.1*. Note that Gal4 lines, if not specifically mutated, have expression in the salivary glands. Moreover *esg*-Gal4 is expressed in the male hub but not in the ovary. Notably, the entire hindgut is *escargot* negative. In addition was observed a very specific pattern of expression in the central brain (fig. 1.5 F). In particular, we observed *escargot* expression in a bilateral circuit of eight neurons projecting dorso-ventrally, which could correspond to olfactory neurons. Interestingly, in higher organism olfactory neurons are continuously replenished by stem cells. There is not sexual dimorphism for this pattern and currently we do not know if stem cells exist in the adult brain of *Drosophila*.

This *in vivo* expression analysis was compared with data reported in GEO microarray profiles database (fig 1.6). According to this microarray *escargot* is expressed, although at lower levels, also in the hindgut, data that was not confirmed in our detailed *in vivo* work. This discrepancy could be explained by the fact that hindgut preparation made for the microarray was done, as indicated in the protocol, dissecting right behind the malpighian tubules where there is still a substantial amount of midgut and hence of *escargot* positive cells. In addition, one of the two malpighian tubules extends posteriorly entangling with the hindgut and the ovaries, increasing the likelihood of tissue contamination. In general, most of the expression profile was confirmed and thus the *esg*-Gal4 line available in our laboratory was considered as an excellent one to recapitulate endogenous *escargot* expression and to induce restricted genetic manipulations.

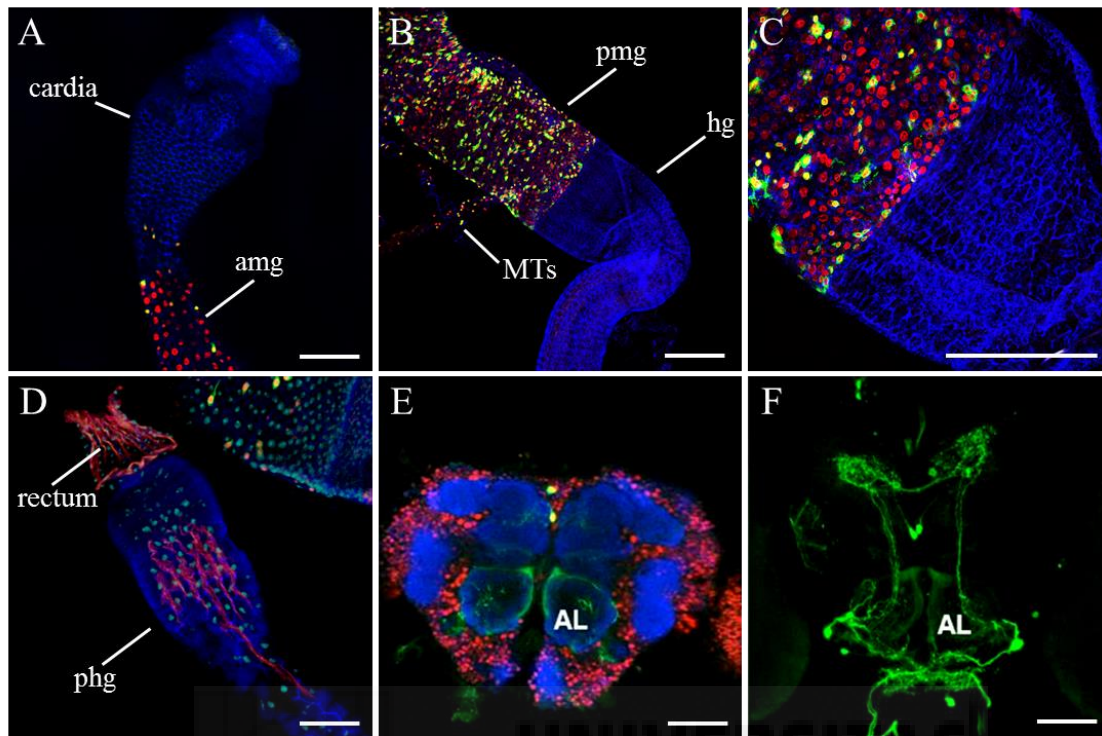


Fig. 1.5 – *escargot-Gal4* adult expression pattern by Dual Differential Marking system. Three channels confocal images: green = CD8::GFP; red = H2B::RFP; blue = anti DLG-1. A) Proventriculus (or cardia) is negative for *esg* expression and has no RFP trace, indicating a different embryonic origin. B) Expression is limited to midgut and malpighian tubules (MTs); hindgut is negative for both reporters. C) Magnification of B; note that the sharp boundary correspond exactly to the pilorus, the midgut-hindgut valve. D) Posterior hindgut and rectum are negative for *esg*. E) Many neurons of the optic lobes and central brain present the RFP trace while only few have GFP. F) Reconstruction of *esg*⁺ neurons: is a bilateral circuit of 8 neurons with dorso-ventral projection. For all panels scale bar = 100μm.

Table 1 – *escargot*-Gal4 adult expression pattern by Dual Differential Marking system (DDM)

<i>Structure</i>		<i>esg-Gal4</i> >	
		CD8::GFP	H2B::RFP
Foregut	crop	✗	✗
	salivary glands	✓	✓
Midgut	proventriculus	✗	✗
	anterior midgut	✓	✓
	“stomach”	✓	✓
	posterior midgut	✓	✓
Hindgut	stem cell zone	✗	✗
	ileum	✗	✗
	rectum	✗	✗
Maphighian tubules	proximal	✓	✓
	distal	✗	✓
Female gonads	tubes	✗	✓
	ovary	✗	✗
	accessory gland	✗	✓
Male gonads	testis	✓	✓
	accessory glands	✗	✓
Brain	central brain	✓	✓
	optic lobes	✗	✓
Carcasses	fat body	✗	✗

CD8::GFP expression denotes actual *esg-Gal4* activity while H2B::RFP indicates *esg-Gal4* previous activity in that cell or in its progenitor during development or tissue turnover. Note that the adult female expression of *esg-Gal4* is restricted to few neurons and only in ISCs and EBs present in the midgut and in the proximal area of the malpighian tubules, making *esg-Gal4* an excellent line to induce restricted genetic manipulations in adult midgut stem and progenitors cells.

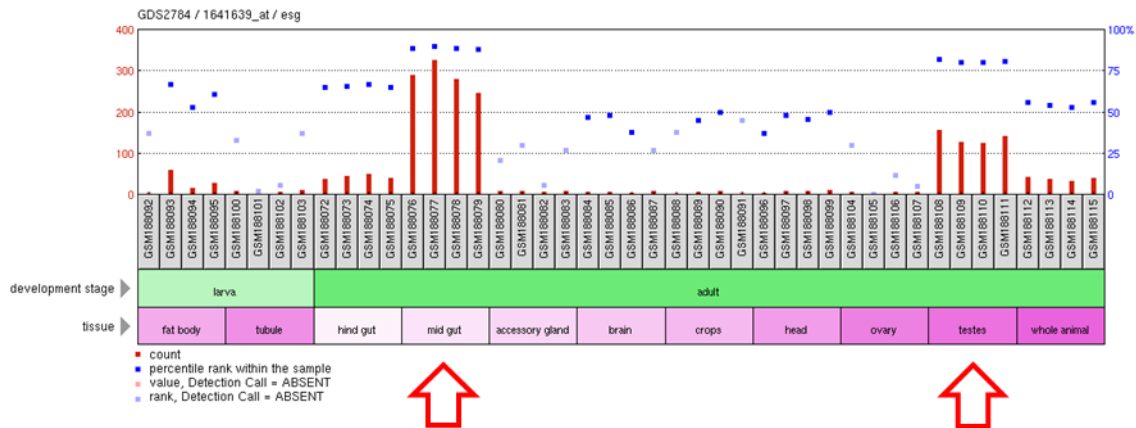


Fig 1.6 - *escargot* expression profiling by microarray indicate strong expression in midgut and testis. For each tissue, 4 biological replicas are reported; tissues are compared to whole animal lysates. In red, level of expression; small cyan and blue squares indicates respectively absent or present. *Esg* is highly expressed in fly midgut and testis (red arrows). In hindgut is expressed as well, with lower levels, in contrast to our results. Due to the contiguity of the midgut and hindgut and the anatomical entangling of the maphighian tubules to the hindgut, is likely an artifact due to dissection protocol. Interestingly, *esg* is called present 3 out of 4 times in central brain and 4 over 4 in whole head strongly suggesting significance even if expression levels at the limit of significance. *esg* is called present 2 out of 4 in the crop, at marginal levels not considerable significant. Source: GEO profiles, DataSet Record GDS2784.

Generation of “*Repressible Dual Differential Marker*” fly stocks to monitor intestinal epithelium homeostasis

We reasoned that the DDM approach could be used in hierarchical systems in which the driver is expressed in the cells upstream (i.e. midgut ISC/EB cells) and then turned off in the descendant cells as described in the previous section. The Gal4/UAS system coupled with a temperature sensitive repressor can allow temporally controlled expression of the tissue specific driver, the so called TARGET system (McGuire et al., 2004)). The DDM approach combined with TARGET would allow (1) to induce

specifically manipulation in the adult flies avoiding embryonic and developmental lethality, which could be a relevant problem with *esg-Gal4* since it is extensively expressed during development; (2) to follow midgut epithelial tissue turnover through the unique identification of stem cells new epithelial descendants among older epithelial cells not labeled (present previous to the temperature shift).

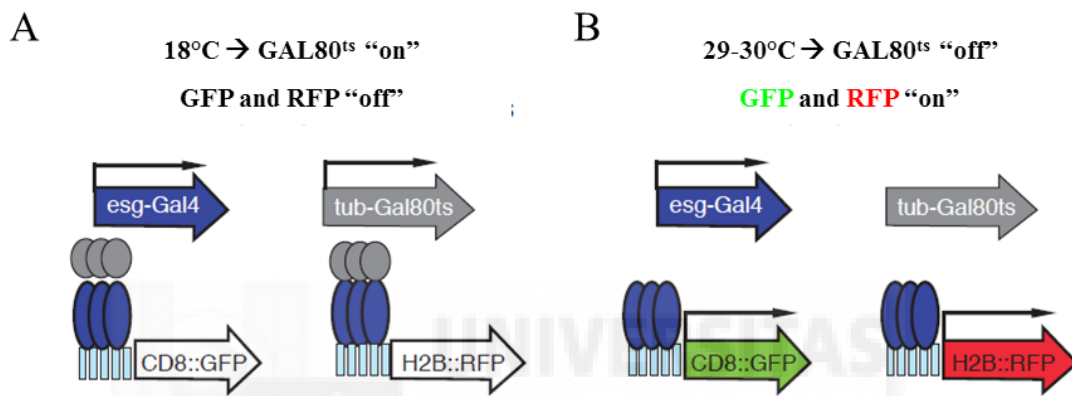


Fig 1.7 - The temperature sensitive GAL80^{ts} allows temporal and regional gene expression targeting (TARGET) A) At the non-permissive temperature the GAL80^{ts} is active ("on") and is bound to the transcription factor GAL4, preventing it from expressing UAS-transgenes, i.e. UAS-CD8::GFP and UAS-H2B::RFP. B) *Viceversa*, at the permissive temperature the repressor is inactive ("off") allowing GAL4 activity and therefore the expression of UAS-transgenes. Turquoise box =UAS sequences; genes = thick arrows; blue ovals = GAL4 transcription factor; grey ovals = GAL80 repressor protein.

The "*escargot-Gal4-DDM*" was then coupled with an ubiquitously expressed temperature sensitive allele of the Gal80 repressor (*tub-Gal80^{ts}*), to generate a TARGET system that we named "Repressible Dual Differential Marker" (ReDDM). At the non-permissive temperature (18°C) the Gal80^{ts} is active ("on") therefore there is not Gal4 mediated transcription, *viceversa*, at the permissive temperature (29-30°C), the Gal80 is

inactive (“off”) allowing Gal4-mediated transcription of UAS-transgene (fig. 1.7). In this manner, flies developed at 18°C did not express the reporter proteins (fig. 1.8 A); when shifted to 29-30°C reporters will start to be expressed only in ISC/EBs cells where *escargot* is constitutively active, while the cells forming the intestinal epithelium, the ECs and ees, will be negative (fig. 1.8 B). In a given time span, epithelial cells turnover will take place and new cells that will integrate will originate from labeled ISCs and EBs and therefore will retain the nuclear red marking, (fig. 1.8 C). Indeed as expected, the *escargot*-ReDDM allowed mapping epithelial cell turnover with a single cell resolution (fig. 1.8 D). Epithelial cells could be identified because *escargot* negative (ECs were never marked by CD8::GFP in the membrane), by nuclear size (visualized by DAPI) or by staining with epithelial markers such as discs large 1 (DLG-1) (fig. 1.8 B). This approach is unique in the manner of labeling stem cells and their progeny in a genetic and hierarchical manner (lineage tracing). MARCM technique, the other commonly used strategy to follow stem cells behavior, labels randomly dividing stem cells upon a heat shock with a permanent marker, allowing therefore a lineage tracing but not providing a global view on the tissue and the whole stem cells population. Importantly, ReDDM has the advantage that can be coupled with any other UAS transgene and maintain the expression specific in the parental cells while allowing to follow the generation and differentiation of daughter cells. A similar method based on an *escargot* / flip-out system (*esg*-Gal4, UAS-*Flp*; *act*>STOP>GFP; *tub*-Gal80^{ts}) has been used to determine gut turnover (Cordero et al., 2014; Cordero et al., 2012b; Jiang et al., 2011; Jiang et al., 2009). However, this method has the main disadvantage that after *escargot* dependent flip out the driver becomes *actin*, which is constitutive, and leads to transgenes miss-expression also in the differentiated progeny. Another secondary disadvantage is that is not differentially labelling undifferentiated cells and

differentiated progeny, making ambiguous the analysis of tissue turnover because dependent on other markers, such as PDM1.

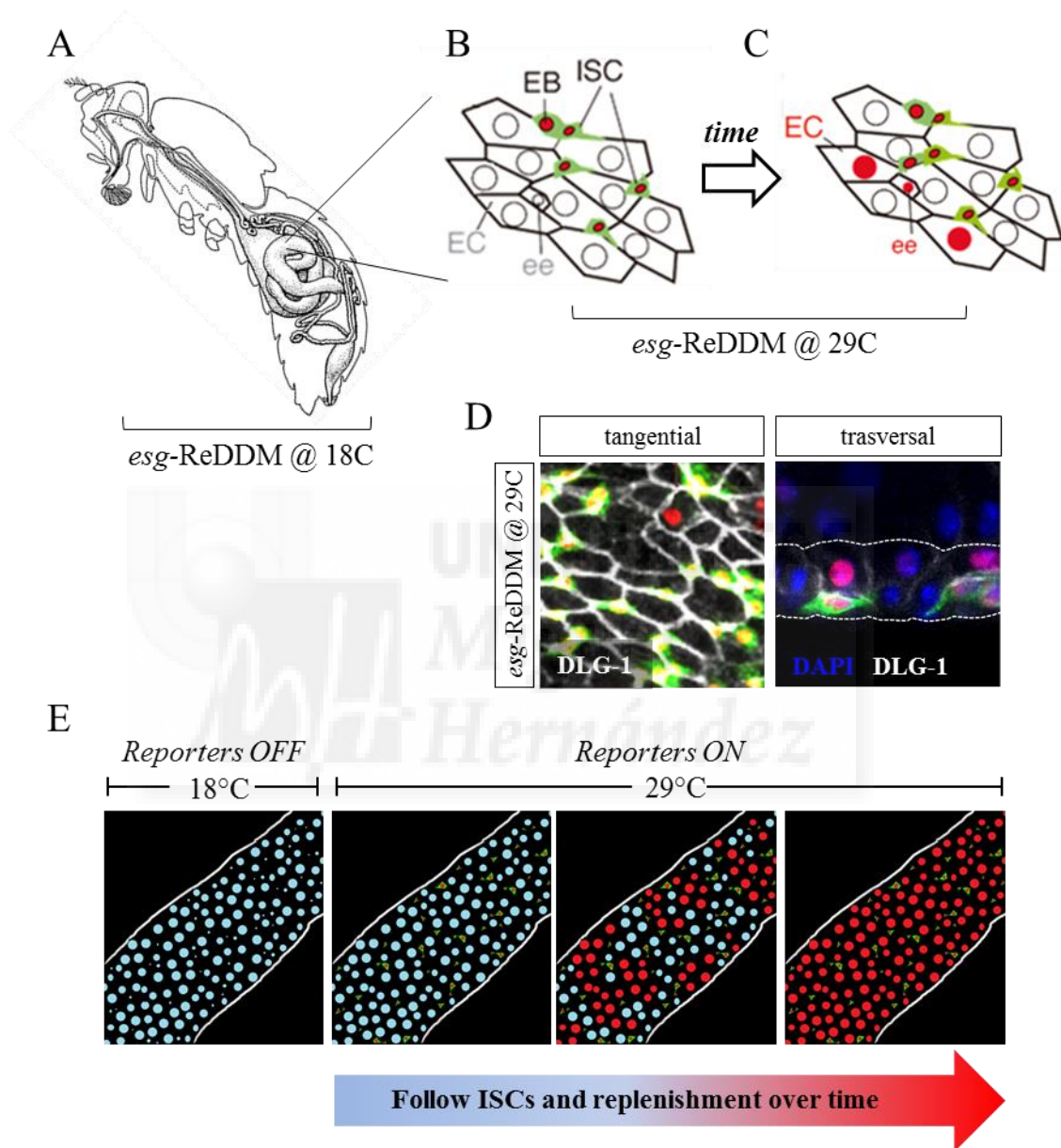


Fig 1.8 – The *escargot*-Repressible Dual Differential Marker (*esg*-ReDDM) allows to temporally monitor cell turnover at the single cell and whole tissue level. A-C) Cartoon showing the ReDDM strategy in the midgut. A) Adult flies developed at 18°C do not express reporter genes and are wild type. B) When shifted to 29°C, ISCs and EBs are double labelled immediately since *escargot* is constitutively

expressed in ISCs/EBs. C) In a given time lapse cells that underwent turnover will be visualized by the perdurance of the nuclear RFP trace (H2B::RFP). D) Tangential and transversal section of midgut epithelium stained with the epithelial marker Disc Large 1 (DLG-1) showing in that the *escargot*-ReDDM has single cell resolution and allows identification of all cell types of the midgut: ISCs/EBs by GFP/RFP double labelling (note basal location and lack of DLG-1 staining), new epithelial cells by the nuclear RFP trace and DLG-1 staining, old epithelial cells by DAPI and DLG-1. E) Cartoon showing how the *escargot*-ReDDM allows to visualize the undifferentiated cell population (ISCs/EBs) and follow whole tissue turn-over (also named replenishment) over time.

Importantly, the ReDDM approach provides an easy manner to observe readily tissue turnover with just DAPI staining. In addition, being every single event of turnover marked by nuclear RFP, ReDDM offers the possibility to determine the exact cell turnover as a percentage of new ECs over old ECs, even with automated countings.

Since *esg*-Gal4 is not specific for ISCs or EBs, we also generated ReDDM lines with the *Dl*-Gal4 and *SuH*-Gal4, two lines which have expression specifically in the ISCs and EBs separately (Zeng et al., 2010). In addition, we screened several other GAL4 lines for midgut (restricted) expression upon crossing over the DDR stock (expression pattern was checked in detail in whole adult flies). The identified lines are summarized in table 1.2. Despite we found other drivers equivalent to *escargot* in the expression pattern in the midgut, like *eyeless* or *krH1*, their expression was not as restricted as for *escargot*. In addition we found that the published *Dl* and *SuH*-Gal4 lines had weak expression and were labelling just a subpopulation of ISCs and EBs. However, when combined in a ReDDM stock they were able to monitor tissue replenishment, indicating that they label ISCs and EBs when they are respectively actively transcribing *Dl* or activating NOTCH. In other terms *Dl* transcription seems not to be constitutive in ISCs while NOTCH activation appears to be transient in EBs.

Indeed we found by loss of function experiments that, although *Dl* is a sufficient marker to identify ISCs, it is not required for their maintenance and proliferation (not shown). Finally, the *Dl* and *SuH-Gal4* lines had extensive expression in other tissues, limiting considerably their use.

Table 2 – ReDDM stocks generated and summary of adult expression pattern

<i>Full genotype</i>	<i>Adult expression pattern</i>	
	<i>Midgut cell types</i>	<i>Midgut restricted?</i>
<i>esg-Gal4</i> , UAS-CD8::GFP/Cyo; <i>Tub-Gal80^{ts}</i> , UAS-H2B::RFP/TM2;	ISCs/EBs	Yes*
<i>ey-Gal4</i> , UAS-CD8::GFP/Cyo; <i>Tub-Gal80^{ts}</i> , UAS-H2B::RFP/TM2;	ISCs/EBs	No
<i>kr-h1-Gal4</i> , UAS-CD8::GFP/Cyo; <i>Tub-Gal80^{ts}</i> , UAS-H2::BRFP/TM2;	ISCs/EBs	No
<i>SuH-Gal4</i> , UAS-CD8::GFP/Cyo; <i>Tub-Gal80^{ts}</i> , UAS-H2B::RFP/TM2;	EBs	No
<i>mir-8-Gal4</i> , UAS-CD8::GFP/Cyo; <i>Tub-Gal80^{ts}</i> , UAS-H2B::RFP/TM2;	EBs	No
<i>klu-Gal4</i> , UAS-CD8::GFP/Cyo; <i>Tub-Gal80^{ts}</i> , UAS-H2B::RFP/TM2;	EBs	No
<i>Tub-Gal80^{ts} /Cyo</i> ; <i>Dl-Gal4</i> , UAS-CD8::GFP, UAS-H2B::RFP/TM2;	ISCs	No

* excluding few neurons and testis.

PART 2 - Global monitoring unveils unexpected dynamics of midgut turnover during homeostasis

Replenishment dynamics by global monitoring indicate a slow and non-homogenous turnover

The *esg*-ReDDM stock described in part 1 was used to monitor globally tissue replenishment over time on standard fly food in non-challenged conditions. Briefly, adult flies developed at the non-permissive temperature (18°C) were collected and shifted to the permissive temperature (30°C) to start tracing tissue turnover. Flies midguts were dissected at different time point and analyzed by automated counting of confocal images. Newly replenished areas could be identified by meaning of H2B::RFP trace and DAPI staining (fig. 2.1 D). Percentage of replenished enterocytes was calculated in each posterior midgut (pmg) as percentage of new ECs over total ECs. As described in the part 1 of the results, the *esg*-ReDDM tracing allows the identification of undifferentiated cells, and their lineage in a time window: stem cells and precursor cells (ISCs/EBs) are identified by double labeling (membrane GFP and nuclear RFP), new enterocytes (ECs) incorporated in the epithelium after temperature shift by persistence of nuclear RFP trace and the old ones by DAPI (fig. 1.8 and 2.1A-C).

Studies based on clonal analysis have assumed that adult midgut stem cells are equivalent in division potential and that midgut epithelium is turned over at a constant and homogeneous rate. These assumptions were required to infer the whole tissue turnover rate from the subpopulation of stem cells and their progeny clonally labeled. Calculations of midgut replenishment by clonal analysis (MARCM) indicated that full tissue turnover was occurring weekly since clones were growing linearly until reaching

a plateau around 7 days (Ohlstein and Spradling, 2006). Unexpectedly, we found that tissue replenishment followed a “patchy” (fig. 2.1A) rather than an homogenous pattern, as expected for a continuously turning-over tissue. In addition, distribution, size, and shape of the renewed patches could differ greatly from intestine to intestine of co-developed age-synchronized animals (compare fig 2.1A, 2.2C second panel, fig 2.3C). Globally, quantification of tissue replenishment at different time points indicated that at 7 days midguts are on average replenished less than 20% (n=26), at 14 days about 60% (n=24) and at 21 days about 80% (n=23) (fig. 2.1 A-D). At 21 days about half of the posterior midguts (pmgs) have still less than 75% replenishment and just 21% of them have 100% replenishment (not shown).

Other “global” approaches (Jiang et al., 2009) provided results similar to the *esg*-ReDDM, suggesting that the MARCM analysis provided an over-estimation of stem cell division and tissue turnover due to an intrinsic property of the approach. MARCM labels randomly dividing stem cells upon a heat shock, it hence labels the group of stem cells that was actively dividing at the time of clonal induction. The discrepancy in turnover rate between global and clonal analysis could indicate that (1) the heat shock accelerates tissue turnover; (2) stem cells do not divide at the same rate. We devised specific experiments, described in the following section, to address these possibilities.

Remarkably, high variability among posterior midguts replenishment rates (fig 2.1 D) and between experiments (not shown) indicated that the midgut model system is not strongly stereotyped as developmental phenotypes. Non-controllable stochastic events could account for this variability. Indeed, ECs tissue densities (fig 2.1 E) were not significantly different, however they had a greater variability at 14 and 21 days, indicating that homeostatic equilibrium could be unbalanced stochastically in some

guts. Hence, to study homeostatic tissue turnover in unchallenged conditions, our following analysis were limited to 7 days post temperature shift, unless otherwise specified.

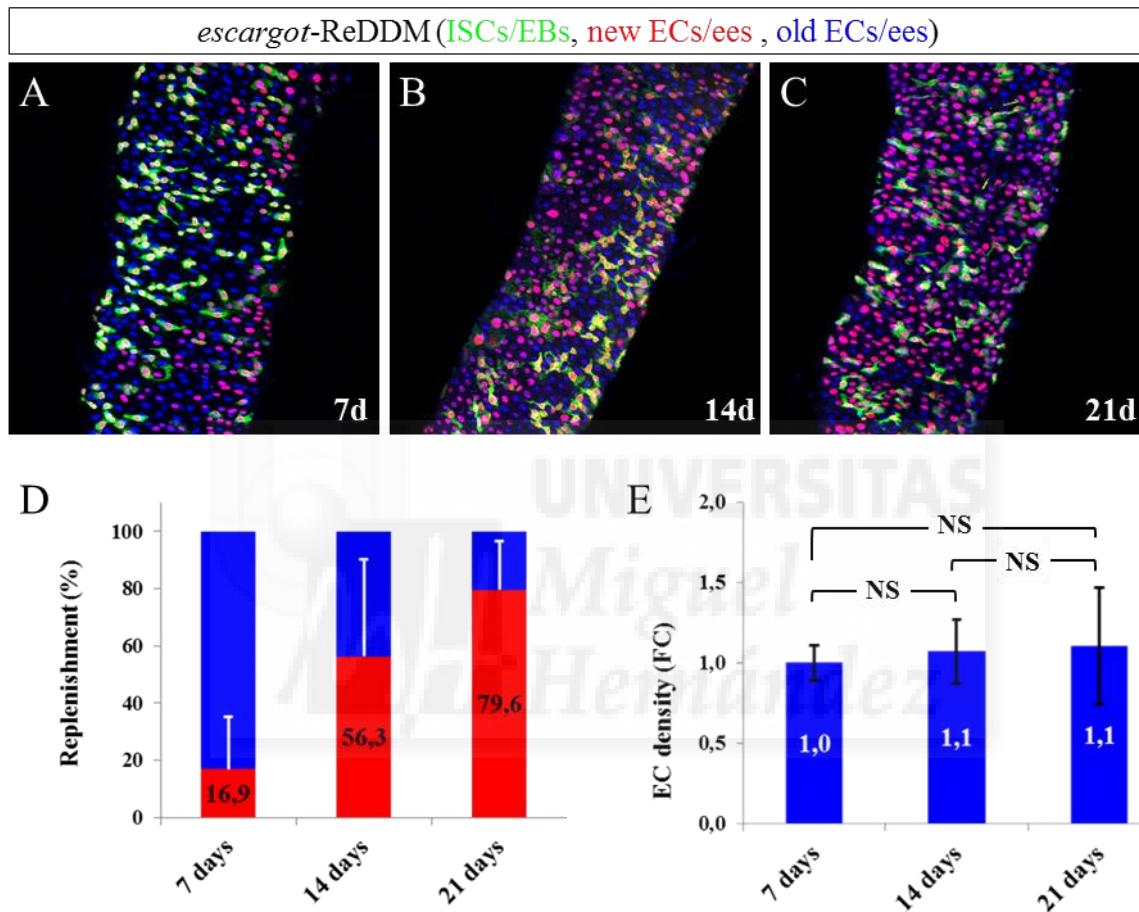


Fig 2.1 - *escargot*-ReDDM allows to follow midgut tissue replenishment over time in a quantitative manner and indicates a slow and “patchy” turnover rate. A-C) Examples of posterior midguts (pmg) at different time points showing progressive tissue replenishment. D) Quantification of tissue replenishment as percentage of new ECs (RFP+, GFP- cells) on total ECs (DAPI) indicates that whole pmg turnover occurs between 2 and 3 weeks. E) Total EC density (expressed as fold change to 7days density) is not significantly changed at 7, 14 or 21days, however standard deviations increase at 14 and 21 days indicating a possible departure from homeostasis for certain guts.

Heat shock induces tissue replenishment

Most used protocols to induce stem cell clones in adult *Drosophila* midgut indicate a 60 minutes heat shock at 37 °C (Lin et al., 2008; Micchelli and Perrimon, 2006; Ohlstein and Spradling, 2006) even for repetitive times (Buchon et al., 2010). This indicates that midguts have a very low tissue proliferation rate and need very long induction time compared to clones induced in epithelial cells of the developing imaginal discs, which have much higher tissue proliferation rate.

To investigate if the prolonged 37 °C heat shock could account for the difference in midgut turnover between clonal and global analysis, we measured tissue replenishment with *esg*-ReDDM with and without 60 minutes heat shock (fig. 2.2 A). We found that the heat shock caused an increase of midgut replenishment at 7 days (fig. 2.2 B, C). Mitosis occurrence was also augmented (fig. 2.2 D), at a similar level of the ones detectable in control clonal analysis experiments (not shown). Importantly, the total EC density was not changed indicating that the heat shock was not inducing strong cell loss, a characteristic of regenerative responses. Indeed the increase in proliferation was just of 2 folds while it can reach about 20 folds increase during bacterial infection (Buchon et al., 2010; Buchon et al., 2009b) or even 100 fold increase by genetically inducing cell death of ECs (Jiang et al., 2009). Since tissue integrity is maintained, replenishment and proliferation induced by heat shock could still be considered within the homeostatic response, but accelerated with respect to flies that did not suffer any 37°C heat shock. Nevertheless, over-estimation of tissue turnover rate (1 week *versus* 2-3 weeks) by clonal approaches could not only be explained by the heat shock since it could not “rescue” the whole difference in tissue replenishment. Heat shock could only

bring the posterior midgut turnover from 15% (fig 2.1 D, fig 2.2 B) to an average of 50% (fig 2.2 B) and not 100%.

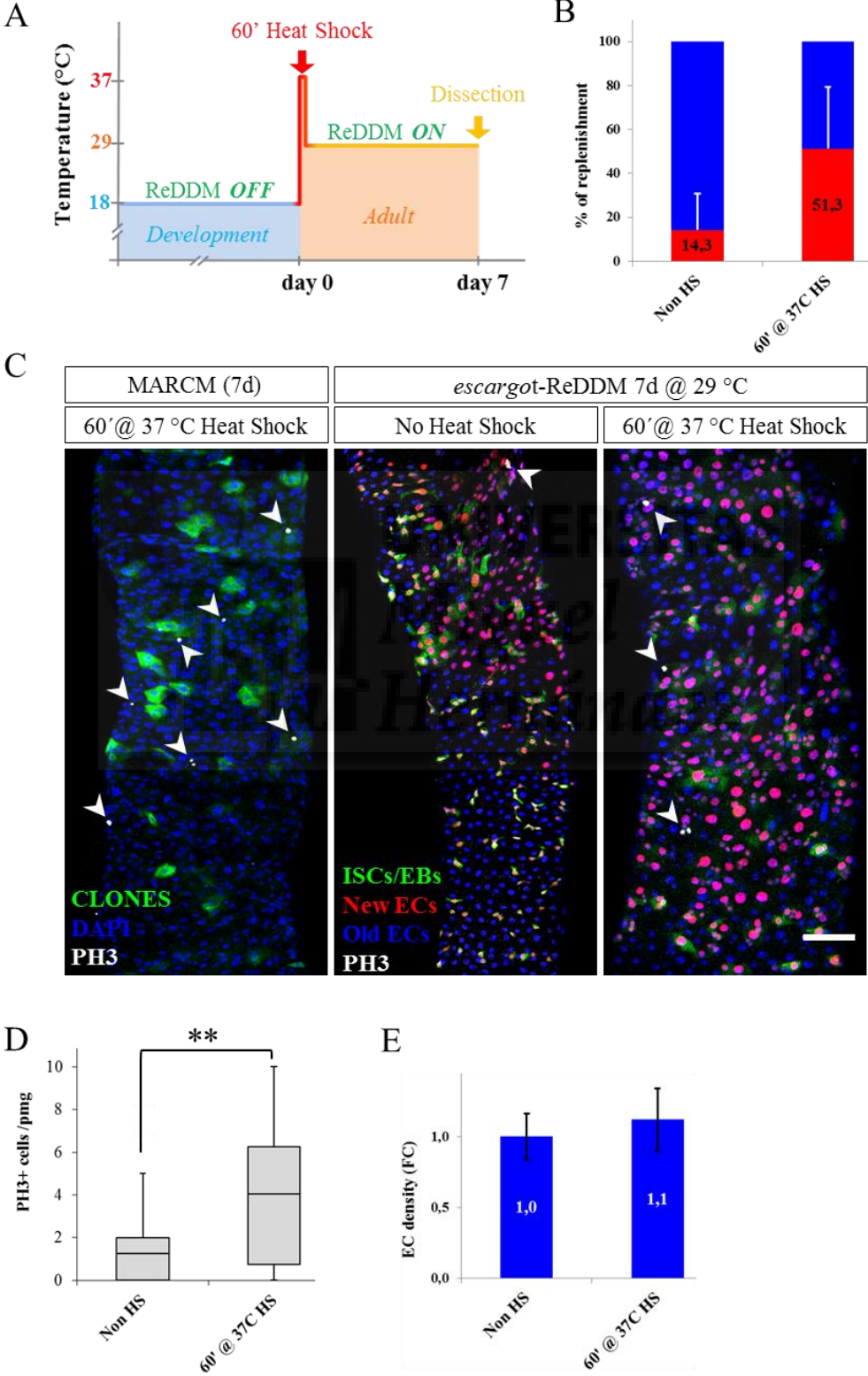


Fig 2.2 – Heat Shock induces tissue replenishment. A) *esg-ReDDM* flies were developed at 18 °C and once eclosed were heat-shocked (HS) or not for 60' at 37°C, as in normal clonal analysis, and then moved to 29 °C to monitor tissue replenishment after 7 days. B) Average ECs turnover (tissue replenishment) at 7 days is quantified as percentage of total ECs; in blue percentage of old ECs, in red of new ones. C) Examples of tissue replenishment of posterior midguts (PMG) after one week in non- and HS conditions in comparison with standard MARCM analysis. In MARCM clones a subset of dividing ISC and their progeny has been labelled by GFP. Non marked ISCs cannot be followed. In *esg-ReDDM*, all ISCs/EBs are double labelled by CD8::GFP and H2B::RFP, new ECs by H2B::RFP persistence, old ones by DAPI staining. Mitotic ISCs are marked by anti-PH3 (white) and indicated by arrowheads. Scale bar = 50µm. D) Heat shock induces a significant increase (p-value < 0,05) of about 2 folds in the number of mitotic cells per posterior midgut (PH3+ cells/pmg shown as box plot with mean and standard deviations). E) The average EC cellular density is unchanged, indicating that tissue structure is preserved upon heat shock

Stem cells proliferation rate correlate with replenishment degree and fluctuates locally

As described in the previous section, rather than uniform and rapid turnover, we observed a global slow turnover rate which occurs non-homogenously following irregular but continuous domains, forming “patches” of new cells (fig 2.1 A, fig 2.2 C second panel and fig 2.3 C). Importantly, we could not recognize any anatomical specificity in the behavior of the tissue since no particular area in the gut showed with consistency to be actively replacing or not. Moreover, there was no specificity at the single animal level, as different organ areas exhibited patterns of replenishment with different shapes and sizes (fig 2.3 C and 2.4 A). These observations suggest that posterior midgut tissue replacement is asynchronous and apparently stochastic, rather than spatially and temporally determined as developmental processes. Given these remarks, it is also conceivable that homeostatic ISCs have different proliferation rate according to local differences in demand. If the case, MARCM approach would give an

over-representation of ISCs which are rapidly dividing because within or close to areas with high turnover rate, resulting in a whole tissue turnover over-estimation. To assess this possibility and test if asynchronous tissue replenishment go along with local differences in ISCs proliferation, were performed (1) a correlative analysis of mitosis and replenishment degree of the whole midgut to confirm that tissue demand increases ISCs proliferation (fig 2.3 A, B); and (2), a spatial distribution analysis of mitosis and replenished areas to assess local differences (fig 2.3 C-F).

Mitotic events resulted to increase exponentially to the replenishment degree in whole midguts from flies of the same age (fig. 2.3 A) indicating that demand and proliferation have an exponential relationship. Indeed, ISCs can tune their proliferation rate accordingly to the demand in non-homeostatic paradigms (Conder and Knoblich, 2009; Lucchetta and Ohlstein, 2012) and undergo symmetric cell division (de Navascues et al., 2012; Knoblich, 2008; O'Brien et al., 2011; Simons and Clevers, 2011b). In addition, the cohort of flies which had similar replenishment degree independently of the age had a similar proliferation rate (fig 2.3 B). To analyze the spatial distribution of mitosis in relationship with replenishment, intestinal epithelium was spatially divided in renewed and not renewed areas. Not renewed areas were further split in proximal and distal areas, respectively the 1-cell-wide ring of old enterocytes surrounding a renewed patch and the remaining area occupied by old enterocytes (fig 2.3 C). Mitotic events were more frequent in replenished areas and their surrounding rather than in non-replenished ones (fig 2.3 D-F), indicating that ISCs proliferation rate fluctuates locally and correlates with replenishment degree. The mitotic events frequency decrease with the distance from the renewed patch, indicating that, as previously described, diffusing signals control ISCs behavior. However, the current

established feedback model (Jiang et al., 2011; Jiang et al., 2009) in which dyeing/damaged ECs signal to ISCs to proliferate, predict that not-yet-renewed areas should have higher mitotic index. On the contrary, replenished areas represent continuous areas of cells newer than their surroundings hence should have a lower proliferation index. The opposite result that we found suggests a replenishment mechanism in which stem cells divide prior to tissue replenishment. Observing the distribution of undifferentiated cells (fig. 2.3 C, second panel) is patent that not-yet-renewed areas present a much higher number of *escargot* positive cells than renewed patches. The higher mitotic index in newly renewed areas could be explained by the need of regenerating the pool of progenitors. This new hypothesis and its implications will be object of specific investigations, which results are shown in the following part 3 and 4.

In summary, these analyses confirmed our hypothesis, born from the “patchy” replenishment pattern, that ISCs proliferation and tissue replenishment are asynchronous between different areas: both are linked but follow flexible and likely unpredictable domains. Finally, the local fluctuation of stem cells proliferation rate provided a further explanation of the discrepancy of tissue turnover calculated by clonal analysis (MARCM) and global tracing (*escargot*-ReDDM or *escargot*-FLP-OUT). Tissue turnover rate calculated by MARCM was an overestimation due not only to the stress induced by the heat shock but also to the over-representation of clones born in areas actively replenishing.

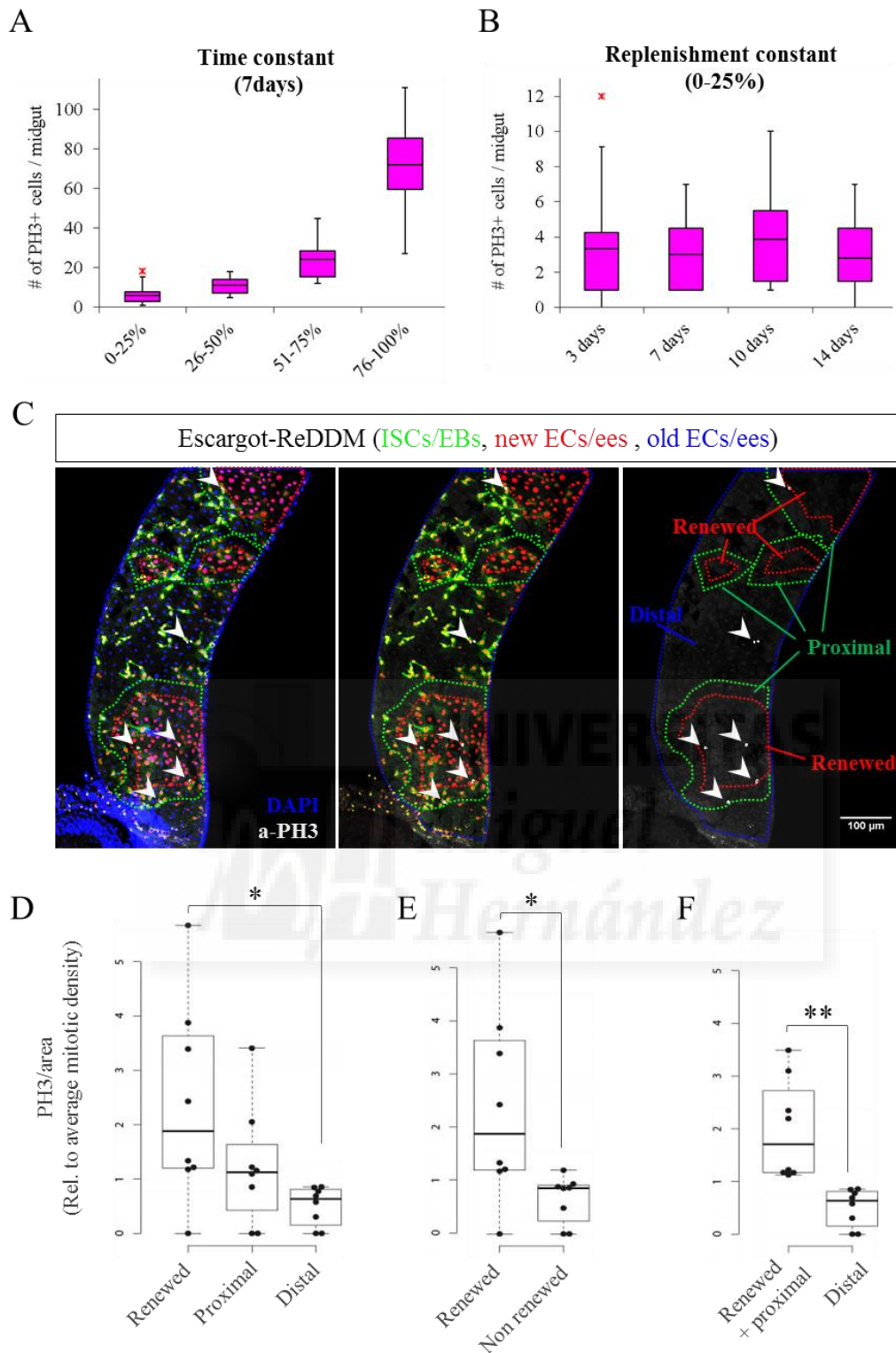


Fig 2.3 – Stem cells proliferation rate correlate with replenishment degree and fluctuates locally.

A) Box plots representing the number of mitotic events (PH3+ cells) per midgut (absolute numbers, y-axis) in *esg*-ReDDM flies of the same age and time after temperature shift to 30 °C (7 days) grouped by similar replenishment degree (percentage, x-axis). B) Box plots showing the number of mitotic events (PH3+ cells) per midgut (absolute numbers, y-axis) in *esg*-ReDDM flies of the same replenishment

degree but of different time after temperature shift to 30 °C (3-7-10-14 days, x-axis). C) Example of the analysis of the spatial distribution of mitosis in relationship with replenishment monitored by Esg-ReDDM as described earlier (all ISCs/EBs are double labelled by CD8::GFP and H2B::RFP, new ECs by H2B::RFP persistence, old ones by DAPI staining, here in blue): arrows indicate mitotic events (anti-PH3 in white), dashed lines delimit the different areas. Scale bar = 100µm. D-F) box/dot plots representing mitotic events per area normalized for the average mitotic density of the considered intestine (mitotic density = tot mitotic events/area). Each dot is an independent midgut. D) Comparison of renewed, proximal and distal areas. E) Comparison of renewed and non-renewed areas. F) Comparison of renewed and proximal with distal area.

Jak/Stat pathway is locally activated to initiate replenishment

Cytokine/Jak/Stat signaling mediates regeneration and homeostasis in the *Drosophila* midgut coordinating ISCs proliferation and EBs differentiation (Beebe et al., 2010; Jiang et al., 2009; Lin et al., 2010; Liu et al., 2010). The canonical JAK/STAT signaling cascade in *Drosophila* comprises the extracellular diffusible ligands Unpaired (Upd), Upd2, and Upd3, a transmembrane receptor named Domeless (Dome), a single Janus tyrosine kinase called Hopscotch (Hop), and the Stat92E transcription factor. Enterocytes that are subjected to apoptosis, enteric infection, or JNK-mediated stress signaling produce JAK/STAT ligands that promote ISCs rapid division. UPD/JAK/STAT activity also promotes and is required for progenitors cell differentiation (Jiang et al., 2009). Paracrine Unpaired signaling from underlying musculature has also been described to control self-renewal and lineage differentiation of *Drosophila* intestinal stem cells (Lin et al., 2010; Osman et al., 2012). Importantly, loss of JAK/STAT signaling by depleting the UPD receptor, Dome, results in atrophic intestines with reduced enterocytes number but does not influence ISCs basal divisions (Jiang et al., 2009) indicating that JAK/STAT signaling has a primary role in progenitors differentiation, although high levels of cytokines are sufficient for inducing ISCs proliferation. Indeed, monitoring tissue replenishment by *esg*-ReDDM in a Dome

loss of function condition by RNAi, we found that tissue replenishment was totally blocked but ISCs could keep proliferating, resulting in undifferentiated tumors (not shown).

To further explore our finding that tissue replenishment occurs following local cues rather than homogenous and continuous signals we analyzed the pattern of activation of JAK/STAT signaling in relationship with tissue replenishment using a JAK/STAT sensor combined with the tracing system of the ReDDM approach (fig 2.4). JAK/STAT activity was detected in all *escargot* expressing cells indicating, as expected from previous work, that all ISCs and EBs receive signals to activate the pathway before integrating into the epithelium (fig 2.3 A-C). Importantly, once *escargot* expressing cells terminally differentiate to generate a new ECs integrated in the epithelium (only nuclear RFP mark), the JAK/STAT activity drops as clearly visible comparing in fig 2.3 panel C-C', F-F' and H-H'. Notice that in this genetic and experimental set-up, new ECs could be univocally distinguished only by DLG-1 staining and perdurance of the H2B::RFP signal since the GFP expression was not dependent on the *escargot* promoter but on the presence of JAK/STAT signaling.

We found that the sensor activity could differ greatly within the same posterior midgut from area to area (fig 2.4 A). Replenishing areas, identified by the presence of new ECs, presented in their surroundings *escargot* positive cells with stronger reporter signal compared to areas that were not (fig 2.4, compare panel B and C). The quantification of JAK/STAT activity by measuring the intensity of the GFP reporter (see methods) indicated about a 2 folds increase (fig 2.4 D). Cells with strongly activated JAK/STAT signaling presented enlarged polyploid nucleus and wide-ranging protrusions (fig 2.4 H, H'), as expected for maturing EBs.

Altogether, these analyses indicated that JAK/STAT signaling is locally activated to initiate tissue replenishment, in agreement with our finding that homeostasis follow flexible and adaptive mechanisms.

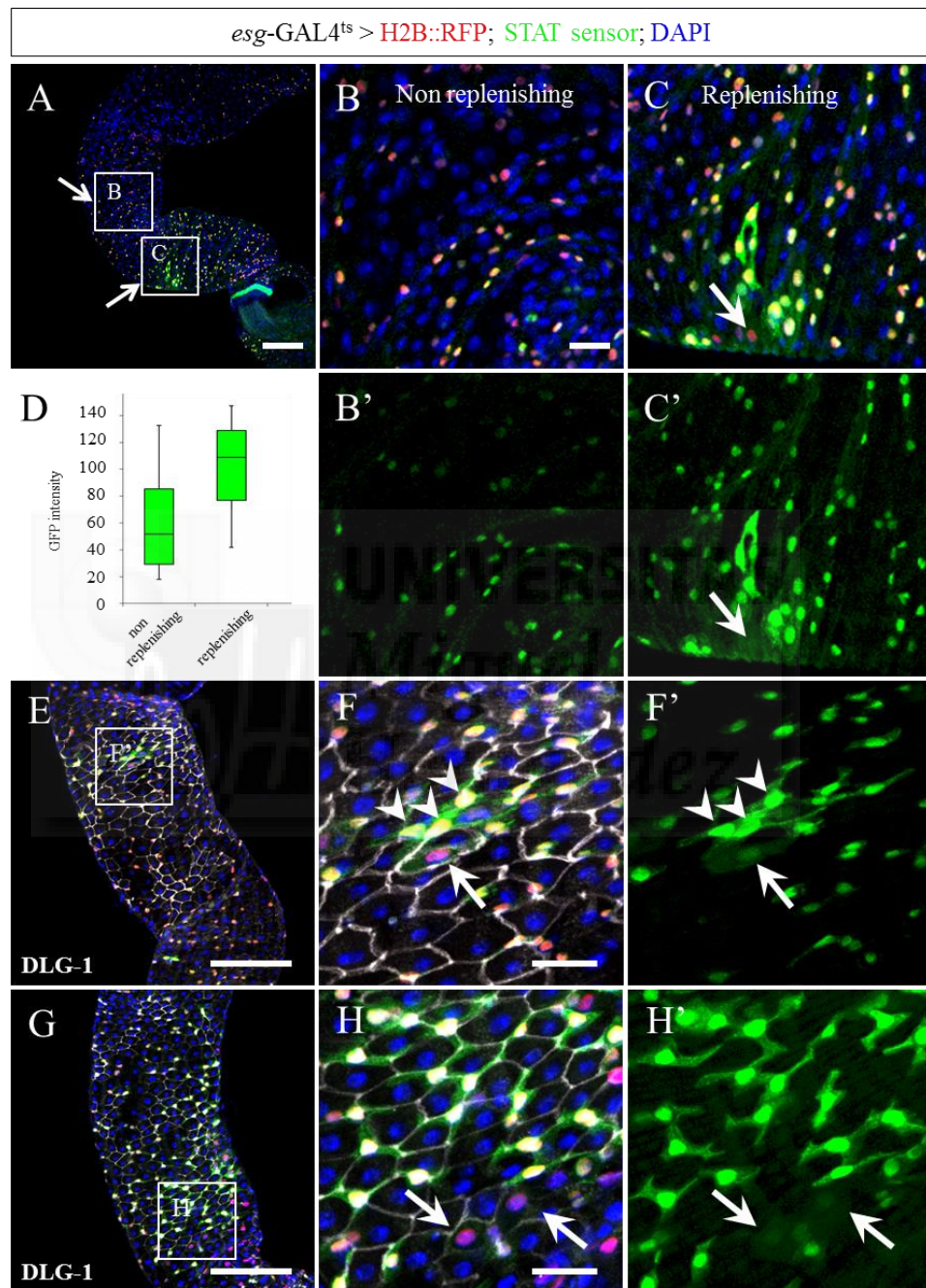


Fig 2.4. Jak/Stat signaling is basally active in all ISC/EBs and is locally increased to initiate replenishment. A, E, G) panoramics of a 7 days posterior midgut (pmg). All *esg*⁺ cells (cells with red nucleus, diploid or polyploidy but not integrated in the epithelium, arrow-heads) are GFP⁺ indicating

STAT signaling, however some present stronger activation of the reporter. Scale bar = 100 μ m. B, C) insets within the same pmg shown in A representing two areas with different levels of JAK/STAT sensor activation. New enterocytes (ECs) present the H2B::RFP trace allowing the identification of replenishing areas. Scale bar = 20 μ m. D) Box-plot showing reporter intensity quantification in *esg*⁺ cells proximal to replenishing and non-replenishing areas. E-H) New ECs are univocally identified by DLG-1 immunostaining (in white) and are negative for STAT activity (C', F' and H', arrows). Cells with strongly activated JAK/STAT signaling presented enlarged polyploid nucleus and wide-ranging protrusions (H, H'), as expected for maturing progenitors (EBs). E, G scale bar = 100 μ m; F, H scale bar = 20 μ m).

Progenitors have plastic differentiation behavior in space and time

To further investigate at which level ISCs/EBs and replenishment have plastic behavior and in particular how stem cells control their domains of replenishment choosing which cells to replace, we compared the behavior of several ISCs simultaneously marking them by clonal means, but univocally. We therefore combined the multicolor Flybow 2.0 cassette (fig 3.1 A) (Hadjieconomou et al., 2011) with the classical MARCM method to differentially label dividing stem cells and their lineages (Fig. 3.1). In this set of experiments, midguts were analyzed 14 days after clone induction (ACI, $n = 15$) to have extensive replenishment (at least 50% in most midguts). FlyBow-MARCM clones ($n > 100$ clones scored) displayed variations in shapes and sizes further highlighting that intestinal replenishment follows highly plastic patterns (Fig. 3.1 B) and not homogeneous renewal (results part 2). In the majority of clones, there was continuity between the labelled cells (Fig. 3.1 B) in agreement with previous work using monochrome MARCM clones (Ohlstein and Spradling, 2006) and consistent with individual ISCs renewing a local domain. However, FlyBow-MARCM also revealed intermingling of cells from two neighbor lineages (arrows in Fig. 3.1 B-D) and fragmentation of some clones that indicated ISCs's progeny mixing. Thus, ISCs and EBs are responsible to

replenish flexible domains of tissue and, to some degree, midgut homeostasis might involve their migration (Fig. 3.1 G).

FlyBow MARCM method is based on membrane tethered fluorescent reporters that put in evidence that EBs can grow quite large protrusion and have distinctive front-back cell polarity as shown previously in this thesis by *esg*-ReDDM (previous *esg*-ReDDM figures and fig. 3.1 E, F). However, EBs invariably adopt a more regular hexagonal shape as they terminally differentiate and become residents in the existing epithelium (fig 3.1 E). A nearest-neighbor analysis pointed out that the shape change characteristic of terminal EB differentiation was coincided with the onset of a local demand and not to the EB birth time (fig 3.1 E, F). To understand this result it is necessary to consider that at the time of clonal induction there is an equal probability that the mitotic recombination will result in a labeled ISC or EB, which will result over time in a multi-cellular clone or a single-cell clone, respectively, which will have always the same “age” after clonal induction. The midguts in this set of experiments were analyzed two-weeks after clone induction but we unexpectedly could observe, together with multicellular clones constituted of differentiated and undifferentiated cells, single cell clones not yet integrated in the epithelium and retaining still undifferentiated features, such as long protrusion (Fig. 3.1 F). Multi-cellular clones with differentiated cells imply that EBs born after clone induction had already differentiated whereas, other single-cell clones within the same midgut, which were born at the same time of clonal induction, retained undifferentiated state for up to 14 days.

In summary, the Flybow-MARCM analyses further supported our perspective in which tissue replenishment follow local rules and indicated that EBs can retain undifferentiated state for long periods of time. This analysis showed that tissue turnover

PART 3 – A delayed progenitors differentiation strategy mediates adaptive responses to homeostatic demand

Our previous results based on the analysis of tissue homeostasis by *esg*-ReDDM indicate that progenitors (EBs) are generated ahead of demand and are characterized by a flexible differentiation capacity both in space and time (fig 3.1 and results in part1). These observations question the current model for intestinal homeostasis in which the ISCs are the main players in tissue homeostasis. ISCs can sense ECs loss (Jiang et al., 2009) and EBs maturation (Choi et al., 2011) to adjust perfectly their proliferation rate, however much less is known on the role of progenitors during homeostasis.

Progenitors have mesenchymal traits

We observed that progenitor cells (EBs) are present as a pool in the *Drosophila* midgut and hold undifferentiated to replenish the tissue where and when needed. To achieve such cellular behavior would be required mechanisms (1) to sense cell by cell the neighborhood to substitute the appropriate cell (2) to retain undifferentiated state until terminal differentiation is needed.

escargot (*esg*), which labels all undifferentiated cells (ISCs and EBs) of *Drosophila* midgut (fig. 3.1 A and results in part 1), encodes a zinc finger motif found in *snail*-related genes (Whiteley et al., 1992). As previously mentioned, *escargot* is the ancestor gene of the *snail* gene family (Barrallo-Gimeno and Nieto, 2009; Boulay et al., 1987; Manzanares et al., 2001; Nieto, 2002). We thought that the molecular mechanisms controlling the flexible cellular behavior of EBs could be related to the mesenchymal to epithelial transition (MET), the reverse counterpart of the more studied

epithelial to mesenchymal transition (EMT), in which the *snail* family genes have a prominent role. EMT and MET events occur during embryonic development, tissue construction, and physio-pathological conditions such as wound healing and cancer (Barrallo-Gimeno and Nieto, 2005; Nieto, 2009). Indeed, pluripotent stem cells are involved in all of these processes, including cancer. In addition, stemness and mesenchymal traits have been directly linked, although just *in-vitro* (Mani et al., 2008; Scheel and Weinberg, 2012).

Labeling stem cells (ISCs) and progenitor cells (also named enteroblasts, EBs) with membrane targeted GFP (*esg-Gal4>UAS-CD8::GFP* or *esg-ReDDM*) we noticed a peculiar mesenchymal-like cellular morphology, in particular in progenitor cells (fig 3.1 A, C). The CD8 fusion reporter proteins allow visualization of structures with high surface/area ratio, like axons or dendrites (Lee and Luo, 1999) otherwise not noticeable with other reporters. We found that EBs, identified as large *escargot* positive (fig 3.1 B, B') or *Su(H)-lacZ* positive cells (fig 3.1 C, C'), persist undifferentiated in non-regenerated areas and send long explorative protrusions along enterocytes borders (fig 3.1 B', arrow), outlined by DLG-1 staining. ISCs instead have a round morphology without strong signs of polarity (fig 3.1 C) although they could present lamellopods-like structures (fig. 3.1 G). The protruding structures detected in EBs were able to accumulate actin filaments (fig 3.1 E) however, since standard fixed preparation can profoundly alter cellular structures, especially membrane protrusions, we further analyzed un-fixed tissue of flies harboring different protein-fusion reporters. We observed that EBs accumulate moesin around the nucleus and in the protruding extremities, strongly suggesting a migratory behavior (fig. 3.1 G). We found that cellular projections can present tubulin (fig. 3.1 F), suggesting stabilization of the

protrusion. In addition, the presence of growth-cone like structures (fig. 3.1 F) indicated directionality in the formation of protrusions and further suggested cellular motility.

Indeed, the location of ISCs and EBs throughout the midgut is not fully regular, leaving small areas free of progenitors (fig 3.1 A, B) that therefore might need to move in the process of replenishing those areas. We proved cellular displacement among the *escargot* population by time lapse microscopy on whole gut explants (CD, suppl. video 1). Displacing cells present the typical fibroblastic movements: extension of a leading edge, cell body displacement and trailer process retraction (CD, suppl. video 2). Although specific drivers to label ISCs or EBs in a reliable manner were and are still lacking, we identified the moving cells as EBs by nuclear size and GFP signal intensity, which is much higher than in ISCs (fig. 3.1 C). In addition GFP signal in ISCs was almost undetectable in this live-video set-up due to the strong auto-fluorescence of the preparation. We therefore concluded, also considering ex-vivo preparations, that the imaged cells were EBs, but still we cannot not exclude that also ISCs can move.

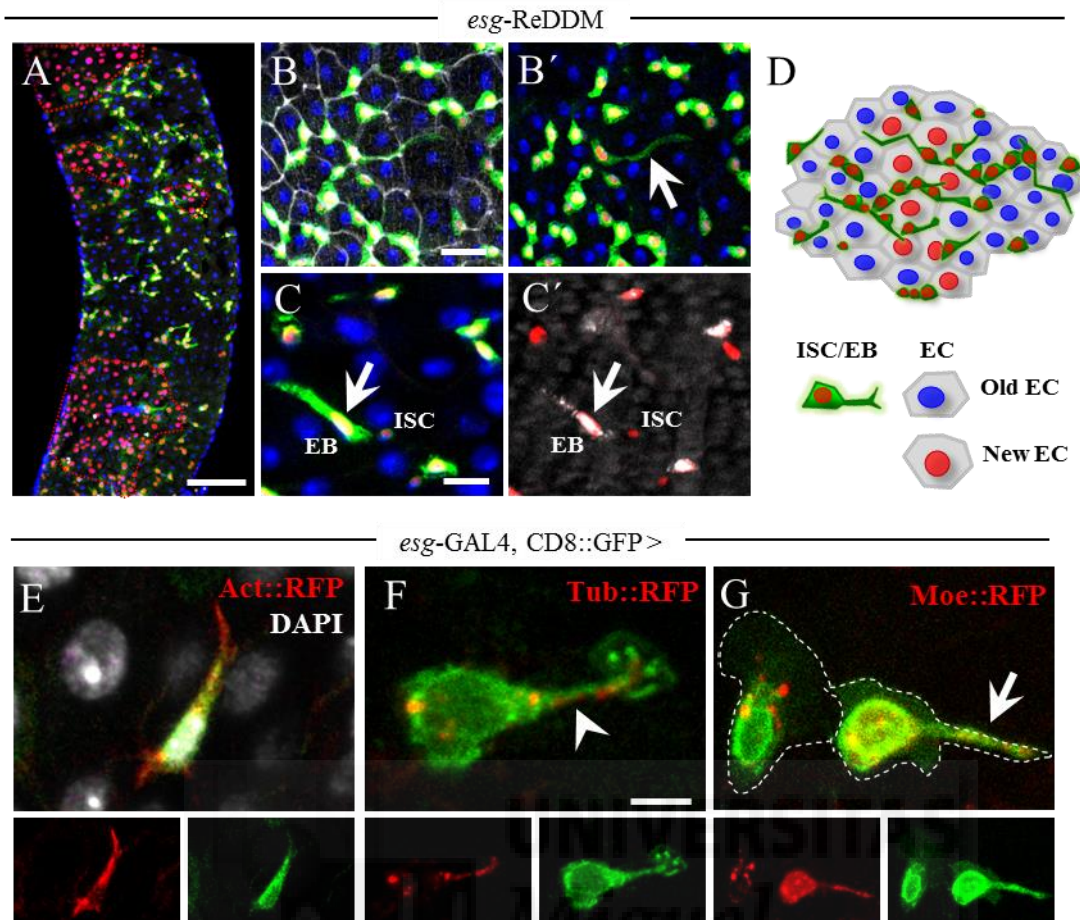


Fig 3.1 – *Drosophila* midgut progenitor cells have mesenchymal traits. (A-D) *escargot*-ReDDM analysis of midgut tissue replenishment at 7 days indicate that enterocytes (ECs) turnover occurs locally. A) *esg*-ReDDM 7 days traced midgut. Dashed red line outline discrete patches of new ECs. Scale bar = 100 μ m. B, B') Large *escargot* cells persist undifferentiated in non-regenerated areas and send long explorative protrusions along ECs borders (arrow), outlined by DLG-1 staining. Scale bar = 40 μ m. C, C') Explorative *escargot* positive cells colocalize with *Su(H)*-lacZ marker indicating that they are enteroblasts (EBs). Scale bar = 20 μ m. D) Cartoon representing replenishment monitored by *esg*-ReDDM. Intestinal stem cells (ISCs) are double labelled, new ECs have red nucleus and old ECs are marked by DAPI. E-G) *escargot* positive cells in fixed and non-fixed preparations expressing different cellular reporter together with the membrane-tethered GFP (*CD8::GFP*). Scale bar = 5 μ m. E) *escargot* expressing cells have actin rich protrusion (arrowheads). Fixed preparation. DNA is visualized by DAPI. F) α -tubulin accumulates in protrusion (arrowhead) and in vesicles in the cell body. Growth-cone like structure can be seen at the end of the protrusion. Non-fixed preparation. G) Enteroblasts have moesin accumulation in cellular protrusion (arrowhead) and nucleus while ISCs have moesin in vesicles and present lamellopods. ISCs are identified by small nucleus and basal location. Non-fixed preparation.

***escargot* is required for mesenchymal traits of enteroblasts and sufficient to retain their undifferentiated state**

Motivated by the role of *escargot* in EMT/MET in other contexts (Nieto, 2009, 2011) and the link between EMT and stemness (Mani et al., 2008; Scheel and Weinberg, 2012), we explored the morphology of ISCs and EBs observing in EBs a characteristic mesenchymal phenotype (fig 3.1) and behavior (supplementary videos in the attached CD). We then assessed directly the role of *escargot* gene in these cellular types by gain and loss of function experiments.

Enhancer traps for *escargot* (*esg*-Gal4) are commonly used to mark stem cells (ISCs) and precursor cells (EBs) of the midgut because are strongly and evenly expressed in all ISCs/EBs from anterior midgut to pylorus boundary (fig. 1.5 A-C), however an endogenous function for the this gene in ISCs/EBs was still not explored. At present-day, to label specifically ISCs or EBs, the only cell-type-specific drivers available are the *Delta*-Gal4 and the *Su(H)*-Gal4 (ISC or EB marker respectively) which however presented strong shortcomings. We found that these drivers were not labelling robustly the whole ISC or EB population, possibly because of variations of Delta/NOTCH signaling related to non-homogeneous replenishment along the midgut. In addition these drivers had expression in several other adult tissues (table 1.2) resulting in high lethality when manipulating *escargot*. Therefore, to distinguish *escargot* gene specific functions in ISCs and in EBs using the *escargot*-ReDDM, we reasoned that we could monitor replenishment and proliferation at early or late time points. This would allow to discriminate the role of *escargot* in each cell type. In fact, at the time of the induction of the gain or loss of function by temperature shift (from 18°C to 29°C, see ReDDM method), we invariably found a pool of EBs already present few

hours after temperature shift. These cells were not rapidly differentiating but were taking 2 to 3 weeks to renew, progressively, the whole midgut (fig 2.1). Hence, we concluded that in homeostatic conditions tissue renewal at early time points (3-5 and 7 days) depends directly from an EB pool. Instead, assessing mitosis frequency and the number of *escargot* positive cells with prolonged induction times (2 to 3 weeks) we could draw conclusions on ISCs division and long term maintenance (self-renewal). In addition, MARCM clonal analysis and regenerative paradigms which induce ISCs proliferation, such as injury, allowed discerning direct effects on ISCs proliferation. Other parameters that we considered to determine if we were altering homeostasis were enterocyte density, enterocyte size, organ size (posterior-midgut diameter) and animal survival.

We found that short term (3-5 and 7 days) down-regulation of *escargot* by *esg*-ReDDM leads to increased and altered replenishment pattern (fig. 3.2 A, B). The increased replenishment indicated that *escargot* is required to retain EB undifferentiated. Notably, the new ECs instead been in patches as in controls, they were homogenously distributed (fig. 3.2 A, B). This pointed out that *escargot* is required to control spatially the replenishment pattern, possibly allowing local exploring and movement. Indeed at the cellular level mesenchymal phenotype was lost (fig. 3.2 C, D) providing support to this explanation. EBs presented total disruption of protrusion and capacity to terminal differentiate integrating in the epithelium, as demonstrated by DLG-1 staining (fig. 3.2 C). Nevertheless, new ECs presented smaller size, indicating that *escargot* loss was leading to differentiation ahead of time and further supporting that *escargot* is required to retain undifferentiated state of EBs.

Conversely, gain of function of *escargot* lead to fully penetrant block of tissue replenishment (fig. 3.1 A, B) and appearance of undifferentiated tumors in 40% of flies within 14 days (fig. 3.1 A, inset in the third panel). The tumoral phenotype was not fully penetrant and not homogeneous along the midgut, indicating that appearance of tumors could also be locally determined and not directly driven by *escargot*. In other terms, such phenotype suggested that *escargot* was not promoting ISCs proliferation, although the appearance of tumors, but was sufficient to retain EBs undifferentiated blocking replenishment.

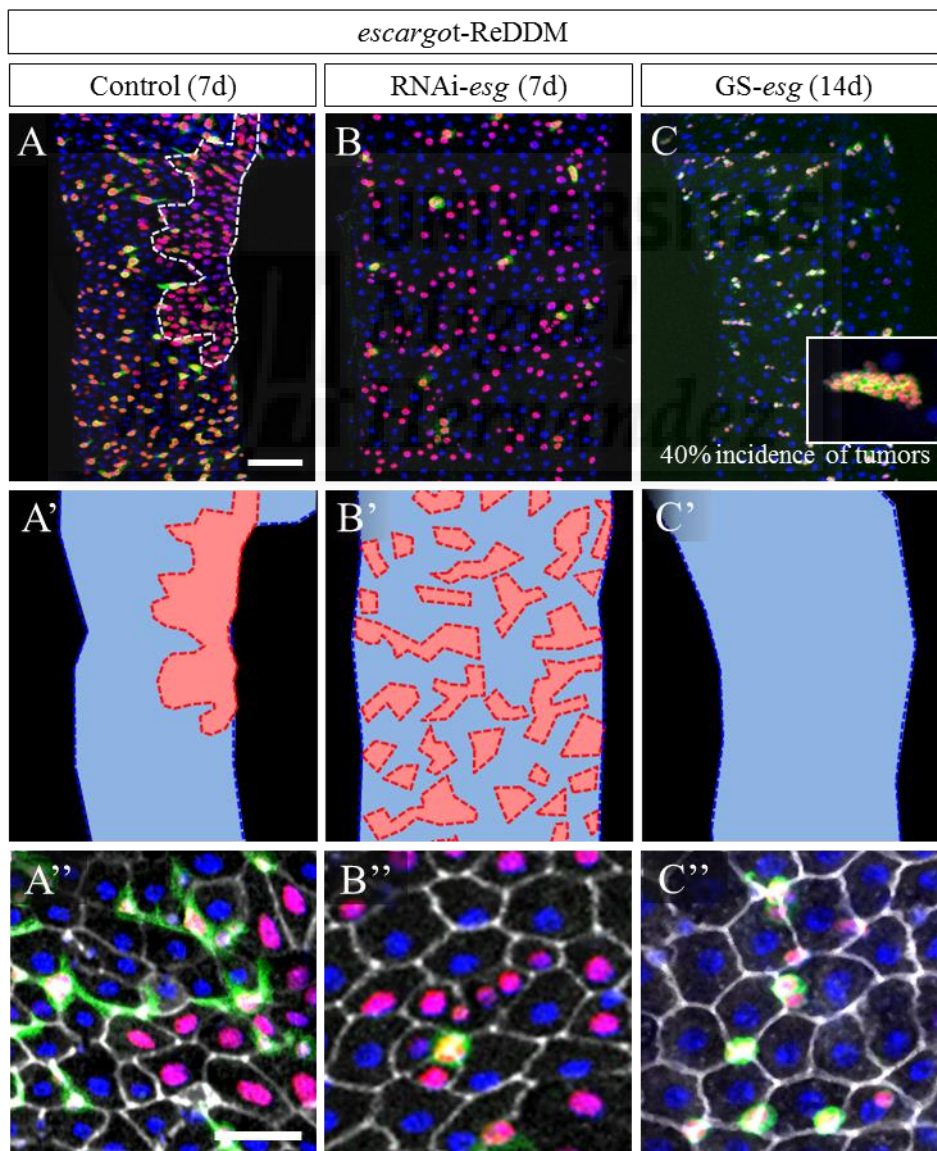


Fig 3.2 – *escargot* (*esg*) is required for mesenchymal traits of EBs and sufficient to retain undifferentiated state. A-C) *esg*-ReDDM analysis of loss (RNAi-*esg*) and gain of function (GS-*esg*) conditions compared to control. Scale bar = 100 μ m. Tissue replenishment in controls occurs by patches (A, dashed red line outline discrete patches of new ECs) while downregulation of *esg* leads to increased and homogeneous replenishment pattern (B). Gain of function of *esg* leads to total block of replenishment even at longer time points (C, 14 days) leading to tumors in 40% of flies (inset in panel C). A'-C') Cartoons representing the outcome of downregulating or increasing *Esg* expression on the replenishment pattern as described in A'-C'. A''- C'') Details of intestines in A-C with DLG-1 staining to highlight terminally differentiated epithelial cells (ECs) and morphology of undifferentiated ISCs/EBs, scale bar = 10 μ m. Loss of *esg* leads to loss of protrusions and integration of EBs which integrate properly in the epithelium, although making smaller ECs (B''). In gain of function of *esg* mesenchymal phenotype is also lost but differentiation cannot occur (C'').

***escargot* is required for stem cells division and long term maintenance**

The results just described clearly indicated that *escargot* is required and sufficient to retain undifferentiated state of progenitors. Surprisingly, although replenishment was enhanced, we noticed that mitotic events were reduced (not shown). In wild type flies, as shown in the part 2 of the results, there is a local increase in proliferation rate upon EB differentiation (fig 2.1C) and ISCs proliferation rate increases exponentially to the replenishment degree in the short term (fig 2.1B). In the loss of *escargot* condition, the observed uncoupling between gain of EB differentiation and ISC proliferation rate was suggesting that *escargot* might be also required for ISCs division, although not sufficient since tumoral phenotype had low expressivity and was not fully penetrant.

To further investigate the role of *escargot* in ISCs we pursued 3 different tactics:
1) we devised an injury protocol in which was expected increased tissue replenishment but also increased stem cells proliferation (fig. 3.3); 2) we investigated the effect of our manipulation at longer time points in which stem cells are expected to have replenished

the EB pool (fig. 3.4); and 3) we performed MARCM clonal analysis in which the genetic manipulation occurs specifically in dividing ISCs allowing to directly assess effects on cell division (fig. 3.5).

For the injury protocol, adult flies of 3-7 days of age developed at non permissive temperature were shifted at 29°C for 3 days to induce transgenes expression. At day 3, half of the flies were gently pinched with tweezers in the abdomen and let recover for 24 hours before dissection (fig. 3.3 A). In damaged control flies, proliferation (fig. 3.3 B) and replenishment (fig. 3.3 C) were induced as expected. In *escargot* loss of function flies, proliferation was not induced upon the damage indicating impaired stem cells divisions (fig 3.3 B). Importantly, upon damage, the integrity of the epithelium was not restored as in controls likely because the EB pool was already differentiated as shown by non-damaged *esg*-RNAi condition and previous figure 3.2 A, B. For the *escargot* gain of function conditions we used two independent lines that gave analogous results, the transgenic UAS-*esg* and the gene-search GS-*esg* line which overexpresses *escargot* from the endogenous locus. In both, replenishment was totally blocked even upon damage indicating that *escargot* is sufficient to retain undifferentiated state not only during homeostasis (fig 3.2 A) but also during regeneration (fig 3.3 C). Importantly, proliferation was still induced although significantly less than in control situation (fig. 3.2 B), showing that *escargot* is not sufficient to induce proliferation, and rather, might not affect or even might reduce damage-induced proliferation.

Sustained *escargot* downregulation over time (14 days) resulted in complete depletion of *escargot* positive cells (fig 3.4 A), indicating that this gene is required not only for stem cells division but also for their maintenance. Accordingly, guts after

passing through initial hypertrophy due to differentiation ahead of time of progenitors, became atrophic (fig 3.4 B) resulting in reduced flies' survival (fig. 3.4 C). Rescue experiments coexpressing the anti-apoptotic protein P35 and TUNEL assays indicated that ISCs were not lost by cell death (not shown) but were likely losing self-renewal capacity and differentiating upon down-regulation of *escargot*.

Finally, clonal analysis further demonstrated the requirement for *escargot* in stem cell proliferation but not its sufficiency. *escargot* loss of function clones by RNAi or using *g66b* and *l2* mutant alleles (Whiteley et al., 1992) showed reduced size and increased proportion of single cell clones. Gain of function clones presented the same number of cells of control clones, indicating similar division capability. Importantly, over-expression of *escargot* leads to undifferentiated clones that do not integrate in the epithelium and that retain mesenchymal features (i.e. protrusion and capacity to disperse).

In summary, the lack of *escargot* caused loss of mesenchymal phenotype of EBs, their premature differentiation, loss of stem cells self-renewal and long term maintenance, altogether resulting in altered homeostasis and impaired regenerative capacity of the intestine.

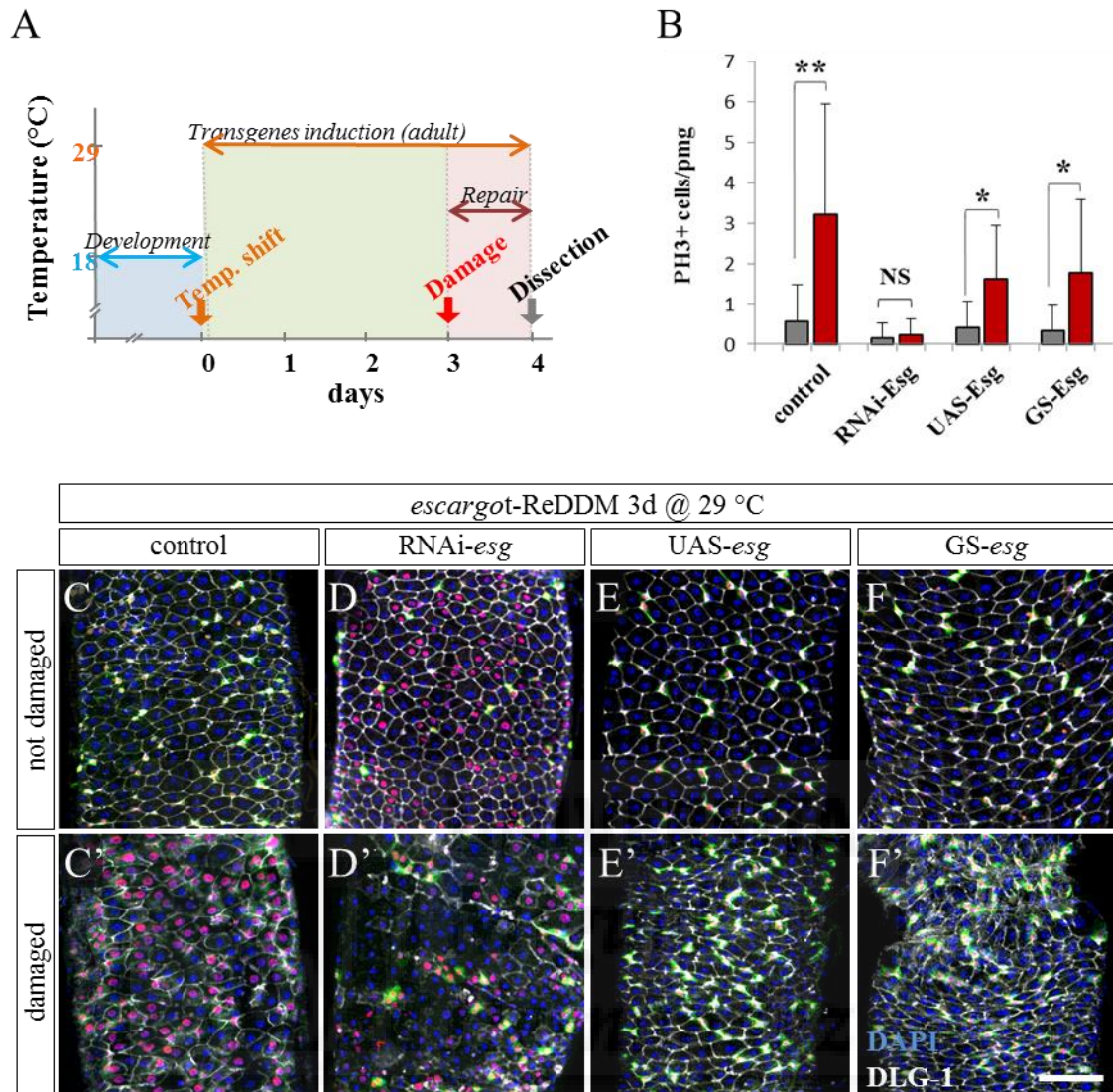


Fig 3.3 – *escargot* is required for ISCs proliferation and is sufficient to retain ISCs/EBs undifferentiated state in regenerative condition. A) Protocol used to induce a regenerative response in midguts. *esg*-ReDDM adult flies of 3-7 days of age developed at non permissive temperature are shifted at 29 °C for 3 days to induce transgenes expression. At day 3, half of the flies are gently pinched with tweezers in the abdomen and let recover for 24 before dissection. B) *escargot* is required for mechanical damage induced ISCs proliferation. PH3+ cells per posterior midgut increase 3 folds in *Esg*-ReDDM wild type flies upon damage. In loss of function condition this induction does not occur. In gain of function condition induction is still possible although reduced. *esg*-ReDDM non-damaged (C-F) and damaged (C'-F') posterior midguts of loss (D-D') and gain of function of *escargot* (E, F, E',F') stained with the epithelial marker DLG-1 (grey) and DAPI (blue). All images have the same magnification, scale bar = 100 μ m. In control flies damage induces replenishment and repair of the epithelium, which is visualized by DLG-1. *esg*-RNAi results in forced replenishment without damage (D) and improper repair upon injury (D'). Gain of expression of *escargot* results instead in total block of replenishment (E, F), also in damaged condition (E', F').

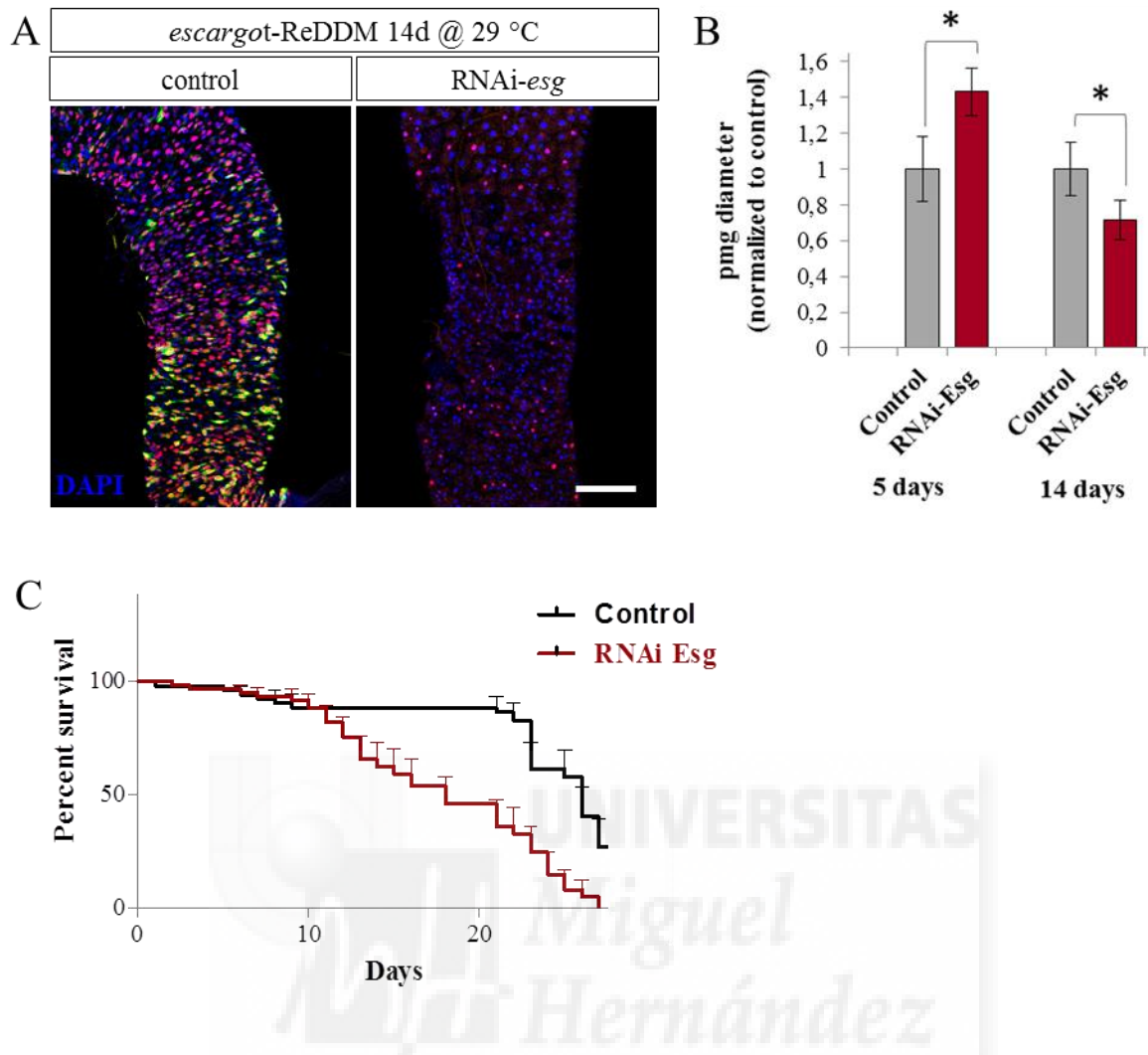


Fig 3.4 – *escargot* is required for stem cells maintenance. A) Panoramics of *esg*-ReDDM controls and RNAi of *escargot* (BL_28514) after 14 days of sustained downregulation. Intestines were completely depleted of *escargot* positive cells, presenting only traced differentiated ECs. Scale bar = 100 μ m. B) Quantification of intestines diameters normalized to controls. Guts after passing through initial hypertrophy due to differentiation ahead of time of progenitors, became atrophic, indicating loss of homeostatic control. C) Quantification of flies survival represented as percentage of survival along time. Log-rank (Mantel-Cox) analysis indicated that *escargot* depletion from stem cells significantly reduced flies' survival ($p < 0.0001$).

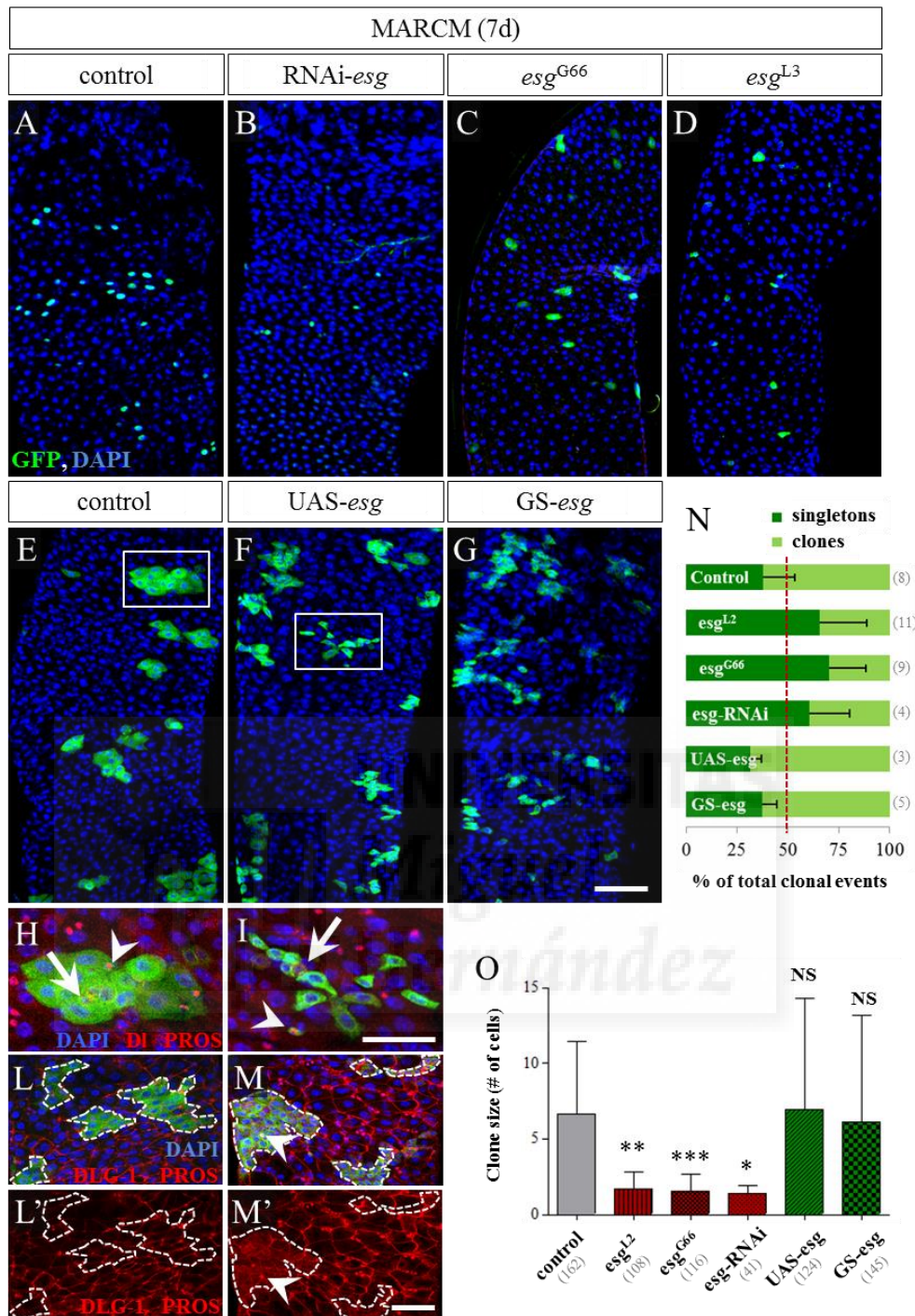


Fig 3.5 – *escargot* is required but not sufficient for ISCs proliferation but required and sufficient to retain undifferentiated state. MARCM clonal analysis of loss and gain of function of *escargot*. A-D) Panoramics of posterior midguts (pmgs) with *Escargot* loss of function clones by RNAi (BL_28514) or by mutant alleles (g66b and l2 allele) showing smaller clones and more singletons than controls. E-G) Pmgs panoramics showing that *esg* GOF clones either by transgene (UAS-*esg*) or overexpression from the endogenous locus (GS-*esg*) presented similar size but were more fragmented than controls. H, I) magnification of control clones (E) and *esg* GOF (F) showing similar size but fragmentation and cells

with undifferentiated characteristics. Arrows indicate stem cells labelled by DI antibody; arrowheads indicate enteroendocrine cells labelled by anti-Prospero. L, M and L', M') magnification of control and *esg* GOF clones stained with the epithelial marker DLG-1 show that *esg* GOF blocks tissue integration, also in clones that are apparently cohesive. N) Quantification of the number of singletons and clones per posterior midgut represented as percentage of total clonal events. Dotted red line indicates the 50% theoretical ratio. 7 days control clones have about 50% or fewer singletons, similarly to *esg* GOF, while *esg* LOF have increased singletons proportion (between parenthesis the number of pmg per condition). O) Quantification of the average size of the total clonal events per genetic condition indicate that *escargot* is required for stem cells division but not sufficient. (between parenthesis the total number of clones per condition). A-G scale bar = 100 μ m. H-M scale bar = 20 μ m.

***mir-8* is expressed in late enteroblasts**

We showed that *Drosophila* midgut tissue homeostasis and regeneration crucially depend on *escargot* expression in stem cells and enteroblasts. *escargot* is required and sufficient in both cell types to retain their undifferentiated state. Its loss makes ISCs to lose long term self-renewal capacity and EBs to prematurely differentiate, altogether resulting in altered tissue homeostasis and regeneration. After recognizing *escargot* as a crucial gene to retain undifferentiated state of ISCs and EBs, and ISC maintenance, we looked for the genetic mechanisms controlling terminal differentiation.

We identified the microRNA miR-8 as a crucial player in midgut homeostasis. *Drosophila* miR-8 is the sole homologue of the human miR-200 family and in *Drosophila* has been related to growth control (Hyun et al., 2009; Jin et al., 2012; Morante et al., 2013) and patterning (Kennell et al., 2008) but in other systems, including human cancer cell lines, has been implicated in suppression of mesenchymal phenotype and metastatic behaviour (Vallejo et al., 2011). In addition miR-8 has been characterized as a regulator of the actin cytoskeleton (Loya et al., 2014) and of cell

adhesion proteins during synapse formation in the *Drosophila* neuromuscular junction, and of planar cell polarity in *Zebrafish* (Flynt and Patton, 2010).

We found that a *mir-8*-Gal4 enhancer trap is expressed in few cells with large nuclei scattered along the midgut (fig. 3.6 A, C). These cells are not localized in any specific midgut domain, however, if present, they are in proximity of each other, in a limited area (fig. 3.6 A, C). *mir-8*-Gal4 cells co-localize with the ISCs/EBs reporter *esg-lacZ* (fig. 3.6 A), indicating that are undifferentiated cells, likely enteroblasts due to their large nucleus. To univocally identify which cell type the *mir-8*-Gal4 was marking, we crossed it with the stem and progenitors cell reporter lines, respectively *Dl-lacZ* and *Su(H)-lacZ*, using the membrane tethered GFP (UAS-CD8::*GFP*) to characterize morphology, or the nuclear GFP (UAS-*NLS*::*GFP*) to highlight ploidy. In addition we co-stained with anti-Delta since *Dl-LacZ* might give non-specific signal in EBs due to transgene perdurance, and with anti-Prospero, the enteroendocrine cells marker. *mir-8*-Gal4 positive cells resulted *Dl-lacZ* and anti-Dl negative (fig 3.6 B-D) and, although not highly polarized, presented protrusion (fig 3.6 B, B'). Their large nucleus, suggesting polyploidy (fig. 3.6 C, C') and the co-staining for the progenitors marker *Su(H)-lacZ* (fig 3.6 E, E') strongly indicated that *mir-8*-Gal4 positive cells were enteroblasts.

Importantly, not all *mir-8* positive cells were marked by *Su(H)-LacZ* nor not all *Su(H)-LacZ* cells were labelled by *mir-8*, suggesting that *mir-8* could mark a temporal or maturation stage of EBs. We therefore proceeded in a detailed cellular characterization and noticed that *mir-8*-Gal4 cells maintain basal location but can have an apical accumulation of DLG-1 protein which however had not the typical apico-lateral distribution of enterocytes (ECs) (fig. 3.7 A, B and A', B'). In addition, their nuclear size, visualized by DNA staining with DAPI, was larger size than diploid stem

cells marked by *Dl*-Gal4 or progenitors marked by *Su(H)*-Gal4 (fig 3.8 C-F'). Together this observations supported the view that *mir-8*-Gal4 expression occurs in late steps of enteroblasts (EBs) maturation after the onset of Notch dependent asymmetry, when EBs start to endoreplicate. Finally, ECs and enteroendocrine cells (ee) do not have *mir-8* locus active, suggesting that *mir-8* is not expressed once terminal differentiation occurred.

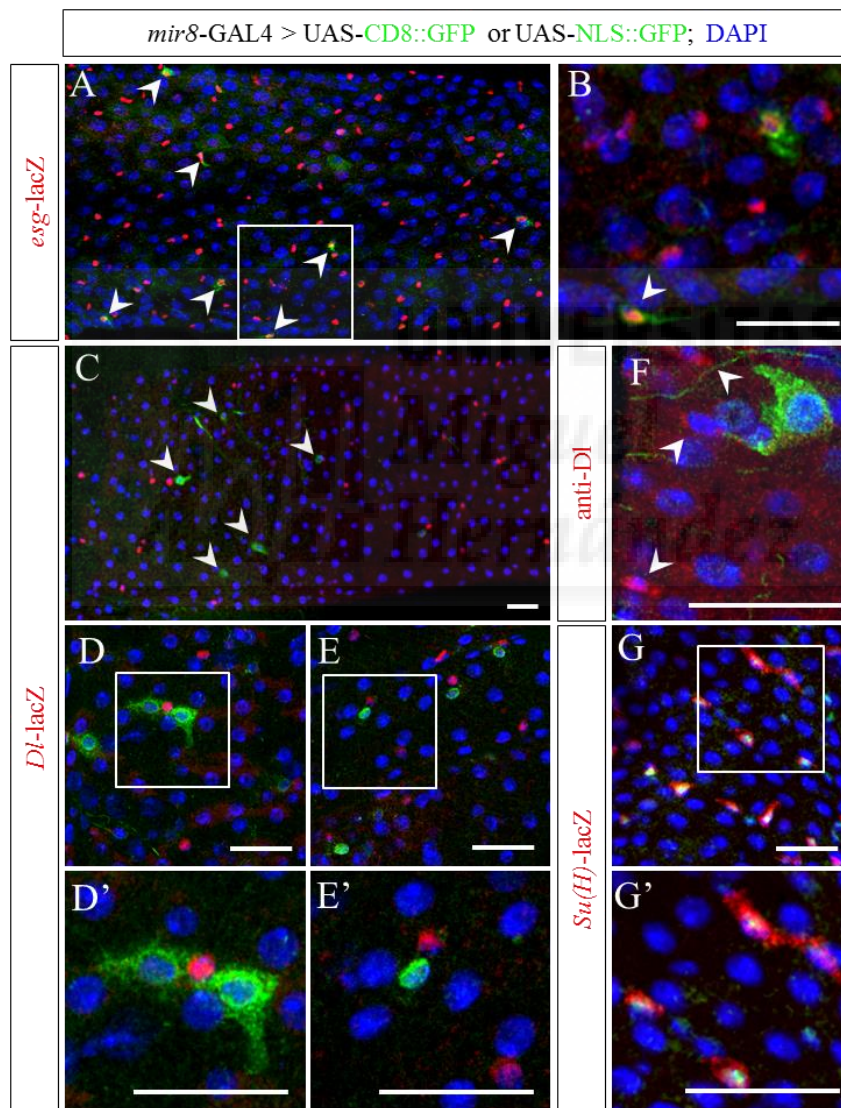


Fig 3.6 – *mir-8* is a marker of progenitor cells. A) Panoramic of a posterior midgut (pmg) showing that *mir-8*-Gal4 cells, visualized by CD8::GFP expression (arrows), co-localize with undifferentiated cells (ISCs and EBs) marked by *esg*-LacZ. B) Magnification of double positive *mir-8*-Gal4/*esg*-LacZ, showing

protrusions and basal location (arrowhead). C-F) *mir-8* positive cells are *Dl*-LacZ and anti-Delta negative. C) Panoramic of a pmg showing that *mir-8*-Gal4 cells visualized by CD8::GFP expression (arrows) do not co-localize with *Dl*-LacZ. D, E and D', E') magnifications highlighting morphology of *mir-8*-Gal4 cells by CD8::GFP (D, D') and nuclear size by NLS::GFP (E, E'), co-stained for *Dl*-LacZ. Note large size and protrusions of miR8 cells. F) Immunostaining for the stem cell marker Delta showing that *mir-8*-Gal4 cells are negative for it. G, G') *mir-8*-Gal4 cells visualized by NLS::GFP co-localize with *Su(H)*-LacZ progenitor cells. The scale bar for all panels is 25 μ m.

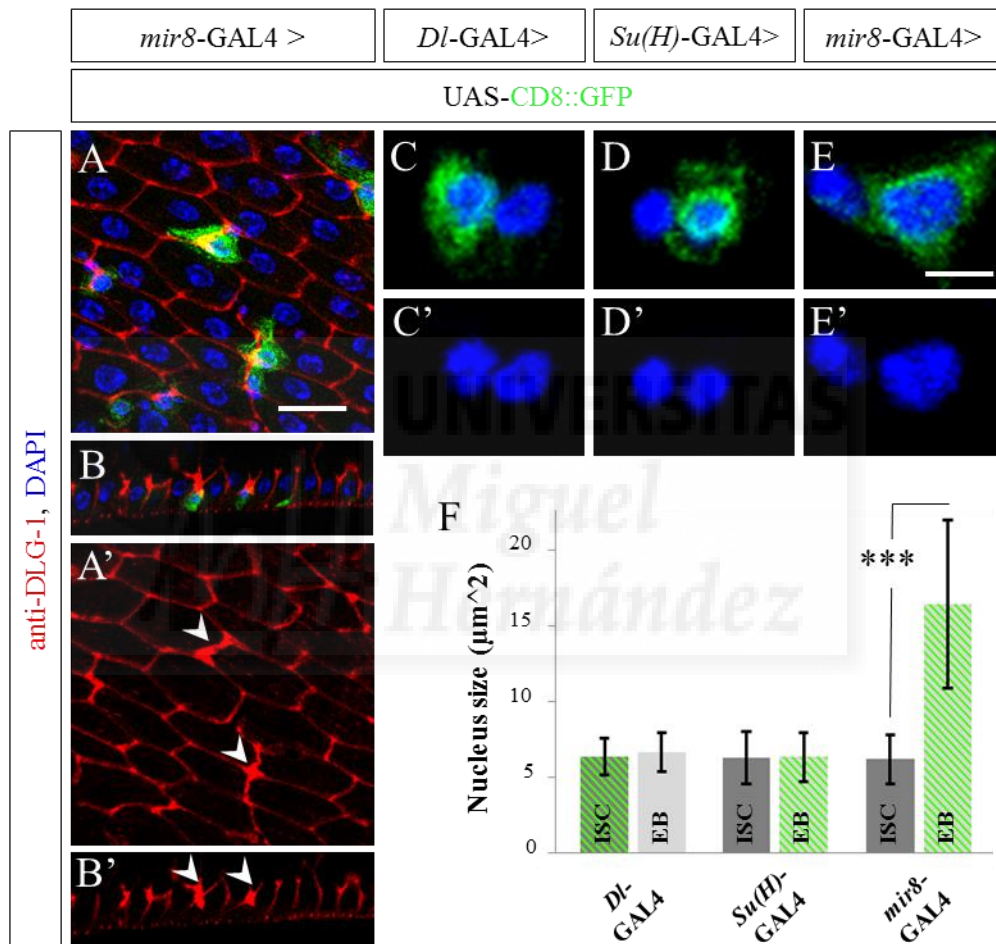


Fig 3.7 – *mir-8* is a marker of late progenitor cells. A, A') Tangential view of the posterior midgut (pmg) epithelium stained with the apico-lateral marker DLG-1. Nuclei are visualized by DAPI staining. *mir-8* positive cells, visualized by CD::GFP expression, localize between enterocytes (ECs) at DLG-1 enriched spots (A', arrowheads). B, B') Transversal view of pmg epithelium showing that *mir-8* cells have nuclei more basally located than ECs and have an apical accumulation of DLG-1 protein and not the typical apico-lateral distribution of epithelial ECs (compare to surrounding ECs), altogether showing that *mir-8* cells are not integrated in the epithelial monolayer. Scale bar = 25 μ m. C-F) Analysis of *mir-8*-Gal4 cells nuclear size in comparison to *Dl* and *Su(H)*-Gal4 lines. Cells are visualized by CD8::GFP expression

(C-E) and nucleus by DAPI (C'-E'). Nuclear size is measured in the marked cell and in its non-labelled sibling (the closest nucleus forming a duplet with the considered cell). *mir-8* cells present nuclei significantly larger than the diploid ISC sibling, while D1 or Su(H) have similar size to their corresponding sisters. Scale bar = 10 μ m

***mir-8* is induced during tissue replenishment**

The cellular characterization of *mir-8* cells identified them as late stage progenitor cells since they present large size, big nucleus but are not fully integrated in the epithelium. We therefore tested functionally if *mir-8* expression was involved in progenitor's maturation and differentiation.

To specifically test whether *mir-8* is involved in progenitor's maturation and differentiation we tested if mechanical damage (fig 3.3 A), which induces tissue replenishment in wild type flies (fig 3.3 C), was able to increase the number of *mir-8* positive cells. We found that the number of *mir-8* cells per posterior midgut was significantly increased in damaged condition compared to undamaged controls (fig. 3.8 A-C). In addition, we noticed that in damaged intestines the cells presented larger size (compare outlined cells in fig 3.8 A' and B') and GFP signal was stronger in intensity (compare GFP signal histogram profiles, fig. 3.8 A'' and B''). A cell-by-cell analysis of size and fluorescence intensity confirmed a significant increase for both measurements (fig. 3.8 D, E). A correlative analysis of average GFP signal intensity and cell size indicated a significant correlation both in control ($P < 0,05$) and damaged conditions ($P < 0,0001$) (fig. 3.8 F). Importantly, these correlations suggested that *mir-8* expression is related to progenitor's maturation, however they did not directly assessed if *mir-8* expressing cell terminally differentiate, integrating in the epithelium. In addition, the increase in number of *mir-8* positive cells could have been related to damage-induced

stem cell proliferation (fig. 3.3 B). To directly tackle this question, we took advantage of the ReDDM method to trace the fate of *mir-8* expressing cells in a regenerative context in which proliferation is not significantly induced. We therefore used a short exposure time to paraquat (4 hours) and observed tissue replenishment (H2B::RFP tracing) and the number of *mir-8* expressing cells (CD8::GFP). Paraquat (1,1'-dimethyl-4,4'-bipyridinium dichloride) is commonly used to generate oxidative stress (Bus and Gibson, 1984). Oxidative damage in response to paraquat exposure has been demonstrated in a wide variety of organisms and in the *Drosophila* midgut (Albrecht et al., 2011; Biteau et al., 2008; Choi et al., 2008a; Choi et al., 2008b; Hochmuth et al., 2011; Myant et al., 2013; Park et al., 2012). Paraquat is generally administered by feeding flies a paraquat/sucrose solution for 24-48 hours. However, in this time course, paraquat is inducing proliferation of ISCs, increasing the number of *escargot*⁺ cells (Biteau et al., 2008; Choi et al., 2008a). Since it has been shown that stem cells do not increase their proliferation in the first 4 hours after bacterial infection (Buchon et al., 2010), we defined a similar short paraquat exposure time to observe the progenitors dependent replenishment without the confounding effects of induced proliferation or excessive tissue loss due to induction of regeneration. In these conditions, we could observe both in control and paraquat-fed flies enterocytes labelled by the H2B::RFP trace. This result indicated that *mir-8* expressing progenitor cells undergo terminal differentiation and stop to express *mir-8* (fig. 3.9 A, A', B, B'). In addition, we detected a significant increase of tissue replenishment indicating that paraquat-mediated oxidative stress was leading to tissue turnover (fig. 3.9 D). Importantly, the number of *mir-8* expressing cells was also significantly increased (fig. 3.9 A'', B'') as indicated by quantification of GFP⁺ cells (fig. 3.9 C). Since the mitotic marker PH3 was not significantly increased (fig 3.9 E), as expected by our experimental design, the increase

in the number of *mir-8* cells could be attributed directly to a relative increase of *mir-8* expressing cells among the progenitors cell population, suggesting that tissue demand induces expression of *mir-8* leading to their terminal differentiation.

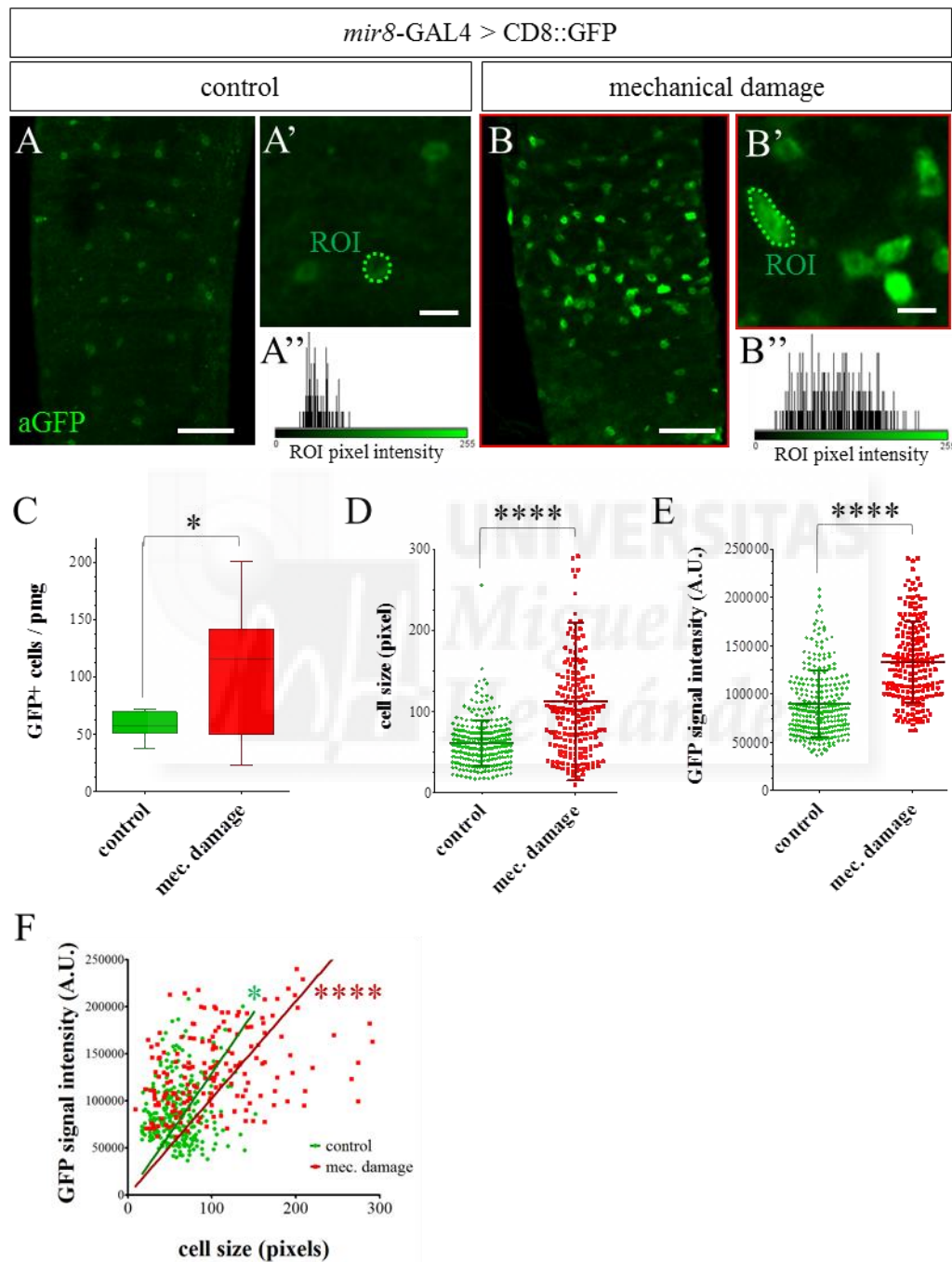


Fig 3.8 – *mir-8* is induced upon epithelial damage and its expression correlate with cell size increase. Analysis of non-damaged (control, in green) and mechanically damaged (mec. damage, in red) posterior midguts (pmg) of *mir-8*-Gal4 flies. A, B) Panoramics of control and mec. damaged pmgs. Cells are

visualized by expression of CD8::GFP and immunostaining for GFP. A', B') Detail showing increased fluorescence and size of *mir-8* cells upon damage. Scale bar = 10 μ m. A'', B'') Histogram profile of GFP signal per pixel from the selected cell in A' and B' respectively, indicating increased GFP signal (intensity per pixel on X axis). C) Quantification of the number of GFP+ cells per pmg show a significant increase in damaged condition. D-F) Cellular analysis of cell size and GFP intensity in control and damaged condition of cells selected as shown in A', B'. Each dot corresponds to a cell. D) Scatter dot plot showing average cell size (in pixels) with population mean and standard deviation. P-value < 0,0001. E) Scatter dot plot showing average pixel GFP signal intensity (mean value per cell, arbitrary units, A.U.) with population mean and standard deviation. P-value < 0,0001. F) Correlative analysis of average GFP signal intensity and cell size indicate significant correlation both in control (P < 0,05) and damaged conditions (P <0,0001). Linear regression analysis show significant linear increase. Best fitting line with (0;0) origin are shown for both population.



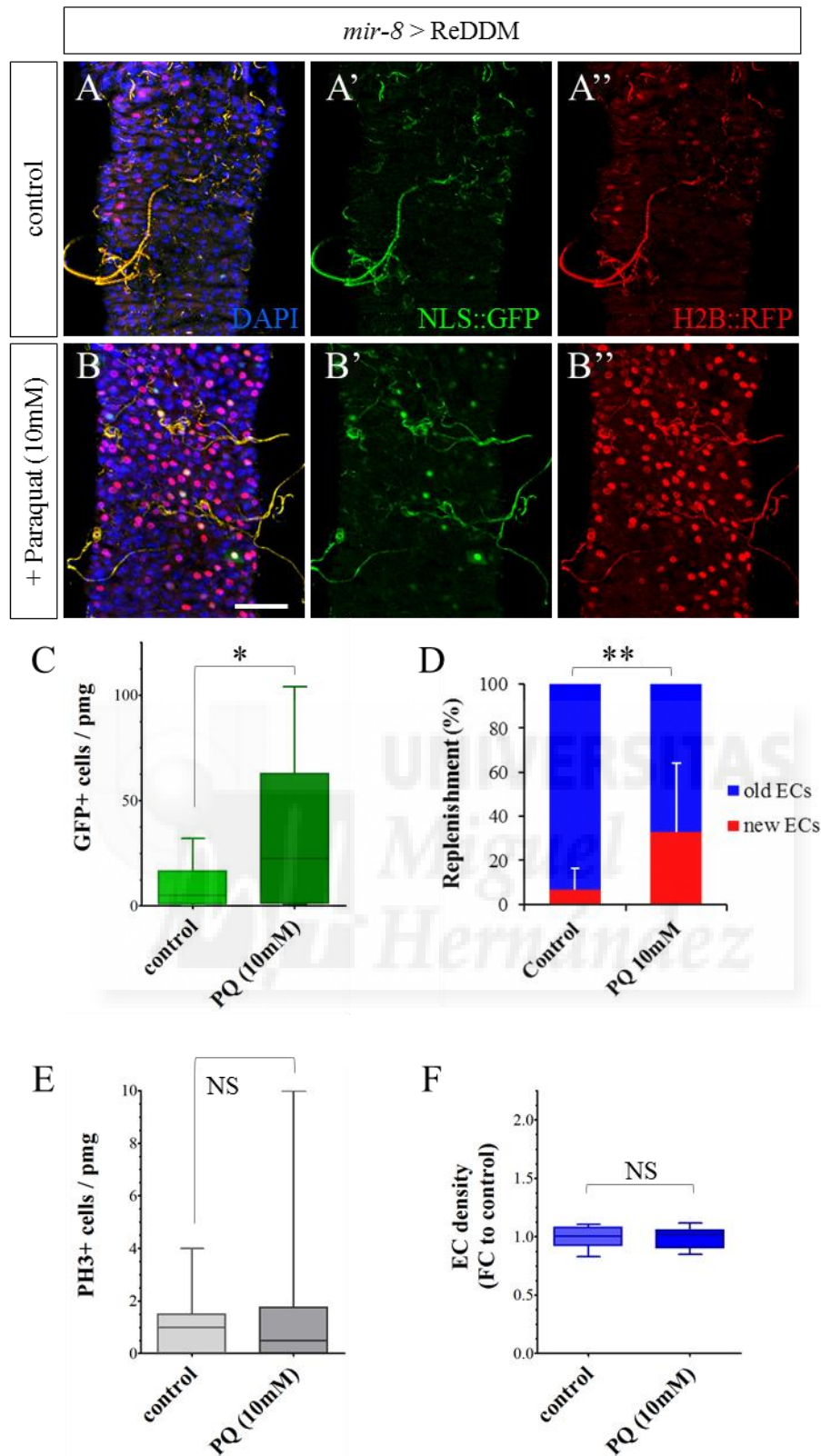


Fig 3.9 – *mir-8* is activated in progenitors cells to replenish the epithelium upon damage. A-F) analysis of sucrose-fed (control) and 10mM paraquat-fed (PQ) posterior midguts (pmg) of *mir-8*-ReDDM flies. A, B) Panoramics of control and PQ pmgs. *mir-8* expressing cells are visualized by *mir-8*-Gal4

expression of NLS::GFP (A', B') while tissue replenishment by H2B::RFP tracing (A'', B''). Scale bar = 50µm. C) Quantification of GFP+ cells indicate a significant increase upon 4h 10mM PQ feeding. D) Stacked bar representing tissue replenishment indicate that PQ induced significant increase in tissue replenishment, shown as mean percentage of H2B::RFP traced cells with standard deviations. E-F) Analysis of the impact of the PQ mediated damage protocol on homeostatic balance. E) Average mitotic cells per pmg (PH3+ cells/pmg). F) Enterocytes (ECs) density fold change to control. E and F together indicate that this protocol neither significantly increases stem cells proliferation nor induces unbalanced tissue loss, therefore remaining in an homeostatic range. Box and whiskers plot show median and data range (from min to max) in fig C, E and F.

Adult *mir-8* mutants have impaired homeostasis and regeneration

Expression pattern of *mir-8*-Gal4 in late-stage progenitor cells and its induction upon damage suggested that *mir-8* might have an important role for homeostatic epithelium integrity through the control of progenitor's differentiation. To test this hypothesis we analyzed *mir-8* mutants and performed miR-8 gain and loss of function experiments.

Adult flies homozygous (d2/d2) or trans-heterozygous mutants (d2/d3) for a *mir-8* locus deletion were viable and had the midgut epithelium apparently normal within 2-3 days upon eclosion (fig. 3.10 A-E) but constituted of significantly smaller enterocytes (fig. 3.10 F), which had also smaller nuclei (fig. 3.10 G) compared to w¹¹¹⁸ and heterozygous controls. The whole posterior midgut size was however not changed (fig 3.10 H) indicating a higher number of epithelial cells, possibly due to a developmental compensation to maintain organ size. The reduction of enterocytes cell size was in agreement with previous data indicating that miR-8 null flies have reduced growth due to higher levels of the conserved insulin pathway inhibitor USH/FOG2, which is his direct target (Hyun et al., 2009). In addition, nuclear size reduction (measured as DAPI area), suggested that in miR-8 mutants enterocytes fail to reach

their normal ploidy, and point to a role for miR-8 in endoreplication. Indeed, parallel work from our laboratory has shown that miR-8 d2/d2 mutant have glia with smaller nuclei and that miR-8 is sufficient to rescue dup/dct1 deficiency (Morante et al., 2013), an essential endoreplication factor (Whittaker et al., 2000). To test whether miR-8 has a role in adult homeostasis we checked 7 days old flies in which normally tissue turnover has already started. At this time point, the epithelium replenishment reaches about 20% on average and epithelium integrity is maintained through perfect balance of cell loss with cell replacement, without picks in proliferation (see results part 2, fig. 2.1 and 2.3). Visualizing the epithelium with the apico-lateral marker DLG-1, we found in miR-8 null flies altered epithelial architecture (fig. 3.10 I-O). Enterocytes presented non-uniform DLG-1 staining, irregular size and shape and also pignotic nuclei, as seen by DAPI. The geometric alteration of cell shape was indicative of cell loss compensated by neighbouring epithelial cells and not by cell replacement, leading to an overall evident loss of tissue density (not quantified). Importantly, miR-8 mutants had strongly augmented proliferation as seen by PH3 marker (fig. 3.10 P) and evident increased in the number of stem cells (seen by Delta staining, not shown). These observation indicated that miR-8 loss of function was not impairing stem cells division, and possibly proliferation increase was due to sustained tissue demand or increased EGF signalling via augmented levels of *spitz* (fig 3.13 and Morante et al., 2013). In either case, this result pointed to impaired tissue replenishment and a role for miR-8 in precursor's differentiation but not in stem cells proliferation, in accordance to the expression pattern described for the *mir-8-Gal4* enhancer trap (fig. 3.6 – 3.7). We further tested *mir-8* mutants for survival upon mechanical damage. Briefly, adult flies were let age for 3 days and then pinched as described for previous experiments and let recover. Their survival was monitored daily for the following 7 days. We detected a significant

reduction in flies survival rate (fig. 3.10 Q), indicating that *mir-8* mutant flies have not only impaired homeostasis but also impaired regenerative capacity.

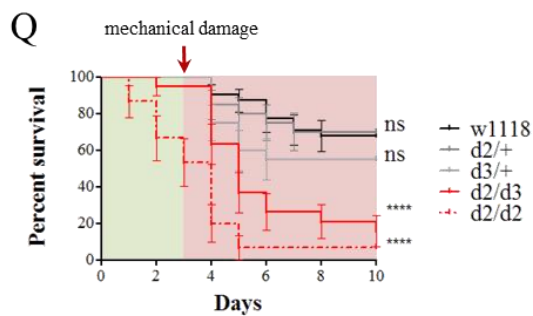
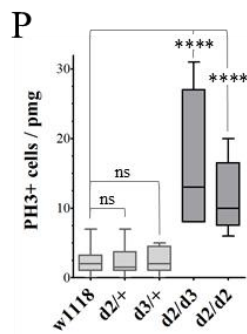
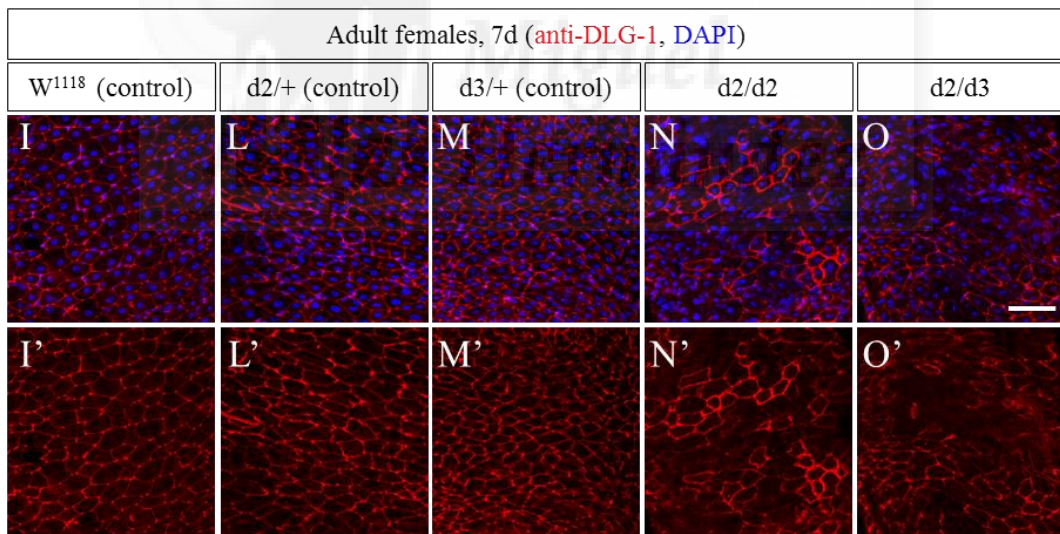
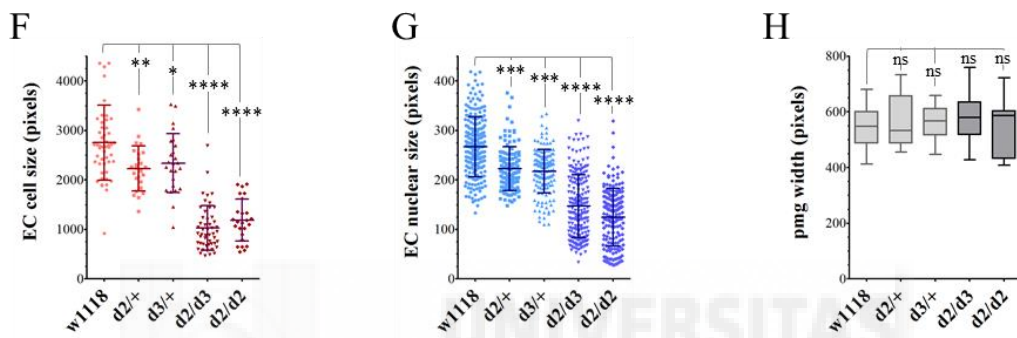
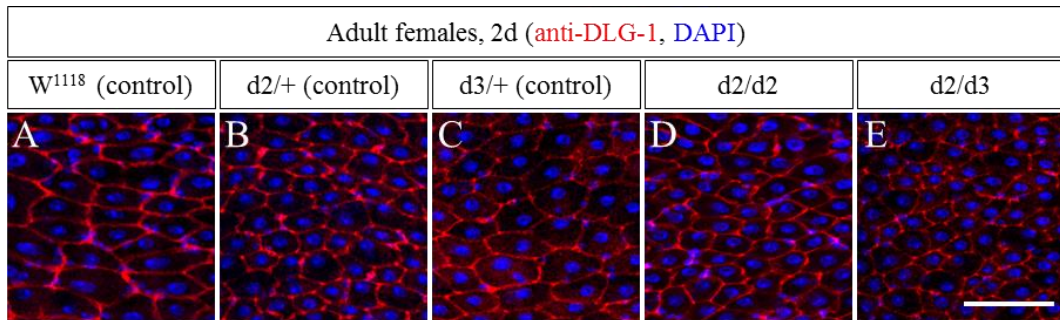


Fig 3.10 – Adult *mir-8* mutant flies have impaired homeostasis and regeneration. A-H) analysis of posterior midgut epithelium of 2 days old flies of the indicated genotypes stained with the epithelial marker Disc Large-1 (DLG-1, in red). Homozygous (D, *d2/d2*) or trans-heterozygous mutants (E, *d2/d3*) for *mir-8* had intact midgut epithelium at 2 days upon eclosion compared to controls (A-C) however enterocytes were smaller (F) with smaller nuclei (G), although gut width was not increased (H). F, G) Scatter dot plot showing significant reduction in cell size and nuclear area. Each dot corresponds to a cell analyzed from randomly selected intestines. H) Box and whiskers plot showing median and data range (from min to max) of midguts width. I-O, I'-O') analysis of posterior midgut epithelium of 7 days old flies as in previous panel (DLG-1, in red). Homozygous (N, *d2/d2*) or trans-heterozygous mutants (O, *d2/d3*) for *mir-8* have non-uniform DLG-1 staining, enterocytes with irregular size and shape and also pignotic nuclei, as seen by DAPI resulting in a disorganized epithelium. P) Box and whiskers plot showing median and data range (from min to max) of PH3+ cells per posterior midguts in each genetic condition. *miR-8* null flies have significantly increased mitotic events. Q) Quantification of flies survival represented as percentage of survival along time. At day 3 after eclosion, flies were mechanically damaged and monitored daily for survival. Log-rank (Mantel-Cox) analysis indicated that *mir-8* depletion significantly impairs survival. Scale bar = 50µm in all panel.

miR-8 is required and sufficient for EBs differentiation and resembles *escargot* phenotypes

To address directly the role of miR-8 in progenitors and tissue replenishment, we proceeded with gain and loss of function experiments in adult flies using the ReDDM method with different cell-specific drivers. *escargot*-ReDDM was used to drive expression in both stem cells and enteroblasts while *SuH*-ReDDM (Zeng et al., 2010) and *Klu*-ReDDM (unpublished driver characterized in this thesis, table 1.2) in enteroblast exclusively.

Loss-of-function (LOF) conditions for microRNAs have been successfully obtained overexpressing constructs carrying several binding sites for the microRNA of interest (Loya et al., 2009). These constructs act like “sponges”, sequestering the microRNA from its endogenous targets. Expression of a miR-8 “sponge” has been

fruitfully used to induce miR-8 loss of function conditions (Kennell et al., 2012; Loya et al., 2014; Lu et al., 2014). Its expression with the *escargot*-ReDDM in stem cells and enteroblasts resulted in strong reduction of tissue replenishment at 14 days without altering the number of “steady state” undifferentiated cells (fig. 3.11 B). Conversely, already at 7 days miR-8 gain of function forced tissue renewal and lead to total depletion of undifferentiated cells, including stem cells (no *escargot* positive cells visualized by UAS-CD8::GFP were present, fig. 3.11 D). Rescue experiments performed coexpressing the anti-apoptotic protein P35 and TUNEL analysis indicated that ISCs were not lost by cell death (not shown) but were likely losing self-renewal capacity and differentiating upon *mir-8* expression. Analogous results were obtained with the enteroblast specific drivers *SuH*-ReDDM (fig. 3.11 E-H) and *Klu*-ReDDM (fig. 3.11 I-K) which confirmed necessity and sufficiency of miR-8 in enteroblast for terminal differentiation and tissue replenishment.

The gain and loss of function experiments of miR-8 resembled respectively the loss and gain of function of *escargot* in terms of stem cells maintenance, tissue replenishment degree/pattern (patches *versus* homogenous replenishment) and cellular morphology (compare fig. 3.2 with fig.3.11 and fig. 3.12). RNAi of *escargot* lead to loss of “stemness” and differentiation of progenitors while its overexpression in block of tissue replenishment (fig. 3.12 A-C, A'-C'), similarly to *mir-8* overexpression and depletion respectively (fig. 3.12 D-F). At the cellular level, loss of *escargot* resulted in suppression of mesenchymal phenotype of progenitors and generation of smaller enterocytes (fig. 3.12 B). Overexpression of *mir-8* gave similar loss of mesenchymal traits and premature expression of the epithelial marker DLG-1 in cells still expressing *escargot* (as seen by CD8::GFP expression) and not properly intercalated (fig. 3.12 D).

These prematurely epithelialized progenitors finally could integrate properly but generating smaller enterocytes (fig 3.12 E).

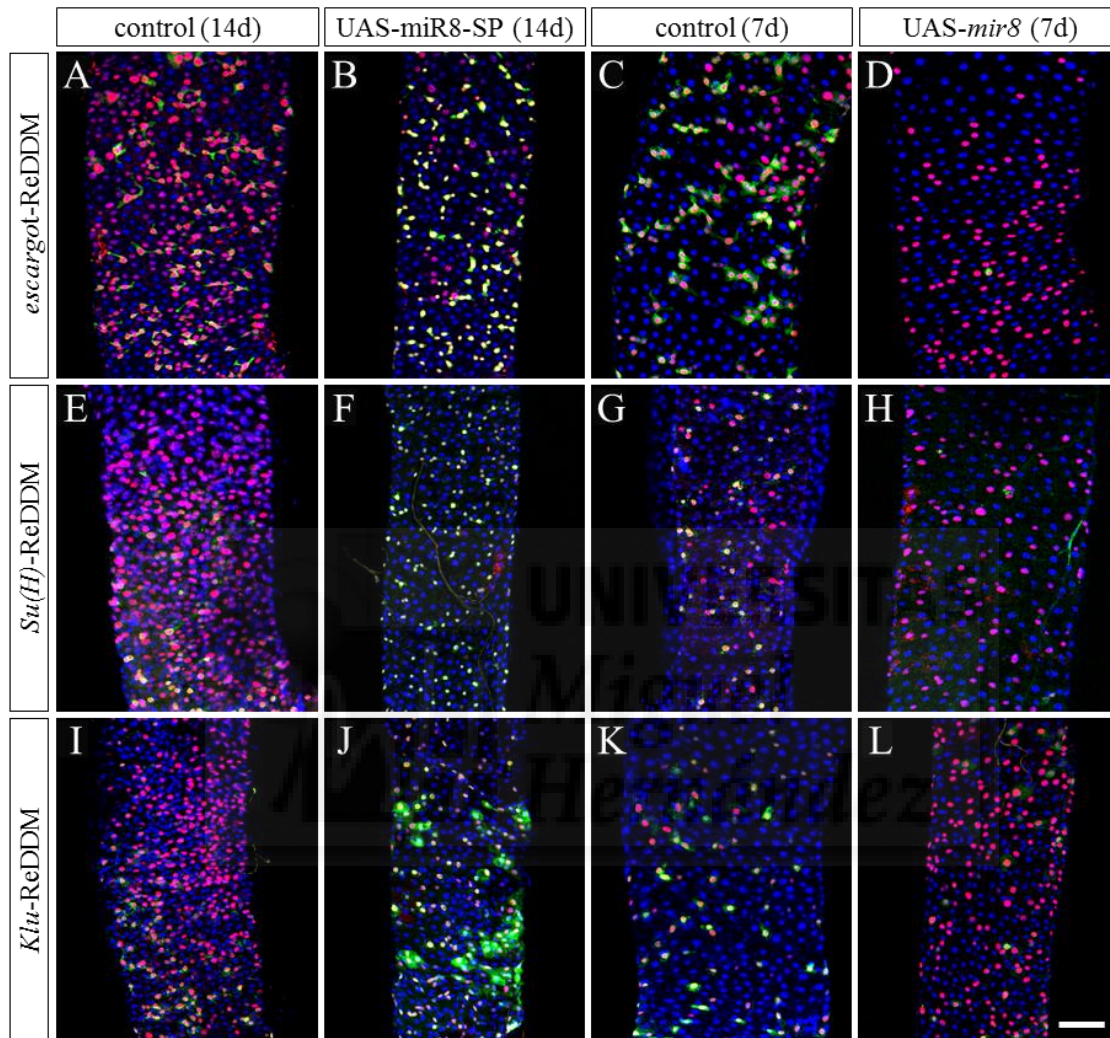


Fig 3.11 – miR-8 is required and sufficient for tissue replenishment. Analysis of posterior midgut tissue replenishment by ReDDM in loss and gain of function conditions for miR-8 with different drivers at the indicated time points (14 or 7 days to highlight in comparison to control block or enhancement of replenishment, respectively). Scale bar = 50 μ m in all panel. Nuclei are stained with DAPI. A-B) Expression of miR-8 sponge (UAS-miR8-SP) in stem cells and enteroblasts by *escargot*-ReDDM leads to block of tissue replenishment, clearly seen at 14 days when controls have extensive replenishment. C-D) Overexpression of *mir-8* (UAS-*mir-8*) leads to depletion of undifferentiated cells and enhancement of replenishment, as seen at 7 days when controls have low replenishment and a vast pool of undifferentiated progenitors. E-F) Expression of miR-8 sponge in enteroblasts by Suppressor of Hairless – ReDDM (*SuH*-ReDDM) leads to block of tissue replenishment. G-H) Overexpression of *mir-8* leads to

depletion of *SuH* positive progenitors and enhancement of replenishment. I-J) Expression of miR-8 sponge in enteroblasts by *Klumpfuss* – ReDDM (*Klu*-ReDDM) leads to block of tissue replenishment. G-H) Overexpression of *mir-8* leads to depletion of *Klu* positive progenitors and enhancement of replenishment.

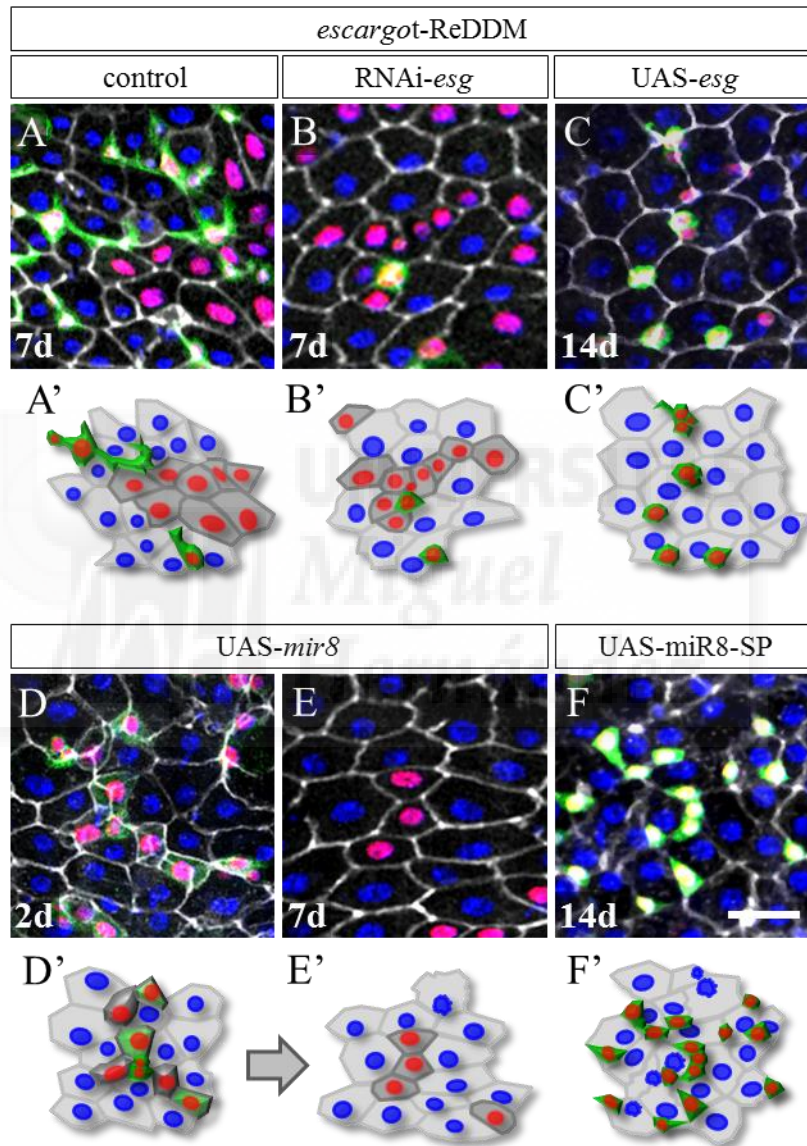


Fig 3.12 – miR-8 gain and loss of function resemble *escargot* phenotypes. Comparison of gain and loss of function of *escargot* (*esg*) and miR-8 in stem and progenitor cells (EBs) on posterior midgut tissue replenishment with disc-large 1 immunostaining (DLG-1, in grey). Scale bar = 20 μ m in all panel, time point indicated in every image. Nuclei are stained with DAPI. A) In controls, enteroblasts have mesenchymal morphology and new ECs are perfectly integrated in the tissue and have similar size to old ECs (DAPI only staining). B) downregulation of *esg* (RNAi-*esg*) leads to EBs differentiation. New ECs

have smaller size and small nucleus. Remaining *esg* positive cells have lost mesenchymal morphology. C) overexpression of *esg* causes total block of differentiation D) Overexpression of *mir-8* (UAS-*mir-8*) leads within 2 days to premature expression of the epithelial marker DLG-1 in undifferentiated cells (cells are not intercalated in the epithelium and are still *esg* positive as seen by CD8::GFP expression). E) At day 7, all undifferentiated cells are differentiating in new ECs with smaller size and nucleus similarly to RNAi-*esg* in panel B. F) Expression of miR-8 sponge leads to block of tissue replenishment likewise gain of *esg* in panel C. A'-F') Cartoons of the observed phenotypes. Undifferentiated cells are in green with red nucleus, their differentiated progeny have nuclear red trace but not green trace (ReDDM tracing) and dark grey body. Old enterocytes have blue nucleus and light grey body.

Antagonistic activity of *Escargot* and miR-8 modulate enteroblast mesenchymal to epithelial transition

Given that *mir-8* is required and sufficient for EBs differentiation and resembles *escargot* phenotypes, we examined by epistatic analysis the genetic relationship between these two genes.

escargot gain of function (UAS-*esg*, fig. 3.13 B) and miR-8 loss of function (miR-8-SP, fig. 3.13 C) caused differentiation blockage while *escargot* loss of function (RNAi-*esg*, fig. 3.13 D) and miR-8 gain of function (UAS-*mir-8*, fig. 3.13 E) enhancement of differentiation. When co-overexpressed (UAS-*esg* + UAS-*mir-8*, fig. 3.13 F), we found an intermediate phenotype with areas totally differentiated and others in which some progenitors were abnormally big and still undifferentiated, indicating an antagonistic effect between *escargot* and miR-8. However over time, *mir-8* overexpression was sufficient to counterbalance *escargot* differentiation blockage and sufficient to completely deplete the midgut of undifferentiated cells. This indicated that in enteroblasts miR-8 acts downstream of *escargot* program and that antagonistic activity of *escargot* and miR-8 balance the maintenance of undifferentiated/mesenchymal state and terminal differentiation/epithelialization process. When

simultaneously depleting *escargot* and miR-8 from undifferentiated cells (miR-8-SP + RNAi-*esg*, fig. 3.13 G) we observed that loss of function of *escargot* counteracts the effects of loss of function of miR-8, indicating that *escargot* is a genetic target of this microRNA.

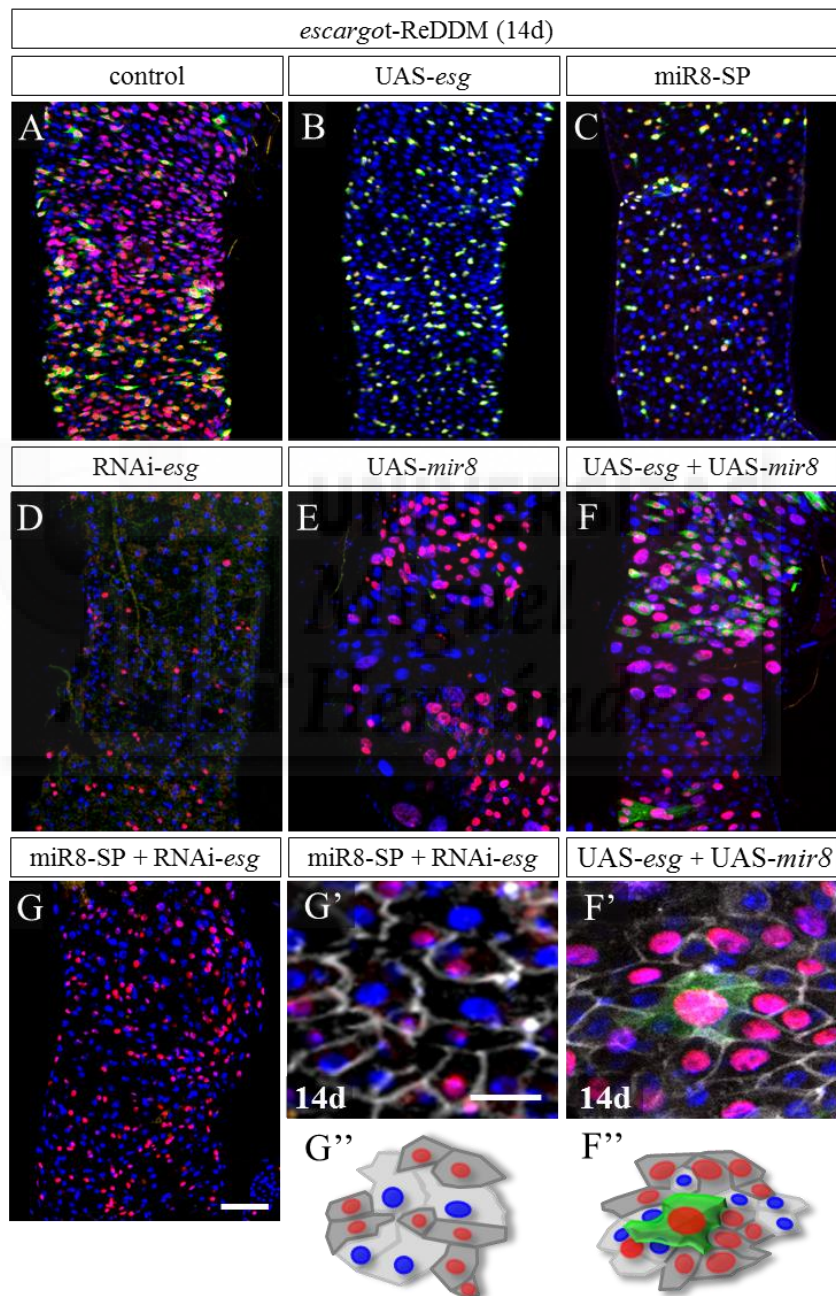


Fig 3.13 – Antagonistic activity of *escargot* and miR-8 modulate enteroblast mesenchymal to epithelial transition. Epistasis analysis of *escargot* and miR-8 in posterior midgut tissue replenishment at

14 days. Scale bar = 50µm in panels A-G, 20µm in G'-F'. Nuclei are stained with DAPI. A) Control midguts present extensive tissue replenishment and a pool of undifferentiated cells. B, C) Gain of *escargot* expression or loss of miR-8 leads to block of replenishment and persistence of undifferentiated state. D, E) loss of *escargot* or gain of miR-8 leads to differentiation of progenitors. F) Co-overexpression causes an intermediate phenotype with areas totally differentiated and others with progenitors still undifferentiated. F') Detail of co-overexpression condition showing a progenitor abnormally big but not integrated in the epithelium, as shown by the epithelial DLG-1 staining. G) Epistasis of *escargot* and miR-8 showing that loss of function of *escargot* counteracts the effects of loss of function of miR-8 leading to differentiation. G') Detail of the epistasis condition showing progenitors differentiated and integrated in the epithelium. G'', F'') Cartoons representing observed phenotypes shown G' and F'. Undifferentiated cells are in green with red nucleus, their differentiated progeny have nuclear RFP trace but not green trace (as designed with ReDDM tracing) and dark grey body. Old enterocytes have blue nucleus and light grey body.

***escargot* is a direct target of miR-8 *in silico* and *in vitro*.**

Loss of function of the *escargot* rescued miR-8 loss of function. This epistasis experiment suggested a functional hierarchy in which *escargot* is regulated directly or indirectly by the microRNA miR-8. In addition, co-overexpression of the two, suggested that they have antagonistic effects. This antagonisms was compatible with direct targeting of *escargot* by miR-8 since UAS-*escargot* construct was made cloning *escargot* cDNA from the initiator Met to the terminator codon plus about 500 bases of 3' untranslated sequences (Fuse et al., 1994), meaning that UAS-*escargot* transgene include almost his whole 3' UTR (636 bp as shown in fig. 3.14 E). Therefore, we first tested if *escargot* mRNA level was higher in miR-8 null condition and secondly investigated if *escargot* could be a direct target of miR-8 by predictive algorithms and *in vitro* Luciferase assay.

Measuring *escargot* mRNA levels by quantitative PCR in *mir-8* mutant L3 larvae indicated an increase of 1.6 folds compared to the average of the three controls, which included *w¹¹¹⁸* as background control and the two individual deletions in heterozygosis (fig. 3.14 A). As a proof of principle we tested also the levels of *zfh-1* (fig. 3.14 B), the fly homologue of the mammalian ZEB which is a described target of miR-200 (Burk et al., 2008; Christoffersen et al., 2007; Gregory et al., 2008; Hurteau et al., 2007; Korpál et al., 2008; Park et al., 2008; Wellner et al., 2009), and *spitz* (fig. 3.14 C), a *Drosophila* EGF ligand which has been shown to be a miR-8 target in larval glia (Morante et al., 2013). As expected, we found that also these transcripts levels augmented. This result confirmed that *escargot* is regulated, directly or indirectly by miR-8. To further investigate the nature of this relationship, we initially approached *in silico* analysis. Various computational methods have been generated, and are still being developed, for miRNA target prediction. These algorithms are based on thermodynamics principles of bases pairing but are also including biological criteria such as conservation among species, target site accessibility and abundance. In example, TargetScan predicts biological targets of microRNAs by searching for the presence of conserved 8mer and 7mer sites that match the seed region of each microRNA (Lewis et al., 2005; Ruby et al., 2007). However, the presence of conserved seed sites has been reported not to guarantee a biological relevant interaction, suggesting that sequences outside the common microRNA seed domain may have a critical role in miRNA target specificity (Vallejo et al., 2011). As a result of such complexity, the lists of candidate target genes from different algorithms often do not overlap (Ekimler and Sahin, 2014). As a matter of fact, we found that TargetScanFly does not predict *escargot* as a putative miR-8 target while Miranda algorithm (Miranda et al., 2006) report two putative target sites in its 3' untranslated terminal region, UTR

(fig. 3.13 E). To test this prediction we performed *in vitro* Luciferase assays as previously described (Morante et al., 2013; Vallejo et al., 2011). In detail, we used a tubulin-*luciferase* reporter that contained the full length 3' UTR of *escargot* mRNA (*escargot* 3' UTR, 636 bp, fig. 3.14 E). The Luciferase activity of this construct was measured in *Drosophila* Schneider cells (S2) that were co-transfected with either a tubulin-*mir-8* or tubulin-*mir-8* mutated (*mir-8-MUT*, fig. 3.14 F) to validate specificity of binding. Luciferase activity was reduced by 70% when wild type *mir-8* expressing vector was transfected. This effect was reversed to a statistically non-significant 30% reduction when was expressed the mutated *mir-8* (fig. 3.14 G). Altogether, these results indicated that *escargot* is a direct target of miR-8, which through downregulation of its target regulates differentiation and epithelialization of enteroblasts.



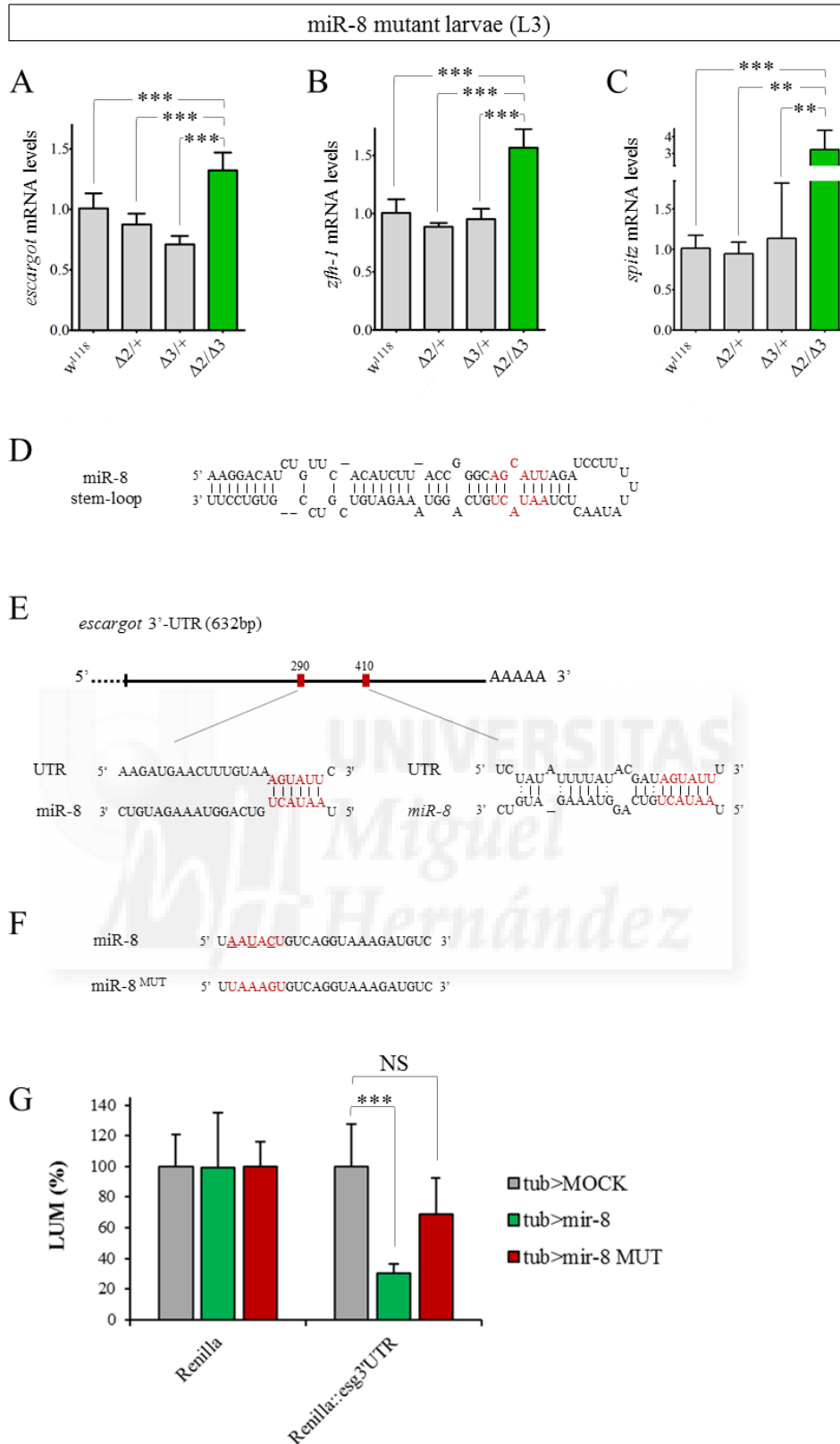


Fig 3.14 – *escargot* mRNA levels are higher in *mir-8* mutants and is predicted as a direct miR-8 target. A-C) Quantitative PCR of *escargot*, *zfh-1* and *spitz* RNA in *mir-8* trans-heterozygous $\Delta 2/\Delta 3$ mutant wandering larvae (L3) compared to w¹¹¹⁸ and $\Delta 2/+$, $\Delta 3/+$ heterozygous controls. A) *escargot*

mRNA levels are increased 1.3, 1.5 and 1.9 folds. B) *Zinc finger homeobox-1 (zfh-1)* mRNA levels are increased 1.5, 1.8 and 1.6 folds. C) *Spitz* mRNA levels are increased in $\Delta 2/\Delta 3$ mutants 3.2, 1.8 and 2.8 folds. Each RNA sample is from 10 to 15 larvae at L3 stage. ** = P value < 0,005; *** = P value < 0,0005. D) Schematics of the miR-8 stem-loop with seed region highlighted in red. E) Schematics of the two predicted target site in *escargot* 3' UTR by miRanda. F) mature miR-8 sequence with the seed highlighted in red and the bases that were mutagenized to generate the *mir-8* mutant underlined. G) Luciferase assay in S2 cells cotransfected with the vectors tub>MOCK (grey), tub>mir8 (green) or tub>mir8 MUT (red) with mutations in the seed sequence as shown in F. Each data point is an average of 4 experimental replicas shown with standard deviation. *** = P value < 0,0005; NS = non-significant.

Escargot represses *mir-8* locus expression *in vivo*

We found that *mir-8* endogenous expression correlated with progenitor cells having bigger size and nucleus (figs. 3.7 and 3.8) and to be induced upon damage (figs. 3.8 and 3.9). Its loss caused block of progenitors in undifferentiated state, not allowing their proper growth and integration in the epithelium (figs. 3.11, 3.12 and 3.13). Co-overexpression, epistasis analysis and *in vitro* Luciferase assay, indicated that miR-8 has an antagonistic activity on *escargot* in terms of differentiation and growth of progenitor cells (fig. 3.13) through direct down-regulation of *escargot* mRNA (fig. 3.14). In human cancer cell lines (Burk et al., 2008; Vetter et al., 2010) and embryonic stem cell lines (Gill et al., 2011), it has been shown that miR-200 family members were repressed by Snail. It has also been shown that ZEB1 can repress the expression of these microRNAs (Burk et al., 2008; Wellner et al., 2009). Escargot has been shown to act as a transcriptional repressor and to negatively regulate endoreplication in abdominal histoblasts (Fuse et al., 1994). This function is compatible with a role in maintaining stem cells diploid and antagonize endoreplication in progenitor cells. We therefore explored if Escargot could regulate the expression of *mir-8* by overexpressing *escargot*

and monitoring the activity of the endogenous *mir-8* locus by measuring the signal from a GFP reporter.

mir8-Gal4 is expressed in small subset of differentiating progenitors in a dynamic and transient manner (figs. 3.6, 3.7 and 3.8) therefore we choose to observe GFP signal intensity in the proventriculus (fig. 3.15 A) and enteric fat (fig. 3.15 D), where it is strongly and homogeneously expressed. To temporally control our manipulation and avoid developmental effects, we used the ReDDM approach (*mir8-ReDDM*). Escargot gain of function by *UAS-escargot* or *GS-escargot* was sufficient to reduce the levels of *mir-8* locus expression in proventriculus (fig. 3.15 B, B', C, C' and G) and enteric fat (fig. 3.15 E, F and H). In addition, enteric fat nuclei were significantly altered in their morphology and presented reduced size compared to control (fig. 3.15 D-F and I). Quantification of transgene expression levels performed in L3 larvae under heat-shock-inducible promoter indicated that *UAS-escargot* and *GS-escargot* were able to raise the levels of *escargot* transcript of about 45 and 70 folds respectively.

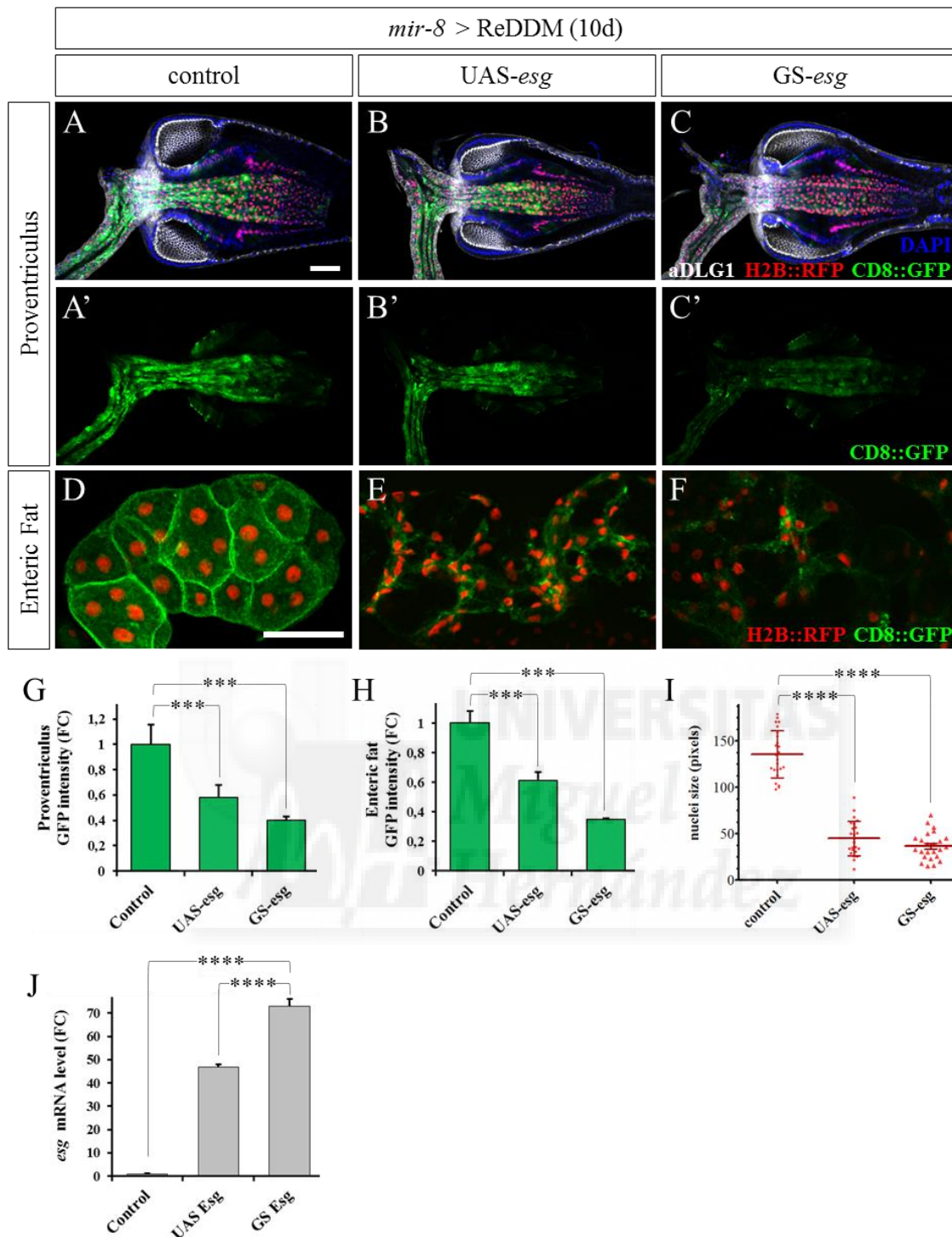


Fig 3.15 – *escargot* overexpression represses *mir-8* locus *in vivo*. Analysis of *mir-8* locus activity by *mir-8*-ReDDM upon 10 days of *escargot* overexpression, either by UAS or GS. A-C) Illustrative images of proventriculus (anterior left, posterior right) showing the expression of *mir-8* in control or *escargot* overexpression condition. A'-C') CD8::GFP channel for the respective panels to highlight expression levels differences. D-F) Representative images of enteric fat showing differences in *mir-8* expression

levels and nuclear size between controls and *escargot* overexpressions. G, H) Quantification of GFP intensity measured as mean pixel value and expressed as fold change to control for proventriculus and enteric fat. I) Scatter dot plot showing mean and standard deviation of nuclei size. Each dot correspond to a nucleus randomly chosen among 5 samples per condition. J) quantitative PCR of *escargot* mRNA levels using heat shock controlled overexpression in L3 larvae. Scale bar = 50 μ m in all panels. Nuclei are visualized by DAPI, proventriculus epithelium by DLG-1 and mir-8 locus expression by CD8::GFP and H2B::RFP (ReDDM). *** = P value < 0,0005; **** = P value < 0,00005.



Discussion

“Every single cell in the human body replaces itself over a period of seven years. That means there's not even the smallest part of you now that was part of you seven years ago.”

Steven Hall, *The Raw Shark Texts*, 2007.



How homeostasis and regeneration resemble each other? A “spot the differences game” with a novel method

Knowledge on regulation of stem cells proliferation and progenitors differentiation during homeostasis was mainly gained through regenerative studies, i.e. during bacterial infection, oxidative stress and other types of damages (Amcheslavsky et al., 2009; Buchon et al., 2010; Chatterjee and Ip, 2009; Guo et al., 2013; Jiang et al., 2011; Jiang et al., 2009; Myant et al., 2013; Takeishi et al., 2013). Even though mechanisms controlling ISCs self-renewal (Bardin et al., 2010; Lin and Xi, 2008; Lin et al., 2008; Xu et al., 2011) and cell lineages specification (Ohlstein and Spradling, 2007) were described, is still poorly explored how stem cells proliferation and progenitors differentiation is regulated during normal homeostasis and little is known about how homeostatic tissue maintenance differs from regeneration (Pellettieri and Sanchez Alvarado, 2007; Rando, 2006). Homeostatic cell replacement can be seen as a “wear and tear process” in which during normal function cells become inefficient by intrinsic mechanisms of aging and/or usage, while regeneration can be seen as sudden rupture of tissue homeostasis. Clearly, cell replacement in homeostatic conditions (continuous or periodic replacement of “selected” sub-optimal cells) or during regeneration (sudden replacement of acutely damaged cells) must have critical differences, although might share common pathways and mechanisms.

Feed-back signals that induce stem cell proliferation during regeneration might control stem cell division kinetic during homeostasis or, on the other extreme, homeostatic stem cell might stochastically and infrequently entry into the cell cycle independently of tissue demand, as in stem cell basal proliferation paradigms. Since it has been postulated that intestinal epithelium undergo continuous and periodical tissue

replenishment during homeostasis, both feed-back and stochastic stem cell entry in cell cycle are compatible with tissue integrity maintenance, but not clear evidence support either possibility. How stem cells regulate their proliferation during homeostasis remains an open question in part because homeostatic stem cells divide rarely and cell turnover is difficult to detect, not allowing correlative analysis with tissue feed-backs. Instead, regeneration paradigms in flies and mammals are easily observable examples of stem cell behavior in response to tissue demand and provided clear evidence that feed-back signaling mechanisms from damaged cells modulate stem cells division rate. In summary, homeostasis and regeneration are completely different contexts that might or might not share common principles.

In *Drosophila* midgut, stem cell division and tissue turnover rate were inferred by MARCM clonal analysis (Ohlstein and Spradling, 2006), in which a random subset of dividing stem cells is labelled by a constitutive marker to follow lineage tracing. Counting the number of cells within clones over time allowed the estimation of stem cells division rate and tissue turnover. However, population dynamics inferences from a subset of tracked stem cells are possible only accepting at least the basic assumption that all stem cells are equal in division and differentiation potential and that midgut turnover occurs in an homogenous fashion. These assumptions were used by *in silico* models of midgut turnover which are able to fit experimental data such as ISC/EB numbers, their distribution and progeny specification (de Navascues et al., 2012; Kuwamura et al., 2010, 2012). However, such assumptions were not directly supported experimentally and although were sufficient to predict most observation taken during regeneration, were overestimating the homeostatic turnover calculated by global monitoring methods, such as the *escargot-Flip/Out* (Cordero et al., 2014; Cordero et

al., 2012b; Jiang et al., 2011; Jiang et al., 2009). This discrepancy raised the possibility that there are different stem cells populations with different division potential (slow and fast cycling ones) or, alternatively, that local differences could modulate their behavior also during homeostasis, similarly to regeneration. The purpose of this work was to tackle these problems.

To understand basic mechanisms of midgut epithelial homeostasis, we undertook a global monitoring approach to correlate stem cells behavior and epithelial tissue turnover without inducing challenging conditions or assuming homogeneity in the stem cells population. We therefore devised a novel method to simultaneously label the whole intestinal stem and progenitor cell population (ISCs/EBs) and their differentiated epithelial progeny (enterocytes, ECs) at a single cell resolution and in a temporal manner, conserving the ability to genetically manipulate only ISCs and EBs. We defined this method Repressible Dual Differential Marker (ReDDM). We found that the whole posterior midgut turnover rate calculated by this approach resulted to be between 2 and 3 weeks rather than the 1 week calculated by MARCM, similarly to results reported for another global monitoring approach based on the Flp/Out technique. To point out if MARCM tissue replenishment overestimation was due to a technical issue or to an intrinsic property of the system (either non homogenous division rate or different stem cells populations) we tested tissue replenishment by ReDDM under MARCM conditions. We found that heat shock was inducing overall faster turnover (1 week *versus* 2-3 weeks) and increased proliferation (2 folds) however it could not “rescue” the whole difference in tissue replenishment. This result indicated that overestimation of tissue turnover rate by MARCM could not be explained exclusively by a heat shock technical issue. Indeed, we found with the ReDDM method that midgut

epithelial renewal occurred by patches of variable size and shape within the same intestine and from intestine to intestine of co-cultured age-synchronized animals, suggesting that tissue renewal is asynchronous within the same epithelium. In addition we found that mitotic events correlated to local tissue replenishment, suggesting local control of proliferation. Taken together these results indicated that previous works incorrectly assumed homogeneous tissue turnover. Clonal analysis simply provided biased data not representative of whole stem cell population but only of stem cells located in actively renewing areas, leading to an overestimation of whole tissue turnover during normal homeostasis.

Importantly, we observed at different time points that there is always a pool of progenitors evenly distributed along the midgut, despite no tissue turnover is detectable. In addition, a careful observation of the mitotic events distribution showed that intestinal stem cells increase locally their proliferation rate but within areas that had already completely renewed and were depleted of progenitors. These observations suggested that replenishment during homeostasis depend on the pool of present progenitors in the first moment, and in a second moment on stem cells. Indeed, we found that mitotic events were very infrequent but constant in non-replenishing midguts of different ages suggesting that during homeostasis stem cells proliferate basally to generate a pool of progenitors which mature slowly or retain undifferentiated state until local demand arises to induce their differentiation. Therefore, only on a second moment proliferation of stem cells occurs, possibly to replenish the reservoir of progenitors. Altogether, these observations indicated that progenitors are not simple transient entities, but active players in tissue homeostasis. In addition, although not centered on

stem cells proliferation, these results suggested that during homeostasis are involved feed-back mechanisms similar to those described in regenerative paradigms.

Since Jak/Stat pathway has been shown to be required for differentiation in both normal and regenerating midgut by loss of function experiments (Jiang et al., 2009) we explored the role of Jak/Stat in local tissue replenishment control. We found by spatial correlation with traced new enterocytes that Jak/stat signaling is increased in progenitor cells in proximity of locally turning-over areas. In addition, in experiments not presented in this thesis, we confirmed published work showing that Jak/Stat signaling is required for homeostatic tissue replenishment since depletion the receptor upstream of Jak/Stat in stem and progenitor cells lead to fully penetrant block of tissue turnover. This loss of function blocked EB maturation since it did not blocked ISCs proliferation, resulting indeed in undifferentiated tumors. Importantly, Jak/stat activation by very short overexpression of its activating ligand UPD, was sufficient for inducing tissue replenishment and ISCs proliferation as previously described but also lead to homogenous and extensive tissue replenishment, similarly to a regenerative response. Altogether these results indicated that homeostasis and regeneration can share the same signaling pathways, nevertheless the replenishment process during homeostasis has unexpected spatial fine tuning mechanisms which might involve other mechanisms to modulate progenitors maturation/differentiation. Indeed, using the flybow-MARCM analysis to generate several univocally identifiable clones, we found that terminal progenitor differentiation was not depending on the progenitor birth time. Also, single cells clones (which represent univocally progenitor cells) could surprisingly persist undifferentiated up to 14 days. This level of plasticity of progenitor cells during tissue homeostasis was previously unforeseen.

Which are the intrinsic mechanisms controlling stem and progenitor cells? The co-option of a metastatic mechanism

Besides the fact that progenitor cells behavior has been poorly explored, little is known about the intrinsic mechanisms required to maintain stem cells and their pluripotent differentiation capacity (“stemness”). Nevertheless, extrinsic signals have been extensively characterized. Intestinal stem cells proliferation is extrinsically modulated by systemic and local signals coming from insulin producing tissues, epithelial cells, visceral muscles and their own progeny. Signaling pathways are integrated to dynamically modulate division rate of intestinal stem cells to cope with tissue demand (Biteau et al., 2011). Importantly, the described regenerative pathways are redundant for stem cell maintenance and basal proliferation and none alone is required. Concerning progenitor’s role, their cellular differentiation implies control of growth, proper tissue intercalation and the contemporary and strictly correlated phenomena of loss of undifferentiated phenotype (e.g. mesenchymal traits). These complementary events (that is, differentiation and loss of undifferentiated phenotype) have to be actively controlled to fit our observations that differentiation of progenitors is locally controlled and birth-time independent. We therefore also investigated for the intrinsic pathways required to retain progenitors undifferentiated.

Driven by the described role in mammals of snail family genes in epithelial to mesenchymal transition (EMT) (Barrallo-Gimeno and Nieto, 2005) and the link between EMT and the gain of stem cell like properties (Mani et al., 2008), we explored the role of *escargot*, which is a gene of the *snail* family, and is commonly used as a midgut stem and progenitor cell marker. Following this parallelism, we identified miR-8, the sole fly homologue of the mammalian miR-200 family, as a novel progenitor’s

marker and regulator of differentiation. In summary, we identified *escargot* and miR-8 as key elements balancing the transition of progenitors towards terminal differentiation. *escargot* is necessary and sufficient to maintain both cell types undifferentiated. The microRNA miR-8 expression starts in late progenitor cells and correlates with cell growth, nuclear size increase and tissue demand, both in homeostatic and regenerative conditions (i.e. mechanical damage and oxidative stress). As demonstrated by gain and loss of function experiments, its expression is necessary and sufficient to drive terminal differentiation. When *escargot* and miR-8 were co-overexpressed, progenitors become abnormally big but persisted undifferentiated and not integrated in the epithelium, indicating an antagonistic action. Their simultaneous depletion from progenitors cells rescued differentiation, indicating that miR-8 dependent differentiation occurs via downregulation of *escargot*. Indeed, Luciferase assay indicated that *escargot* 3' UTR is a direct target of miR-8. Conversely, *escargot* over-expression could negatively regulate *mir-8* locus activity. These results indicate that stemness and maintenance of progenitors in undifferentiated state requires the active repression of the differentiation program, whereas the terminal differentiation toward epithelial cell requires the active repression of undifferentiated traits. The presented results describe a simple and direct antagonism between master elements of mutually exclusive biological processes, able to reciprocally influence their own expression. The break of this reciprocal regulation impacts on homeostasis, resulting in tumor formation or intestinal hypotrophy and dysfunction.

Our results indicate that the mesenchymal traits of progenitors, maintained by *escargot* and negatively regulated by miR-8, are at the base of proper differentiation and epithelial integrity. In addition, could provide the cellular basis to explain how

stochastic loss of stem cells through differentiation or damage (Lopez-Garcia et al., 2010) is compensated by their neighbors. Indeed, *Drosophila* ISCs and EBs have not a defined niche other than the underlying visceral musculature which evenly surrounds the whole midgut providing Wingless signaling (Lin and Xi, 2008; Lin et al., 2008). Such uniform muscular “niche” is compatible with the migration and dynamic reorganization of EBs that we observed.

Overall, the cellular and genetic evidences presented in this work indicate striking analogies between *Escargot*/miR-8 “undifferentiated to differentiated transition” and the *Snail*/miR-200 mesenchymal to epithelial transition (MET). In mammals, miR-200 microRNAs can induce MET by direct targeting the mesenchymal inducers ZEB1 and ZEB2, and other stemness genes. miR-200-dependent MET has been shown to have a pivotal role during the last steps of the metastatic cascade (Dykxhoorn et al., 2009). We observed that progenitors have a front end - back end polarity and can send explorative protrusions along the epithelium, similarly to mesenchymal cells, while hold undifferentiated by *escargot* expression. This phenotype is reversed when cells terminally differentiate integrating into the epithelium upon miR-8 expression. Importantly, we have shown that the mesenchymal features and invasive properties of enteroblasts are a prerequisite for the successful integration of new epithelial cells within the existing epithelium. In fact, precocious expression of miR-8 or downregulation of *escargot* was leading to differentiated cells not properly integrated in the epithelium.

How slow cycling stem cells can elicit rapid responses to unpredictable demand? Ask their daughters

How slow cycling stem cells may elicit rapid responses to homeostatic demands and regeneration remains poorly understood and it is the focus of intense research. Adult tissues are constituted of post-mitotic cells exposed to environmental stress, a pool of differentiating progenitors which substitute damaged cells and long term self-renewing somatic stem cells. Progenitors are originated by asymmetric cell division of stem cells and, after further divisions, undergo a maturation process culminating in terminal differentiation to replenish the tissue. In *Drosophila* midgut, progenitors are post-mitotic therefore the only dividing cells are the stem cells. This makes the system ideal to explore the relationship between stem cells proliferation, progenitors maturation and tissue turnover.

We found that in *Drosophila* midgut there is a pool of progenitors (EBs) ready to differentiate evenly distributed along the midgut, despite no tissue turnover was ongoing. When replenishment was taking place, was following unpredictable domains and leading to a local increase of stem cells divisions which apparently occurred upon, and not prior to, tissue replenishment. The *Drosophila* midgut progenitors population has been reasonably assumed to be transient, but surprisingly has never been explored in detail *how transient*. Our study show that progenitors can hold undifferentiated in areas that do not need replenishment, and that stem cells proliferate at very low but constant rate if replenishment is not taking place. The flybow-MARCM analysis pointed out that the progenitor terminal differentiation was not coincided with the progenitor birth time but with the onset of a local demand. Indeed, single cells clones (which represent univocally progenitor cells) could persist undifferentiated up to 14

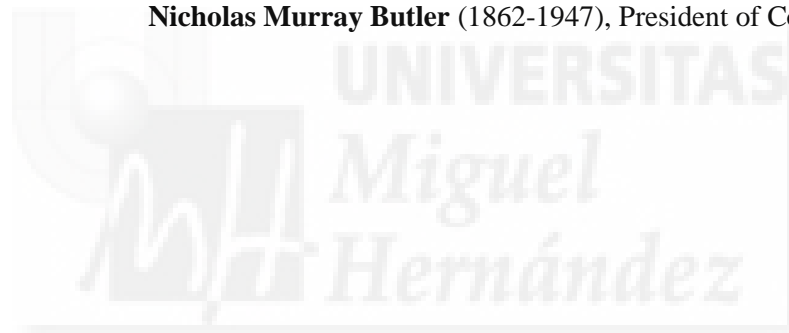
days. Altogether, our observations draw out the attention from stem cells as primary sensors of tissue feed-back and brought the progenitor under the light-spot.

Thus, how slow cycling stem cells may elicit rapid and precise responses? The alternative views that have been postulated focusing on stem cells behaviour envision two opposite and mutually exclusive situation: on one side, stem cells have low proliferation rate and undergo a reversible switch between quiescence and activation of cell cycle in response to demand (Biteau et al., 2011; Liu et al., 2010). Such strategy, although could provide exactly the required number of cells, could generates a delay in the response that may compromise epithelial integrity and animal survival. Alternatively, stem cells might undergo continuous cell division to face with high tissue demand, like has been proposed for the epidermis (Clayton et al., 2007; Doupe et al., 2010), intestine (Lopez-Garcia et al., 2010; Snippert and Clevers, 2011), the *Drosophila* midgut (Micchelli and Perrimon, 2006; Takashima and Hartenstein, 2012) or the male testis (Klein et al., 2010). A continuous division strategy however does not necessarily ensure robustness to fluctuating tissue needs, unless assuming over-production. Overproduction would be a major cost for the organisms and is contrary to the common view that adult stem cells must divide sparingly to minimize stem cell “exhaustion” and the risk of cancer (Arai and Suda, 2007; Cairns, 1975a, b; Orford and Scadden, 2008). However, if we now consider the notion that progenitors could postpone their differentiation and actively contribute to homeostasis responding directly to tissue feedbacks, becomes possible that also slow cycling stem cells could sustain highly variable tissue demands. Stem cells would cope with increased demand thanks to progenitors cells that would buffer their delayed response caused by the time needed to adapt their proliferation rate.

Conclusions

*“An expert is someone who knows more and more about less and less
until he knows everything about nothing”*

Nicholas Murray Butler (1862-1947), President of Columbia University



In this experimental work we used *Drosophila melanogaster* to investigate the homeostatic mechanisms of the adult midgut epithelium in unchallenged conditions. We devised an original method to directly observe the whole stem cells/progenitors population and simultaneously the epithelial tissue replenishment. The main conclusions of this experimental work are listed as follows, grouped as for the results sections.

PART 1 - ReDDM: a novel method to follow stem cell self-renewal and quantify tissue regeneration simultaneously

- 1) *escargot* is a marker of stem cells and progenitors;
- 2) *escargot*-ReDDM method allows monitoring epithelial cell replenishment with a single cell resolution over time;
- 3) *escargot* ReDDM allows spatial correlation studies between ISCs/EBs numbers, tissue replenishment and proliferation;

PART 2 - Global monitoring unveils unexpected dynamics of midgut turnover during homeostasis

- 4) Progenitor cells are evenly distributed along the midgut, despite no replenishment is ongoing;
- 5) Replenishment occurs following flexible and unpredictable domains rather than being homogeneous;
- 6) Stem cells proliferation rate is not homogenous and correlate with areas that have already been replenished;
- 7) Clonal approaches have overestimated tissue turnover because heat shock accelerates tissue replenishment and because stem cell population is not proliferating at the same rate;

- 8) JAK/Stat pathway is activated (and required) for replenishment during homeostasis similarly to regenerative paradigms;
- 9) Progenitors differentiation occurs independently of birth time;

PART 3 - A delayed progenitors differentiation strategy mediates adaptive responses to homeostatic demand

- 10) Enteroblasts present marked mesenchymal features, such as actin rich filopodia, lamellipodia and also short distance cellular movements involving nucleus translocation;
- 11) *escargot* is required for mesenchymal traits of enteroblasts and sufficient to retain their undifferentiated state;
- 12) *escargot* is required for stem cells division and long term maintenance;
- 13) *mir-8* is expressed in late enteroblasts and is induced during tissue replenishment;
- 14) miR-8 is required and sufficient for enteroblasts differentiation and resemble *escargot* phenotypes;
- 15) Antagonistic activity of *escargot* and miR-8 modulate enteroblast mesenchymal to epithelial transition;
- 16) *escargot* is a direct target of miR-8 *in silico* and *in vitro*;
- 17) Escargot represses *mir-8* locus expression *in vivo*.

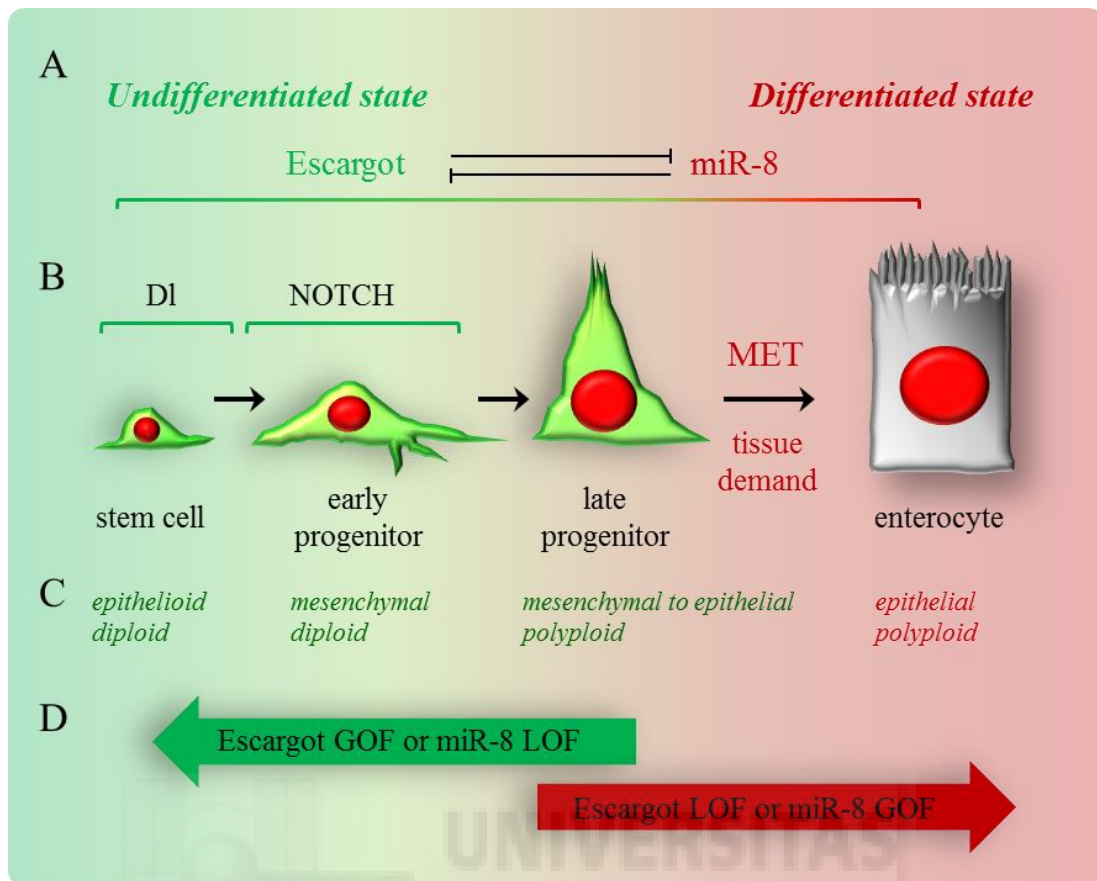


Fig. 1 – Escargot and miR-8 control midgut epithelial homeostasis – A) Escargot and miR-8 control the transition from undifferentiated to differentiated state during *Drosophila* midgut homeostasis by a direct cross-regulation. B) Stem cells generate progenitor cells which are specified through DI-NOTCH signaling. Early progenitors undergo a process of maturation which includes growth, polyploidization and intercalation in the epithelium. Late stage progenitors are marked by *mir-8* expression and are in the process of intercalation, in a mesenchymal to epithelial transition (MET) –like manner. C) Properties of stem cells, progenitors and enterocytes. Stem cells and progenitors are *escargot* positive and are held in undifferentiated state by *escargot* expression, however only progenitors present an evident mesenchymal phenotype. Enterocytes are cuboidal epithelial cells with polyploidy nucleus. Stem cells and early progenitors are diploid however progenitors undergo polyploidization while retaining undifferentiated state. D) The manipulation of Escargot and miR-8 in stem and progenitor cells is sufficient to unbalance toward undifferentiated or differentiated state. (GOF = gain of function; LOF = loss of function; MET = mesenchymal to epithelial transition).

Materials & Methods

“By three methods we may learn wisdom: first, by reflection, which is noblest; second, by imitation, which is easiest; and third, by experience, which is the most bitter.”



Confucius

***Drosophila melanogaster* genetics**

Stocks, maintenance and crosses

Fly stocks were grown on regular glucose-yeast “iberian” food between 25,0 and 26,5°C on a 12-hour light/dark cycle. ‘Iberian’ fly food was made by mixing 15 L of water, 0.75 kg of wheat flour, 1 kg of brown sugar, 0.5 kg yeast, 0.17 kg agar, 130 mL of a 5% nipagin solution in ethanol, and 130 mL of propionic acid.

A copy of each stock in use was kept in the laboratory stock collection at 18°C on 3-4 weeks generation cycle. Crosses were settled between 25,0 and 26,5°C if not otherwise specified. Crosses in which transgene expression was controlled by the temperature sensitive allele of GAL80 repressor (tubGAL80^{ts}) were settled at 18°C then shifted at 30°C to allow UAS transgenes expression. The lines used are listed and described in table 1.

Table 1. Fly stocks used

Stock name	Description	Origin_code or reference
W ¹¹¹⁸	Partial deletion of white gene- is the background of most transgenic strains. Used as control (w ^{-/-} background).	Rabinow and Birchler, 1989
Oregon R	Collected from wild flies in 1925 or earlier by D.E. Lancefield. Used as wild type control	Lindsley and Grell, 1968
Tub-Gal80 ^{ts}	Encodes a temperature-sensitive GAL80 expressed under the control of the α Tub84B promoter	BL_7017
10XSTAT92E-DGFP	Stat92E binding sites upstream of a minimal heat-shock promoter driving the expression of a destabilized GFP reporter. Is a reporter of endogenous JAK/STAT pathway.	Bach et al. 2007

UAS-mCD8::GFP	UAS sequence drive the expression of the coding region for mouse CD8a fused in frame, at its 3' end, to GFP (F64L, S65T).	BL_5137
UAS-NLS::GFP	UAS sequence drives the expression of GFP fused to a peptide recognized for nuclear import (nuclear localization sequence, NLS)	BL_4775
UAS-H2B::RFP	UAS sequences drive expression of His2B, tagged with RFP.	Mayer et al., 2005
UAS-Act::RFP	UAS regulatory sequences drive expression of Act5C, which is tagged at the N-terminus with RFP.	BL_24778
UAS-Moe::RFP	UAS sequence drive expression of the actin-binding domain (the C-terminal 137 residues) of Moesin which is tagged with mCherry RFP.	Millard and Martin, 2008
UAS-Tub::RFP	UAS regulatory sequences drive expression of Hsap α Tub tagged with mCherry RFP.	BL_25774
UAS-esg	UAS driving expression of <i>escargot</i> cDNA, from the initiator Met to the terminator codon plus about 500 bases of 3' untranslated sequences.	DGRC_109127
GS-esg	“Gene search” line inserted in <i>escargot</i> locus resulting in UAS driven expression of endogenous <i>escargot</i> .	<i>Drosophila</i> Gene Search Project, Tokyo, 2012
esg-GFP P01986	GFP fusion/trap in <i>escargot</i> gene.	Le Bras and Van Doren, 2006
esg-lacZ	Enhancer trap of <i>escargot</i> gene.	Samakovlis et al., 1996
RNAi-esg VDRC	UAS regulatory sequences drive expression of an inverted repeat for <i>escargot</i> gene.	GD_9793
RNAi-esg (TRIP)	UAS regulatory sequences drive expression of an inverted repeat for <i>escargot</i> gene.	BL_28514
esgG66	Amorphic allele - The 3.5kb of <i>escargot</i> sequences between coordinates 680 and 4200 have been deleted.	Whiteley et al., 1992 Kassis, 1994
esgL2	Amorphic allele - Part of the <i>escargot</i> transcription unit deleted (S. Hayashi, unpublished observations).	Hayashi et al., 1993 Fuse et al., 1994
mir-8 Δ 2	Imprecise excision of the P{EP}EP2269 insertion, resulting in a 1.8kb deletion that removes the mir-8 gene.	Karres et al., 2007
mir-8 Δ 3	Imprecise excision of the P{EP}EP2239 insertion, resulting in a 26kb deletion that includes mir-8, Ugt37c1, CG5859 and Fen1.	Karres et al., 2007
mir8-GAL4	mir-8 GAL4 enhancer trap.	DGRC_104917
UAS-mir-8	UAS regulatory sequences drive expression of the <i>mir-8</i> miRNA precursor stem loop	Vallejo et al., 2011

	sequence.	
UAS-EGFP::mir-8-SP	UAS driving expression of ten repetitive sequences complementary to miR-8 with mismatches at positions 9–12 for enhanced stability introduced into the 3'UTR of EGFP.	Loya et al., 2009
Su(H)-GBE-lacZ	Three copies of a grh protein binding element (GBE) and two copies of a Su(H)binding site drive expression of <i>Ecol</i> \lacZ.	Furriols et al., 2001
Su(H)-GAL4	Three copies of a grh protein binding element (GBE) and two copies of a Su(H)binding site drive expression of <i>Scer</i> \GAL4.	Zeng et al., 2010
DI-lacZ	<i>Ecol</i> \lacZ is inserted in the <i>Delta</i> gene locus.	BL_11651
DI-Gal4	<i>Scer</i> \GAL4 is inserted in the <i>Delta</i> gene locus. Obtained by modification of BL_11651 by Zeng et al.	Zeng et al., 2010

BL = Bloomington; DGRC = *Drosophila* Genetic Resources Center (Kyoto); FO = FlyORF (Zurich)

VDRC = Vienna *Drosophila* RNAi Center;

Establishment of recombinant lines

Recombination allows combining in the same chromosome different alleles. The frequency of recombination is function of intergenic distance. In *Drosophila* recombination occurs only in females hence is necessary to collect F1 heterozygous female virgins to cross with a balancers line, i.e. If / Cyo; TM1 / MKRS; F2 recombinants can be selected by the intensity of eye color if each allele has a mini-white gene, transgene expression in the case of recombining a Gal4 and a UAS line phenotypically recognizable or genotyping.

Recombinant lines generated during the development of this work are listed in table 2 and are now available from the laboratory collection. For each recombinant one to three different stocks were kept.

Recombinants of a Gal4 line and visible reporters, such as GFP, were selected at larval stage by fluorescence. TubGAL80ts and UAS H2B::RFP recombinants were screened by PCR because both original stocks had bright red eyes. The presence of white eyed flies in the F2 was indication of occurring recombination and allowed to estimate frequency of recombination. For flies genotyping, primers (listed in table 3) were designed using PrimerBlast.

Table 2. **Recombinant flies and stocks generated**

Full genotype

w; <i>esg</i> -Gal4, UAS-CD8::GFP / Cyo; TM2/MKRS
w; +/+; <i>tub</i> -GAL80ts , UAS-H2B::RFP / TM2
w; <i>esg</i> -Gal4, UAS-CD8::GFP / Cyo; <i>tub</i> -GAL80ts , UAS-H2B::RFP / TM2
w; <i>ey</i> -Gal4, UAS-CD8::GFP / Cyo; <i>tub</i> -GAL80ts , UAS-H2B::RFP / TM2
w; <i>mir8</i> -Gal4, UAS-CD8::GFP /Cyo; +/+;
w; <i>mir8</i> -Gal4, UAS-CD8::GFP /Cyo; <i>tub</i> -GAL80ts , UAS-H2B::RFP / TM2;
w; <i>esg</i> -Gal4, UAS RFP ^{myr} / Cyo; +/+;
w; <i>esg</i> -Gal4, UAS RFP ^{myr} , UAS-CD8::GFP /Cyo; +/+;
w; NP1-Gal4 / (Cyo); <i>tub</i> GAL80 ^{ts} , UAS-H2B::RFP / TM2
w; NP1-Gal4, P01986DE / (Cyo); <i>tub</i> -GAL80 ^{ts} , UAS-H2B::RFP / TM2

Balancer allele between parenthesis indicates that the correspondent transgenic chromosome is homozygous viable.

Table 3. **Primer pairs used for genotyping**

Gene	Oligo Name	Sequence (5' to 3')
GAL80	F-GAL80	CATGGACTACAACAAGAGATC
	R-GAL80	TTATAAACTATAATGCGAGATATTG
mRFP	F-mRFP	ACGTCATCAAGGAGTTCAT
	R-mRFP	GGTGTAGTCCTCGTTGTG

Induction of midgut regeneration

Mechanical damage

Esg-ReDDM adult flies of 3-7 days of age developed at non permissive temperature are shifted at 29 °C for 3 days to induce transgenes expression. At day 3, half of the flies are gently pinched with tweezers in the abdomen and let recover for 24 before dissection.

Paraquat exposure

Flies were dry starved for 4 hours and then fed for 4 hours with 5% sucrose \pm 10 mM paraquat solution (methyl viologen, Sigma Aldrich) on filter paper. Intestines were dissected for immunohistochemistry with standard protocol as follows.

Survival curves

Crosses were settled at 18C. Females of the appropriate genotypes and of 3 to 7 days of age were then shifted at 29C. Per genetic condition, were kept no more than 15 flies per

small tube to avoid overcrowding stress. To keep the flies free of contaminations and on fresh food, tubes were changed every 3 day. Flies were daily checked for survival until natural death or experimental endpoint (21 or 28 days). Life tables were constructed combining data from all vials in a genotype group. Survival curves were plotted using Prism GraphPad software, and analyzed by the log-rank test.

Immunohistochemistry

Standard immunohistochemistry protocols were used to evaluate effects of genetic manipulations on intestinal tissue architecture, to identify cell types, intestinal stem cells/progenitors number and cell divisions. Used antibodies, host specie, origin and used dilution are listed in table 1. In detail, D1 staining was used to identify stem cells (ISC), prospero to identify enteroendocrine cells (ee), Disc Large-1 to label the enterocytes (EC) and enteroendocrine cell borders highlighting the epithelium monolayer structure, phospho-histone-3 to identify mitotic cells. Other commonly used antibodies were anti beta-galactosidase and anti-GFP to show reporter's expression. DAPI was used in all preparation to counterstain all nuclei.

Table 4. **Primary antibodies**

Antigen	Host Specie	Source	Dilution
Beta galactosidase	rabbit	Cappel	1:1000
Beta galactosidase	chicken	Abcam	1:1000
Disc large-1 (DLG-1)	mouse	DSHB	1:100

Prospero (PROS)	mouse	DSHB	1:100
Delta (DI)	mouse	DSHB	1:100
PhosphoHistone 3 (PH3)	rabbit	Upstate	1:1000
GFP	sheep	Lifespan Biosciences	1:2000
GFP	rabbit	Molecular Probes	1:1000

DSHB = Developmental Studies of Hybridoma Bank – www.dshb.biology.uiowa.edu

To visualize visceral muscles was used 633-coniugated phalloidin, commercially available from Invitrogen. Phalloidin is a toxin with high affinity for filamentous actin.

Dissection of adult flies intestines

Adult flies of the appropriate genotype are dissected on silicon pads in 1X PBS. Heads are cut-off; thorax and abdomen are separated to expose the anterior portion of the midgut; the intestine is gently pulled by the crop to expose the proventriculus; abdomen is opened from thee most posterior portion using the tweezers, ovaries are discarded and intestine is exposed pulling gently from the rectum. The whole intestinal tube, including crop, midgut, hindgut and malpighian tubules is transferred on ice to proceed with standard immunohistochemistry protocol.

Standard immunohistochemistry protocol

1. Flies or larvae are dissected in phosphate-buffered saline (PBS) and discs or organs of interests are accumulated on ice in concave glass or 0.5 ml eppendorf tubes (max 30 min);
2. Fix for 20 to 40 min shaking at room temperature (RT), in 4% paraformaldehyde (PFA) or formaldehyde (FA) made in PBS;
3. 3 X 5 min washes with abundant PBS;
4. 1 hour blocking in 1% bovine serum albumin – PBS-Triton (BSA-PBT) at RT;
5. Primary antibody at the appropriate dilution in 1% BSA-PBT at 4°C overnight with very slow shaking;
6. 3 X 5 min wash with PBT at RT;
7. Secondary antibody in 1% BSA-PBT for 2 hrs shaking at RT in darkness
8. Optional 4',6-diamidino-2-phenylindole (DAPI) staining:
9. 2 X rapid but abundant PBS washes;
10. 10 min DAPI (Invitrogen, 0.3 mg/ml) shaking at RT in darkness;
11. 2 X rapid but abundant PBS wash;
12. Mount on glass slides with Fluoromount-G (Southern Biotech);
13. Use weights to properly flat the preparation and let it dry in darkness at RT for at least 2 hours, then store at 4°C until confocal scanning.

Relative quantification of gene expression levels

Standard Real-time PCR, (also named quantitative PCR, qPCR) was used to determine expression levels of genes of interests in specific genetic conditions (gain or loss of function) or physiological status (i.e. virgin *versus* mated). Primers used are listed in table 5.

Dissection of adult flies intestines for RNA extraction

Intestines were dissected in the same manner as for immunohistochemistry but midguts (or desired portion of the intestine, i.e. posterior midgut) were separated from proventriculus, salivary glands, malpighian tubules and hindgut. Portion of interest was accumulated in a 10ul drop of RNAlater® (Qiagen) deposited in the dissection silicon pad. Once 10 to 20 samples were collected, they were transferred in an eppendorf with the minimum liquid possible, frozen on dry ice then stored at -80C until RNA extraction.

RNA extraction from intestines

RNA isolation was performed by RNeasy® Kit (Qiagen) following manufacturer protocols.

cDNA preparation

cDNA was synthesized from 100 ng to 1 ug of total extracted RNA by TaqMan Reverse Transcription Reagents with random primers and oligo dT primers (Applied Biosystems). Negative controls were prepared using identical retrotranscription mix with water as a substitute of polymerase.

Real Time PCR

SYBR Green real-time PCR in the ABI Prism 7500 Sequence Detection System (Applied Biosystems). Quantitative PCRs were performed in 96-well optical reaction plates (Applied Biosystems). Primers (listed in table 5) were designed using PrimerBlast. For each sample technical triplicates were run and required to be within 0.1 standard deviation to be used for further analysis. Negative controls were run as well in triplicates and required to be undetermined or do not present signal before 34 cycles. Each real time reaction was qualitatively evaluated on the basis of reaction kinetics. Primers were systematically evaluated by the presence of a single amplicon in the dissociation curve. Gene's expression levels were normalized to the housekeeping gene encoding for the ribosomal protein RP49. The statistical analysis was done on the Δ CT (dCT) values. The formula used to calculate fold change was $FC = 2^{-(dCT)}$, with dCT calculated as the difference in CT values between the gene of interest and RP49. P-values < 0.05 in unpaired two-tailed Student's t test were considered to be statistically significant.

Table 5. **Primer pairs used for qPCRs**

Gene	Sequence (5' to 3')
<i>rp49</i>	TGTCCTTCCAGCTTCAAGATGACCATC CTTGGGCTTGCGCCATTGTG
<i>escargot</i>	ATATGTCGCCCCGAACTATGCCGA CGGGCAATGGAACTGCTGATGTTT
<i>spitz</i>	GCGGGTGTTTTGTGTGTCAT TTGGAATCGGGTTTCTCTACA

Evaluation of cell death by TUNEL

To exclude that certain genetic manipulations (i.e. *esg*-RNAi or UAS-mir8) were leading to cell death of stem cells, the presence of dying cells in was assessed by in situ cell death detection kit (Roche applied sciences, Grenzach, Germany) according to manufacturer's protocol followed by a DAB-reaction (Thermo Fisher, Schwerte, Germany).

Luciferase assay to test microRNA targets

S2 cells preparation and transfection

For *Drosophila* S2 cell luciferase assays, 250.000 cells were seed in 24-well plates 3-4 hours prior to transfection. Transfection mix includes the tub-mir-8 plasmid (250 ng) (Karres et al., 2007), the luciferase::*esg*-UTR construct (25 ng), and the Renilla luciferase plasmid (25 ng) for normalization. As control, a tub-mutant mir-8 construct was generated by site-directed mutagenesis as described below. The relative luciferase activity was measured 60-72 hours post-transfection using the Dual-Glo Luciferase Assay system (Promega). Each condition was tested in triplicate and the experiment was repeated four times.

***mir-8* mutagenesis**

To mutagenize the tub>miR8 plasmid (JB-25_miR8) was used the QuikChange® II XL Site-Directed Mutagenesis Kit (Stratagene) according to manufacturer protocol. Gradient PCR was used to perform simultaneously different conditions of elongation, in particular were set 2 different temperatures above and 2 below 60C (55.1 – 57.2 – 59.8 – 62.5 – 64.6 C). For transformation were used the XL10 Gold Ultracompetent cells. Mutagenesis was verified by sequencing. Used primers listed in table 6.

Table 6. **Primer pairs used for *mir-8* mutagenesis and sequencing**

Use	Oligo Name	Sequence (5' to 3')
Mutagenesis	miR-8-mut_up	GATCCTTTTTATAACTCTTAAAGTGTCAGGTAAAGATGTCGTCCG
	miR-8-mut_low	CGGACGACATCTTTACCTGACACTTTAAGAGTTATAAAAAGGATC
Sequencing	M8short-up	AAGGGGGCCAATGTTCTAAG
	M8short-low	CCGCTTGICTTTCGCATTATC

Image acquisition, processing and data analysis

Confocal microscopy

Images were acquired using inverted confocal microscopy apparatus from Leica (TCS-SL). Acquisition was routinely at 1024 X 1024 pixels. Collected tiff images were processed and analyzed with FIJI collection of plugins and macros for ImageJ (<http://www.fiji.sc/Fiji>; <http://www.imagej.nih.gov/ij/>).

GFP signal intensity measurements for STAT-GFP reporter and miR8-GAL4 flies.

Enhancer traps, either by direct GFP insertion or GAL-4 mediated expression of a reporter protein, allow determining relative gene expression levels. Fluorescent reporters of Analysis were performed on single stack images acquired with same settings, outlining each cell as a region of interest (ROI) and measuring area and fluorescence as mean of each pixel signals per ROI.

Ex-vivo time lapse imaging

Guts were dissected on ice and mounted on glass slides in PBS with a glass coverslip. Preparations were sealed with nail polish and immediately imaged at room temperature in the inverted confocal with 20X dry objective or 40X oil immersion. Multichannel acquisition was performed every 5 minutes for 2 to 6 hours. Automated stage allowed to sequentially scan more than one position of the preparation. Several Z stacks at 1 μ m distance were taken at each time point. Reconstruction and analysis was performed with FIJI version of Image J.

Bibliography



References

- Alberga, A., Boulay, J.L., Kempe, E., Dennefeld, C., and Haenlin, M. (1991). The snail gene required for mesoderm formation in *Drosophila* is expressed dynamically in derivatives of all three germ layers. *Development* *111*, 983-992.
- Albrecht, S.C., Barata, A.G., Grosshans, J., Teleman, A.A., and Dick, T.P. (2011). In vivo mapping of hydrogen peroxide and oxidized glutathione reveals chemical and regional specificity of redox homeostasis. *Cell Metab* *14*, 819-829.
- Ambros, V. (2001). microRNAs: tiny regulators with great potential. *Cell* *107*, 823-826.
- Amcheslavsky, A., Ito, N., Jiang, J., and Ip, Y.T. (2011). Tuberous sclerosis complex and Myc coordinate the growth and division of *Drosophila* intestinal stem cells. *J Cell Biol* *193*, 695-710.
- Amcheslavsky, A., Jiang, J., and Ip, Y.T. (2009). Tissue Damage-Induced Intestinal Stem Cell Division in *Drosophila*. *Cell Stem Cell* *4*, 49-61.
- Apidianakis, Y., Pitsouli, C., Perrimon, N., and Rahme, L. (2009). Synergy between bacterial infection and genetic predisposition in intestinal dysplasia. *Proc Natl Acad Sci U S A* *106*, 20883-20888.
- Arai, F., and Suda, T. (2007). Maintenance of quiescent hematopoietic stem cells in the osteoblastic niche. *Ann N Y Acad Sci*, *1*.
- Ashraf, S.I., Hu, X., Roote, J., and Ip, Y.T. (1999). The mesoderm determinant snail collaborates with related zinc-finger proteins to control *Drosophila* neurogenesis. *EMBO J* *18*, 6426-6438.
- Bardin, A.J., Perdigoto, C.N., Southall, T.D., Brand, A.H., and Schweisguth, F. (2010). Transcriptional control of stem cell maintenance in the *Drosophila* intestine. *Development* *137*, 705-714.
- Barker, N. (2014). Adult intestinal stem cells: critical drivers of epithelial homeostasis and regeneration. *Nat Rev Mol Cell Biol* *15*, 19-33.
- Barker, N., Ridgway, R.A., van Es, J.H., van de Wetering, M., Begthel, H., van den Born, M., Danenberg, E., Clarke, A.R., Sansom, O.J., and Clevers, H. (2009). Crypt stem cells as the cells-of-origin of intestinal cancer. *Nature* *457*, 608-611.

Barker, N., van Es, J.H., Kuipers, J., Kujala, P., van den Born, M., Cozijnsen, M., Haegebarth, A., Korving, J., Begthel, H., Peters, P.J., *et al.* (2007). Identification of stem cells in small intestine and colon by marker gene Lgr5. *Nature* 449, 1003-1007.

Barrallo-Gimeno, A., and Nieto, M.A. (2005). The Snail genes as inducers of cell movement and survival: implications in development and cancer. *Development* 132, 3151-3161.

Barrallo-Gimeno, A., and Nieto, M.A. (2009). Evolutionary history of the Snail/Scratch superfamily. *Trends in genetics : TIG* 25, 248-252.

Bartel, D.P. (2004). MicroRNAs: Genomics, Biogenesis, Mechanism, and Function. *Cell* 116, 281-297.

Baumann, O. (2001). Posterior midgut epithelial cells differ in their organization of the membrane skeleton from other *Drosophila* epithelia. *Exp Cell Res* 270, 176-187.

Beebe, K., Lee, W.C., and Micchelli, C.A. (2010). JAK/STAT signaling coordinates stem cell proliferation and multilineage differentiation in the *Drosophila* intestinal stem cell lineage. *Dev Biol* 338, 28-37.

Bellen, H.J., Levis, R.W., Liao, G., He, Y., Carlson, J.W., Tsang, G., Evans-Holm, M., Hiesinger, P.R., Schulze, K.L., Rubin, G.M., *et al.* (2004). The BDGP gene disruption project: single transposon insertions associated with 40% of *Drosophila* genes. *Genetics* 167, 761-781.

Bellen, H.J., O'Kane, C.J., Wilson, C., Grossniklaus, U., Pearson, R.K., and Gehring, W.J. (1989). P-element-mediated enhancer detection: a versatile method to study development in *Drosophila*. *Genes & development* 3, 1288-1300.

Bier, E. (2005). *Drosophila*, the golden bug, emerges as a tool for human genetics. *Nat Rev Genet* 6, 9-23.

Bier, E., Vaessin, H., Shepherd, S., Lee, K., McCall, K., Barbel, S., Ackerman, L., Carretto, R., Uemura, T., Grell, E., *et al.* (1989). Searching for pattern and mutation in the *Drosophila* genome with a P-lacZ vector. *Genes & development* 3, 1273-1287.

Biteau, B., Hochmuth, C.E., and Jasper, H. (2008). JNK activity in somatic stem cells causes loss of tissue homeostasis in the aging *Drosophila* gut. *Cell Stem Cell* 3, 442-455.

Biteau, B., Hochmuth, C.E., and Jasper, H. (2011). Maintaining tissue homeostasis: dynamic control of somatic stem cell activity. *Cell Stem Cell* 9, 402-411.

Biteau, B., and Jasper, H. (2011). EGF signaling regulates the proliferation of intestinal stem cells in *Drosophila*. *Development* 138, 1045-1055.

Biteau, B., Karpac, J., Supoyo, S., Degennaro, M., Lehmann, R., and Jasper, H. (2010). Lifespan extension by preserving proliferative homeostasis in *Drosophila*. *PLoS Genet* 6, e1001159.

Blanpain, C., and Fuchs, E. (2009). Epidermal homeostasis: a balancing act of stem cells in the skin. *Nat Rev Mol Cell Biol* 10, 207-217.

Bond, D., and Foley, E. (2012). Autocrine platelet-derived growth factor-vascular endothelial growth factor receptor-related (Pvr) pathway activity controls intestinal stem cell proliferation in the adult *Drosophila* midgut. *J Biol Chem* 287, 27359-27370.

Bonnay, F., Cohen-Berros, E., Hoffmann, M., Kim, S.Y., Boulianne, G.L., Hoffmann, J.A., Matt, N., and Reichhart, J.M. (2013). big bang gene modulates gut immune tolerance in *Drosophila*. *Proc Natl Acad Sci U S A* 110, 2957-2962.

Boulay, J.L., Dennefeld, C., and Alberga, A. (1987). The *Drosophila* developmental gene snail encodes a protein with nucleic acid binding fingers. *Nature* 330, 395-398.

Boutet, A., De Frutos, C.A., Maxwell, P.H., Mayol, M.J., Romero, J., and Nieto, M.A. (2006). Snail activation disrupts tissue homeostasis and induces fibrosis in the adult kidney. *EMBO J* 25, 5603-5613.

Boutet, A., Esteban, M.A., Maxwell, P.H., and Nieto, M.A. (2007). Reactivation of Snail genes in renal fibrosis and carcinomas: a process of reversed embryogenesis? *Cell Cycle* 6, 638-642.

Bowman, S.K., Rolland, V., Betschinger, J., Kinsey, K.A., Emery, G., and Knoblich, J.A. (2008). The tumor suppressors Brat and Numb regulate transit-amplifying neuroblast lineages in *Drosophila*. *Dev Cell* 14, 535-546.

Bracken, C.P., Gregory, P.A., Kolesnikoff, N., Bert, A.G., Wang, J., Shannon, M.F., and Goodall, G.J. (2008). A double-negative feedback loop between ZEB1-SIP1 and the microRNA-200 family regulates epithelial-mesenchymal transition. *Cancer Res* 68, 7846-7854.

Brand, A.H., and Perrimon, N. (1993). Targeted gene expression as a means of altering cell fates and generating dominant phenotypes. *Development* 118, 401-415.

Brumby, A.M., and Richardson, H.E. (2005). Using *Drosophila melanogaster* to map human cancer pathways. *Nature reviews Cancer* 5, 626-639.

Buchon, N., Broderick, N.A., Chakrabarti, S., and Lemaitre, B. (2009a). Invasive and indigenous microbiota impact intestinal stem cell activity through multiple pathways in *Drosophila*. *Genes & development* 23, 2333-2344.

Buchon, N., Broderick, N.A., Kuraishi, T., and Lemaitre, B. (2010). *Drosophila* EGFR pathway coordinates stem cell proliferation and gut remodeling following infection. *BMC biology* 8, 152.

Buchon, N., Broderick, N.A., Poidevin, M., Pradervand, S., and Lemaitre, B. (2009b). *Drosophila* intestinal response to bacterial infection: activation of host defense and stem cell proliferation. *Cell Host Microbe* 5, 200-211.

Burk, U., Schubert, J., Wellner, U., Schmalhofer, O., Vincan, E., Spaderna, S., and Brabletz, T. (2008). A reciprocal repression between ZEB1 and members of the miR-200 family promotes EMT and invasion in cancer cells. *EMBO Rep* 9, 582-589.

Bus, J.S., and Gibson, J.E. (1984). Paraquat: model for oxidant-initiated toxicity. *Environmental health perspectives* 55, 37-46.

Bushati, N., and Cohen, S.M. (2007). microRNA functions. *Annu Rev Cell Dev Biol* 23, 175-205.

Buszczak, M., Paterno, S., and Spradling, A.C. (2009). *Drosophila* stem cells share a common requirement for the histone H2B ubiquitin protease scrawny. *Science* 323, 248-251.

Cairns, J. (1975a). The cancer problem. *Sci Am* 233, 64-72.

Cairns, J. (1975b). Mutation selection and the natural history of cancer. *Nature* 255, 197-200.

Cannon, W.B. (1941). The Body Physiologic and the Body Politic. *Science* 93, 1-10.

Cano, A., and Nieto, M.A. (2008). Non-coding RNAs take centre stage in epithelial-to-mesenchymal transition. *Trends in cell biology* 18, 357-359.

Cano, A., Perez-Moreno, M.A., Rodrigo, I., Locascio, A., Blanco, M.J., del Barrio, M.G., Portillo, F., and Nieto, M.A. (2000). The transcription factor snail controls epithelial-mesenchymal transitions by repressing E-cadherin expression. *Nature cell biology* 2, 76-83.

Casali, A., and Batlle, E. (2009). Intestinal stem cells in mammals and *Drosophila*. *Cell Stem Cell* 4, 124-127.

- Castle, W.E. (1906). Inbreeding, Cross-Breeding and Sterility in *Drosophila*. *Science* 23, 153.
- Clayton, E., Doupe, D.P., Klein, A.M., Winton, D.J., Simons, B.D., and Jones, P.H. (2007). A single type of progenitor cell maintains normal epidermis. *Nature* 446, 185-189.
- Clyne, P.J., Brotman, J.S., Sweeney, S.T., and Davis, G. (2003). Green fluorescent protein tagging *Drosophila* proteins at their native genomic loci with small P elements. *Genetics* 165, 1433-1441.
- Comijn, J., Berx, G., Vermassen, P., Verschuere, K., van Grunsven, L., Bruyneel, E., Mareel, M., Huylebroeck, D., and van Roy, F. (2001). The two-handed E box binding zinc finger protein SIP1 downregulates E-cadherin and induces invasion. *Molecular cell* 7, 1267-1278.
- Conder, R., and Knoblich, J.A. (2009). Fly stem cell research gets infectious. *Cell* 137, 1185-1187.
- Cordero, J.B., Ridgway, R.A., Valeri, N., Nixon, C., Frame, M.C., Muller, W.J., Vidal, M., and Sansom, O.J. (2014). c-Src drives intestinal regeneration and transformation. *The EMBO Journal* 33, 1474-1491.
- Cordero, J.B., Stefanatos, R.K., Myant, K., Vidal, M., and Sansom, O.J. (2012a). Non-autonomous crosstalk between the Jak/Stat and Egfr pathways mediates Apcl-driven intestinal stem cell hyperplasia in the *Drosophila* adult midgut. *Development* 139, 4524-4535.
- Cordero, J.B., Stefanatos, R.K., Scopelliti, A., Vidal, M., and Sansom, O.J. (2012b). Inducible progenitor-derived Wingless regulates adult midgut regeneration in *Drosophila*. *Embo J* 31, 3901-3917.
- Cotsarelis, G., Sun, T.T., and Lavker, R.M. (1990). Label-retaining cells reside in the bulge area of pilosebaceous unit: implications for follicular stem cells, hair cycle, and skin carcinogenesis. *Cell* 61, 1329-1337.
- Cronin, S.J., Nehme, N.T., Limmer, S., Liegeois, S., Pospisilik, J.A., Schramek, D., Leibbrandt, A., Simoes Rde, M., Gruber, S., Puc, U., *et al.* (2009). Genome-wide RNAi screen identifies genes involved in intestinal pathogenic bacterial infection. *Science* 325, 340-343.
- Crosnier, C., Stamatakis, D., and Lewis, J. (2006). Organizing cell renewal in the intestine: stem cells, signals and combinatorial control. *Nat Rev Genet* 7, 349-359.
- Chaffer, C.L., Thompson, E.W., and Williams, E.D. (2007). Mesenchymal to Epithelial Transition in Development and Disease. *Cells Tissues Organs* 185, 7-19.

Chatterjee, M., and Ip, Y.T. (2009). Pathogenic stimulation of intestinal stem cell response in *Drosophila*. *J Cell Physiol* 220, 664-671.

Chien, S., Reiter, L.T., Bier, E., and Gribskov, M. (2002). Homophila: human disease gene cognates in *Drosophila*. *Nucleic acids research* 30, 149-151.

Choi, N.H., Kim, J.G., Yang, D.J., Kim, Y.S., and Yoo, M.A. (2008a). Age-related changes in *Drosophila* midgut are associated with PVF2, a PDGF/VEGF-like growth factor. *Aging Cell* 7, 318-334.

Choi, N.H., Lucchetta, E., and Ohlstein, B. (2011). Nonautonomous regulation of *Drosophila* midgut stem cell proliferation by the insulin-signaling pathway. *Proc Natl Acad Sci U S A* 108, 18702-18707.

Choi, Y.J., Hwang, M.S., Park, J.S., Bae, S.K., Kim, Y.S., and Yoo, M.A. (2008b). Age-related upregulation of *Drosophila* caudal gene via NF-kappaB in the adult posterior midgut. *Biochim Biophys Acta* 10, 7.

Christoffersen, N.R., Silahatoglu, A., Orom, U.A., Kauppinen, S., and Lund, A.H. (2007). miR-200b mediates post-transcriptional repression of ZFHX1B. *RNA (New York, NY)* 13, 1172-1178.

Christofi, T., and Apidianakis, Y. (2013). Ras-oncogenic *Drosophila* hindgut but not midgut cells use an inflammation-like program to disseminate to distant sites. *Gut Microbes* 4, 54-59.

De Craene, B., Denecker, G., Vermassen, P., Taminau, J., Mauch, C., Derore, A., Jonkers, J., Fuchs, E., and Berx, G. (2014). Epidermal Snail expression drives skin cancer initiation and progression through enhanced cytoprotection, epidermal stem/progenitor cell expansion and enhanced metastatic potential. *Cell death and differentiation* 21, 310-320.

de Frutos, C.A., Dacquin, R., Vega, S., Jurdic, P., Machuca-Gayet, I., and Nieto, M.A. (2009). Snail1 controls bone mass by regulating Runx2 and VDR expression during osteoblast differentiation. *EMBO J* 28, 686-696.

de Navascues, J., Perdigoto, C.N., Bian, Y., Schneider, M.H., Bardin, A.J., Martinez-Arias, A., and Simons, B.D. (2012). *Drosophila* midgut homeostasis involves neutral competition between symmetrically dividing intestinal stem cells. *Embo J* 31, 2473-2485.

Dietzl, G., Chen, D., Schnorrer, F., Su, K.C., Barinova, Y., Fellner, M., Gasser, B., Kinsey, K., Oppel, S., Scheiblaue, S., *et al.* (2007). A genome-wide transgenic RNAi library for conditional gene inactivation in *Drosophila*. *Nature* 448, 151-156.

- Domínguez, D., Montserrat-Sentís, B., Virgós-Soler, A., Guaita, S., Grueso, J., Porta, M., Puig, I., Baulida, J., Francí, C., and García de Herreros, A. (2003). Phosphorylation Regulates the Subcellular Location and Activity of the Snail Transcriptional Repressor. *Molecular and cellular biology* 23, 5078-5089.
- Doupe, D.P., Klein, A.M., Simons, B.D., and Jones, P.H. (2010). The ordered architecture of murine ear epidermis is maintained by progenitor cells with random fate. *Dev Cell* 18, 317-323.
- Dykxhoorn, D.M., Wu, Y., Xie, H., Yu, F., Lal, A., Petrocca, F., Martinvalet, D., Song, E., Lim, B., and Lieberman, J. (2009). miR-200 Enhances Mouse Breast Cancer Cell Colonization to Form Distant Metastases. *PLoS ONE* 4, e7181.
- Edwards, P.A. (1999). The impact of developmental biology on cancer research: an overview. *Cancer Metastasis Rev* 18, 175-180.
- Ekimler, S., and Sahin, K. (2014). Computational Methods for MicroRNA Target Prediction. *Genes* 5, 671-683.
- Elgendy, M., Sheridan, C., Brumatti, G., and Martin, S.J. (2011). Oncogenic Ras-induced expression of Noxa and Beclin-1 promotes autophagic cell death and limits clonogenic survival. *Molecular cell* 42, 23-35.
- Evan, G.I., and Vousden, K.H. (2001). Proliferation, cell cycle and apoptosis in cancer. *Nature* 411, 342-348.
- Evdokimova, V., Tognon, C., Ng, T., Ruzanov, P., Melnyk, N., Fink, D., Sorokin, A., Ovchinnikov, L.P., Davicioni, E., Triche, T.J., *et al.* Translational Activation of Snail1 and Other Developmentally Regulated Transcription Factors by YB-1 Promotes an Epithelial-Mesenchymal Transition. *Cancer cell* 15, 402-415.
- Flynt, A.S., and Patton, J.G. (2010). Crosstalk between planar cell polarity signaling and miR-8 control of NHERF1-mediated actin reorganization. *Cell Cycle* 9, 235-237.
- Fodde, R. (2009). The stem of cancer. *Cancer cell* 15, 87-89.
- Foudi, A., Hochedlinger, K., Van Buren, D., Schindler, J.W., Jaenisch, R., Carey, V., and Hock, H. (2009). Analysis of histone 2B-GFP retention reveals slowly cycling hematopoietic stem cells. *Nat Biotechnol* 27, 84-90.

- Fox, D.T., and Spradling, A.C. (2009). The *Drosophila* hindgut lacks constitutively active adult stem cells but proliferates in response to tissue damage. *Cell Stem Cell* 5, 290-297.
- Fre, S., Bardin, A., Robine, S., and Louvard, D. (2011). Notch signaling in intestinal homeostasis across species: the cases of *Drosophila*, Zebrafish and the mouse. *Exp Cell Res* 317, 2740-2747.
- Fuchs, E. (2009). The tortoise and the hair: slow-cycling cells in the stem cell race. *Cell* 137, 811-819.
- Fulda, S., and Vucic, D. (2012). Targeting IAP proteins for therapeutic intervention in cancer. *Nat Rev Drug Discov* 11, 109-124.
- Fuse, N., Hirose, S., and Hayashi, S. (1994). Diploidy of *Drosophila* imaginal cells is maintained by a transcriptional repressor encoded by escargot. *Genes & development* 8, 2270-2281.
- Fuse, N., Hirose, S., and Hayashi, S. (1996). Determination of wing cell fate by the escargot and snail genes in *Drosophila*. *Development* 122, 1059-1067.
- Geminard, C., Rulifson, E.J., and Leopold, P. (2009). Remote control of insulin secretion by fat cells in *Drosophila*. *Cell Metab* 10, 199-207.
- Gill, J.G., Langer, E.M., Lindsley, R.C., Cai, M., Murphy, T.L., Kyba, M., and Murphy, K.M. (2011). Snail and the microRNA-200 family act in opposition to regulate epithelial-to-mesenchymal transition and germ layer fate restriction in differentiating ESCs. *Stem cells (Dayton, Ohio)* 29, 764-776.
- Golic, K.G., and Lindquist, S. (1989). The FLP recombinase of yeast catalyzes site-specific recombination in the *Drosophila* genome. *Cell* 59, 499-509.
- Goulas, S., Conder, R., and Knoblich, J.A. (2012). The Par complex and integrins direct asymmetric cell division in adult intestinal stem cells. *Cell Stem Cell* 11, 529-540.
- Green, D.R., and Evan, G.I. (2002). A matter of life and death. *Cancer cell* 1, 19-30.
- Greenspan, R.J. (2004). Fly pushing : the theory and practice of *Drosophila* genetics, 2nd edn (Cold Spring Harbor, N.Y.: Cold Spring Harbor Laboratory Press).
- Gregory, P.A., Bert, A.G., Paterson, E.L., Barry, S.C., Tsykin, A., Farshid, G., Vadas, M.A., Khew-Goodall, Y., and Goodall, G.J. (2008). The miR-200 family and miR-205 regulate epithelial to mesenchymal transition by targeting ZEB1 and SIP1. *Nature cell biology* 10, 593-601.

- Grun, D., Wang, Y.L., Langenberger, D., Gunsalus, K.C., and Rajewsky, N. (2005). microRNA target predictions across seven *Drosophila* species and comparison to mammalian targets. *PLoS computational biology* 1, e13.
- Guo, Z., Driver, I., and Ohlstein, B. (2013). Injury-induced BMP signaling negatively regulates *Drosophila* midgut homeostasis. *J Cell Biol* 201, 945-961.
- Hadjieconomou, D., Rotkopf, S., Alexandre, C., Bell, D.M., Dickson, B.J., and Salecker, I. (2011). Flybow: genetic multicolor cell labeling for neural circuit analysis in *Drosophila melanogaster*. *Nature methods* 8, 260-266.
- Hanahan, D., and Weinberg, R.A. (2011). Hallmarks of cancer: the next generation. *Cell* 144, 646-674.
- Hayashi, S., Hirose, S., Metcalfe, T., and Shirras, A.D. (1993). Control of imaginal cell development by the escargot gene of *Drosophila*. *Development* 118, 105-115.
- He, S., Nakada, D., and Morrison, S.J. (2009). Mechanisms of stem cell self-renewal. *Annu Rev Cell Dev Biol* 25, 377-406.
- Hochmuth, C.E., Biteau, B., Bohmann, D., and Jasper, H. (2011). Redox regulation by Keap1 and Nrf2 controls intestinal stem cell proliferation in *Drosophila*. *Cell Stem Cell* 8, 188-199.
- Hugo, H., Ackland, M.L., Blick, T., Lawrence, M.G., Clements, J.A., Williams, E.D., and Thompson, E.W. (2007). Epithelial—mesenchymal and mesenchymal—epithelial transitions in carcinoma progression. *Journal of Cellular Physiology* 213, 374-383.
- Hurteau, G.J., Carlson, J.A., Spivack, S.D., and Brock, G.J. (2007). Overexpression of the microRNA hsa-miR-200c leads to reduced expression of transcription factor 8 and increased expression of E-cadherin. *Cancer Res* 67, 7972-7976.
- Hussey, G.S., Chaudhury, A., Dawson, A.E., Lindner, D.J., Knudsen, C.R., Wilce, M.C., Merrick, W.C., and Howe, P.H. (2011). Identification of an mRNP complex regulating tumorigenesis at the translational elongation step. *Molecular cell* 41, 419-431.
- Hyun, S., Lee, J.H., Jin, H., Nam, J., Namkoong, B., Lee, G., Chung, J., and Kim, V.N. (2009). Conserved MicroRNA miR-8/miR-200 and its target USH/FOG2 control growth by regulating PI3K. *Cell* 139, 1096-1108.

Jiang, H., and Edgar, B.A. (2009). EGFR signaling regulates the proliferation of *Drosophila* adult midgut progenitors. *Development* 136, 483-493.

Jiang, H., and Edgar, B.A. (2012). Intestinal stem cell function in *Drosophila* and mice. *Curr Opin Genet Dev* 22, 354-360.

Jiang, H., Grenley, M.O., Bravo, M.J., Blumhagen, R.Z., and Edgar, B.A. (2011). EGFR/Ras/MAPK signaling mediates adult midgut epithelial homeostasis and regeneration in *Drosophila*. *Cell Stem Cell* 8, 84-95.

Jiang, H., Patel, P.H., Kohlmaier, A., Grenley, M.O., McEwen, D.G., and Edgar, B.A. (2009). Cytokine/Jak/Stat signaling mediates regeneration and homeostasis in the *Drosophila* midgut. *Cell* 137, 1343-1355.

Jin, H., Kim, V.N., and Hyun, S. (2012). Conserved microRNA miR-8 controls body size in response to steroid signaling in *Drosophila*. *Genes & development* 26, 1427-1432.

Karpac, J., Younger, A., and Jasper, H. (2011). Dynamic coordination of innate immune signaling and insulin signaling regulates systemic responses to localized DNA damage. *Dev Cell* 20, 841-854.

Karpowicz, P., Perez, J., and Perrimon, N. (2010). The Hippo tumor suppressor pathway regulates intestinal stem cell regeneration. *Development* 137, 4135-4145.

Karres, J.S., Hilgers, V., Carrera, I., Treisman, J., and Cohen, S.M. (2007). The conserved microRNA miR-8 tunes atrophin levels to prevent neurodegeneration in *Drosophila*. *Cell* 131, 136-145.

Keck, B., Wach, S., Goebell, P.J., Kunath, F., Bertz, S., Lehmann, J., Stockle, M., Taubert, H., Wullich, B., and Hartmann, A. (2013). SNAI1 protein expression is an independent negative prognosticator in muscle-invasive bladder cancer. *Annals of surgical oncology* 20, 3669-3674.

Kennell, J.A., Cadigan, K.M., Shakhmantsir, I., and Waldron, E.J. (2012). The microRNA miR-8 is a positive regulator of pigmentation and eclosion in *Drosophila*. *Dev Dyn* 241, 161-168.

Kennell, J.A., Gerin, I., MacDougald, O.A., and Cadigan, K.M. (2008). The microRNA miR-8 is a conserved negative regulator of Wnt signaling. *Proc Natl Acad Sci U S A* 105, 15417-15422.

Kim, M.K., Kim, M.A., Kim, H., Kim, Y.B., and Song, Y.S. (2014a). Expression profiles of epithelial-mesenchymal transition-associated proteins in epithelial ovarian carcinoma. *BioMed research international* 2014, 495754.

- Kim, Y.H., Kim, G., Kwon, C.I., Kim, J.W., Park, P.W., and Hahm, K.B. (2014b). TWIST1 and SNAI1 as markers of poor prognosis in human colorectal cancer are associated with the expression of ALDH1 and TGF-beta1. *Oncology reports* 31, 1380-1388.
- Klein, A.M., Nakagawa, T., Ichikawa, R., Yoshida, S., and Simons, B.D. (2010). Mouse germ line stem cells undergo rapid and stochastic turnover. *Cell Stem Cell* 7, 214-224.
- Knoblich, J.A. (2008). Mechanisms of Asymmetric Stem Cell Division. *Cell* 132, 583-597.
- Korpai, M., Lee, E.S., Hu, G., and Kang, Y. (2008). The miR-200 family inhibits epithelial-mesenchymal transition and cancer cell migration by direct targeting of E-cadherin transcriptional repressors ZEB1 and ZEB2. *J Biol Chem* 283, 14910-14914.
- Kuwamura, M., Maeda, K., and Adachi-Yamada, T. (2010). Mathematical modelling and experiments for the proliferation and differentiation of *Drosophila* intestinal stem cells I. *J Biol Dyn* 4, 248-257.
- Kuwamura, M., Maeda, K., and Adachi-Yamada, T. (2012). Mathematical modelling and experiments for the proliferation and differentiation of *Drosophila* intestinal stem cells II. *J Biol Dyn* 6, 267-276.
- Langevin, J., Le Borgne, R., Rosenfeld, F., Gho, M., Schweisguth, F., and Bellaiche, Y. (2005). Lethal giant larvae controls the localization of notch-signaling regulators numb, neuralized, and Sanpodo in *Drosophila* sensory-organ precursor cells. *Curr Biol* 15, 955-962.
- Lee, T., and Luo, L. (1999). Mosaic analysis with a repressible cell marker for studies of gene function in neuronal morphogenesis. *Neuron* 22, 451-461.
- Lee, T., and Luo, L. (2001). Mosaic analysis with a repressible cell marker (MARCM) for *Drosophila* neural development. *Trends Neurosci* 24, 251-254.
- Lee, W.C., Beebe, K., Sudmeier, L., and Micchelli, C.A. (2009). Adenomatous polyposis coli regulates *Drosophila* intestinal stem cell proliferation. *Development* 136, 2255-2264.
- Leedham, S.J., Brittan, M., McDonald, S.A., and Wright, N.A. (2005). Intestinal stem cells. *J Cell Mol Med* 9, 11-24.
- Leopold, P., and Perrimon, N. (2007). *Drosophila* and the genetics of the internal milieu. *Nature* 450, 186-188.

Lewis, B.P., Burge, C.B., and Bartel, D.P. (2005). Conserved seed pairing, often flanked by adenosines, indicates that thousands of human genes are microRNA targets. *Cell* 120, 15-20.

Li, L., and Xie, T. (2005). Stem cell niche: structure and function. *Annu Rev Cell Dev Biol* 21, 605-631.

Lim, Y.-Y., Wright, J.A., Attema, J.L., Gregory, P.A., Bert, A.G., Smith, E., Thomas, D., Lopez, A.F., Drew, P.A., Khew-Goodall, Y., *et al.* (2013). Epigenetic modulation of the miR-200 family is associated with transition to a breast cancer stem-cell-like state. *Journal of Cell Science* 126, 2256-2266.

Lin, G., and Xi, R. (2008). Intestinal stem cell, muscular niche and Wingless signaling. *Fly* 2, 310-312.

Lin, G., Xu, N., and Xi, R. (2008). Paracrine Wingless signalling controls self-renewal of *Drosophila* intestinal stem cells. *Nature* 455, 1119-1123.

Lin, G., Xu, N., and Xi, R. (2010). Paracrine unpaired signaling through the JAK/STAT pathway controls self-renewal and lineage differentiation of *Drosophila* intestinal stem cells. *J Mol Cell Biol* 2, 37-49.

Liu, W., Singh, S.R., and Hou, S.X. (2010). JAK-STAT is restrained by Notch to control cell proliferation of the *Drosophila* intestinal stem cells. *J Cell Biochem* 109, 992-999.

Liu, Y.N., Yin, J.J., Abou-Kheir, W., Hynes, P.G., Casey, O.M., Fang, L., Yi, M., Stephens, R.M., Seng, V., Sheppard-Tillman, H., *et al.* (2013). MiR-1 and miR-200 inhibit EMT via Slug-dependent and tumorigenesis via Slug-independent mechanisms. *Oncogene* 32, 296-306.

Lopez-Garcia, C., Klein, A.M., Simons, B.D., and Winton, D.J. (2010). Intestinal stem cell replacement follows a pattern of neutral drift. *Science* 330, 822-825.

Loya, C.M., Lu, C.S., Van Vactor, D., and Fulga, T.A. (2009). Transgenic microRNA inhibition with spatiotemporal specificity in intact organisms. *Nature methods* 6, 897-903.

Loya, C.M., McNeill, E.M., Bao, H., Zhang, B., and Van Vactor, D. (2014). miR-8 controls synapse structure by repression of the actin regulator enabled. *Development* 141, 1864-1874.

Lu, C.S., Zhai, B., Mauss, A., Landgraf, M., Gygi, S., and Van Vactor, D. (2014). MicroRNA-8 promotes robust motor axon targeting by coordinate regulation of cell adhesion molecules during synapse development. *Philos Trans R Soc Lond B Biol Sci* 369.

Lucchetta, E.M., and Ohlstein, B. (2012). The *Drosophila* midgut: a model for stem cell driven tissue regeneration. *Wiley Interdiscip Rev Dev Biol* 1, 781-788.

Mani, S.A., Guo, W., Liao, M.J., Eaton, E.N., Ayyanan, A., Zhou, A.Y., Brooks, M., Reinhard, F., Zhang, C.C., Shiptsin, M., *et al.* (2008). The epithelial-mesenchymal transition generates cells with properties of stem cells. *Cell* *133*, 704-715.

Manzanares, M., Locascio, A., and Nieto, M.A. (2001). The increasing complexity of the Snail gene superfamily in metazoan evolution. *Trends in genetics : TIG* *17*, 178-181.

McCurrach, M.E., Connor, T.M., Knudson, C.M., Korsmeyer, S.J., and Lowe, S.W. (1997). bax-deficiency promotes drug resistance and oncogenic transformation by attenuating p53-dependent apoptosis. *Proc Natl Acad Sci U S A* *94*, 2345-2349.

McGuire, S.E., Le, P.T., Osborn, A.J., Matsumoto, K., and Davis, R.L. (2003). Spatiotemporal rescue of memory dysfunction in *Drosophila*. *Science* *302*, 1765-1768.

McGuire, S.E., Mao, Z., and Davis, R.L. (2004). Spatiotemporal gene expression targeting with the TARGET and gene-switch systems in *Drosophila*. *Science's STKE : signal transduction knowledge environment* *2004*, p16.

McLeod, C.J., Wang, L., Wong, C., and Jones, D.L. (2010). Stem cell dynamics in response to nutrient availability. *Curr Biol* *20*, 2100-2105.

Micchelli, C.A., and Perrimon, N. (2006). Evidence that stem cells reside in the adult *Drosophila* midgut epithelium. *Nature* *439*, 475-479.

Micchelli, C.A., Sudmeier, L., Perrimon, N., Tang, S., and Beehler-Evans, R. (2011). Identification of adult midgut precursors in *Drosophila*. *Gene Expr Patterns* *11*, 12-21.

Mingot, J.M., Vega, S., Maestro, B., Sanz, J.M., and Nieto, M.A. (2009). Characterization of Snail nuclear import pathways as representatives of C2H2 zinc finger transcription factors. *J Cell Sci* *122*, 1452-1460.

Miranda, K.C., Huynh, T., Tay, Y., Ang, Y.S., Tam, W.L., Thomson, A.M., Lim, B., and Rigoutsos, I. (2006). A pattern-based method for the identification of MicroRNA binding sites and their corresponding heteroduplexes. *Cell* *126*, 1203-1217.

Morante, J., Vallejo, D.M., Desplan, C., and Dominguez, M. (2013). Conserved miR-8/miR-200 defines a glial niche that controls neuroepithelial expansion and neuroblast transition. *Dev Cell* *27*, 174-187.

- Morin, X., Daneman, R., Zavortink, M., and Chia, W. (2001). A protein trap strategy to detect GFP-tagged proteins expressed from their endogenous loci in *Drosophila*. *Proc Natl Acad Sci U S A* 98, 15050-15055.
- Morrison, S.J., and Kimble, J. (2006). Asymmetric and symmetric stem-cell divisions in development and cancer. *Nature* 441, 1068-1074.
- Morrison, S.J., and Spradling, A.C. (2008). Stem cells and niches: mechanisms that promote stem cell maintenance throughout life. *Cell* 132, 598-611.
- Myant, K.B., Scopelliti, A., Haque, S., Vidal, M., Sansom, O.J., and Cordero, J.B. (2013). Rac1 drives intestinal stem cell proliferation and regeneration. *Cell Cycle* 12, 2973-2977.
- Nakagoshi, H. (2005). Functional specification in the *Drosophila* endoderm. *Dev Growth Differ* 47, 383-392.
- Ni, J.Q., Liu, L.P., Binari, R., Hardy, R., Shim, H.S., Cavallaro, A., Booker, M., Pfeiffer, B.D., Markstein, M., Wang, H., *et al.* (2009). A *Drosophila* resource of transgenic RNAi lines for neurogenetics. *Genetics* 182, 1089-1100.
- Ni, J.Q., Markstein, M., Binari, R., Pfeiffer, B., Liu, L.P., Villalta, C., Booker, M., Perkins, L., and Perrimon, N. (2008). Vector and parameters for targeted transgenic RNA interference in *Drosophila melanogaster*. *Nature methods* 5, 49-51.
- Nieto, M.A. (2002). The snail superfamily of zinc-finger transcription factors. *Nat Rev Mol Cell Biol* 3, 155-166.
- Nieto, M.A. (2009). Epithelial-Mesenchymal Transitions in development and disease: old views and new perspectives. *The International journal of developmental biology* 53, 1541-1547.
- Nieto, M.A. (2011). The ins and outs of the epithelial to mesenchymal transition in health and disease. *Annu Rev Cell Dev Biol* 27, 347-376.
- Nieto, M.A., Sargent, M.G., Wilkinson, D.G., and Cooke, J. (1994). Control of cell behavior during vertebrate development by Slug, a zinc finger gene. *Science* 264, 835-839.
- Nystul, T.G., and Spradling, A.C. (2006). Breaking out of the mold: diversity within adult stem cells and their niches. *Curr Opin Genet Dev* 16, 463-468.

- O'Brien, L.E., Soliman, S.S., Li, X., and Bilder, D. (2011). Altered modes of stem cell division drive adaptive intestinal growth. *Cell* 147, 603-614.
- Oda, H., Tsukita, S., and Takeichi, M. (1998). Dynamic Behavior of the Cadherin-Based Cell–Cell Adhesion System during *Drosophila* Gastrulation. *Developmental Biology* 203, 435-450.
- Ohlstein, B., Kai, T., Decotto, E., and Spradling, A. (2004). The stem cell niche: theme and variations. *Curr Opin Cell Biol* 16, 693-699.
- Ohlstein, B., and Spradling, A. (2006). The adult *Drosophila* posterior midgut is maintained by pluripotent stem cells. *Nature* 439, 470-474.
- Ohlstein, B., and Spradling, A. (2007). Multipotent *Drosophila* intestinal stem cells specify daughter cell fates by differential notch signaling. *Science* 315, 988-992.
- Orford, K.W., and Scadden, D.T. (2008). Deconstructing stem cell self-renewal: genetic insights into cell-cycle regulation. *Nat Rev Genet* 9, 115-128.
- Osman, D., Buchon, N., Chakrabarti, S., Huang, Y.T., Su, W.C., Poidevin, M., Tsai, Y.C., and Lemaitre, B. (2012). Autocrine and paracrine unpaired signaling regulate intestinal stem cell maintenance and division. *J Cell Sci* 125, 5944-5949.
- Overmeyer, J.H., Kaul, A., Johnson, E.E., and Maltese, W.A. (2008). Active ras triggers death in glioblastoma cells through hyperstimulation of macropinocytosis. *Molecular cancer research : MCR* 6, 965-977.
- Pardal, R., Clarke, M.F., and Morrison, S.J. (2003). Applying the principles of stem-cell biology to cancer. *Nature reviews Cancer* 3, 895-902.
- Park, J.S., Kim, Y.S., and Yoo, M.A. (2009). The role of p38b MAPK in age-related modulation of intestinal stem cell proliferation and differentiation in *Drosophila*. *Aging* 1, 637-651.
- Park, J.S., Lee, S.H., Na, H.J., Pyo, J.H., Kim, Y.S., and Yoo, M.A. (2012). Age- and oxidative stress-induced DNA damage in *Drosophila* intestinal stem cells as marked by Gamma-H2AX. *Exp Gerontol* 47, 401-405.
- Park, S.M., Gaur, A.B., Lengyel, E., and Peter, M.E. (2008). The miR-200 family determines the epithelial phenotype of cancer cells by targeting the E-cadherin repressors ZEB1 and ZEB2. *Genes & development* 22, 894-907.

Park, S.Y., Kim, H.S., Kim, N.H., Ji, S., Cha, S.Y., Kang, J.G., Ota, I., Shimada, K., Konishi, N., Nam, H.W., *et al.* (2010). Snail1 is stabilized by O-GlcNAc modification in hyperglycaemic condition. *EMBO J* 29, 3787-3796.

Peinado, H., Del Carmen Iglesias-de la Cruz, M., Olmeda, D., Csiszar, K., Fong, K.S., Vega, S., Nieto, M.A., Cano, A., and Portillo, F. (2005). A molecular role for lysyl oxidase-like 2 enzyme in snail regulation and tumor progression. *EMBO J* 24, 3446-3458.

Pellettieri, J., and Sanchez Alvarado, A. (2007). Cell turnover and adult tissue homeostasis: from humans to planarians. *Annu Rev Genet* 41, 83-105.

Perez-Moreno, M.A., Locascio, A., Rodrigo, I., Dhondt, G., Portillo, F., Nieto, M.A., and Cano, A. (2001). A new role for E12/E47 in the repression of E-cadherin expression and epithelial-mesenchymal transitions. *J Biol Chem* 276, 27424-27431.

Potten, C.S., and Loeffler, M. (1990). Stem cells: attributes, cycles, spirals, pitfalls and uncertainties. Lessons for and from the crypt. *Development* 110, 1001-1020.

Potter, C.J., Tasic, B., Russler, E.V., Liang, L., and Luo, L. (2010). The Q system: a repressible binary system for transgene expression, lineage tracing, and mosaic analysis. *Cell* 141, 536-548.

Rando, T.A. (2006). Stem cells, ageing and the quest for immortality. *Nature* 441, 1080-1086.

Reed, J.C. (1998). Bcl-2 family proteins. *Oncogene* 17, 3225-3236.

Reiter, L.T., Potocki, L., Chien, S., Gribskov, M., and Bier, E. (2001). A systematic analysis of human disease-associated gene sequences in *Drosophila melanogaster*. *Genome research* 11, 1114-1125.

Ren, F., Wang, B., Yue, T., Yun, E.Y., Ip, Y.T., and Jiang, J. (2010). Hippo signaling regulates *Drosophila* intestine stem cell proliferation through multiple pathways. *Proc Natl Acad Sci U S A* 107, 21064-21069.

Rorth, P., Szabo, K., Bailey, A., Laverty, T., Rehm, J., Rubin, G.M., Weigmann, K., Milan, M., Benes, V., Ansorge, W., *et al.* (1998). Systematic gain-of-function genetics in *Drosophila*. *Development* 125, 1049-1057.

Ruby, J.G., Stark, A., Johnston, W.K., Kellis, M., Bartel, D.P., and Lai, E.C. (2007). Evolution, biogenesis, expression, and target predictions of a substantially expanded set of *Drosophila* microRNAs. *Genome research* 17, 1850-1864.

Sahai-Hernandez, P., Castanieto, A., and Nystul, T.G. (2012). *Drosophila* models of epithelial stem cells and their niches. *Wiley Interdiscip Rev Dev Biol* 1, 447-457.

Sarkisian, C.J., Keister, B.A., Stairs, D.B., Boxer, R.B., Moody, S.E., and Chodosh, L.A. (2007). Dose-dependent oncogene-induced senescence in vivo and its evasion during mammary tumorigenesis. *Nature cell biology* 9, 493-505.

Scheel, C., and Weinberg, R.A. (2012). Cancer stem cells and epithelial-mesenchymal transition: concepts and molecular links. *Seminars in cancer biology* 22, 396-403.

Serrano, M., Lin, A.W., McCurrach, M.E., Beach, D., and Lowe, S.W. (1997). Oncogenic ras provokes premature cell senescence associated with accumulation of p53 and p16INK4a. *Cell* 88, 593-602.

Sharpless, N.E., and DePinho, R.A. (2004). Telomeres, stem cells, senescence, and cancer. *The Journal of clinical investigation* 113, 160-168.

Shaw, R.L., Kohlmaier, A., Polesello, C., Veelken, C., Edgar, B.A., and Tapon, N. (2010). The Hippo pathway regulates intestinal stem cell proliferation during *Drosophila* adult midgut regeneration. *Development* 137, 4147-4158.

Shimono, Y., Zabala, M., Cho, R.W., Lobo, N., Dalerba, P., Qian, D., Diehn, M., Liu, H., Panula, S.P., Chiao, E., *et al.* (2009). Downregulation of miRNA-200c Links Breast Cancer Stem Cells with Normal Stem Cells. *Cell* 138, 592-603.

Simons, B.D., and Clevers, H. (2011a). Stem cell self-renewal in intestinal crypt. *Exp Cell Res* 317, 2719-2724.

Simons, B.D., and Clevers, H. (2011b). Strategies for homeostatic stem cell self-renewal in adult tissues. *Cell* 145, 851-862.

Singh, S.R., and Hou, S.X. (2009). Multipotent stem cells in the Malpighian tubules of adult *Drosophila melanogaster*. *J Exp Biol* 212, 413-423.

Singh, S.R., Zeng, X., Zheng, Z., and Hou, S.X. (2011). The adult *Drosophila* gastric and stomach organs are maintained by a multipotent stem cell pool at the foregut/midgut junction in the cardia (proventriculus). *Cell Cycle* 10, 1109-1120.

Slaidina, M., Delanoue, R., Gronke, S., Partridge, L., and Leopold, P. (2009). A *Drosophila* insulin-like peptide promotes growth during nonfeeding states. *Dev Cell* 17, 874-884.

- Snippert, H.J., and Clevers, H. (2011). Tracking adult stem cells. *EMBO Rep* 12, 113-122.
- Soengas, M.S., Alarcon, R.M., Yoshida, H., Giaccia, A.J., Hakem, R., Mak, T.W., and Lowe, S.W. (1999). Apaf-1 and caspase-9 in p53-dependent apoptosis and tumor inhibition. *Science* 284, 156-159.
- Southall, T.D., and Brand, A.H. (2009). Neural stem cell transcriptional networks highlight genes essential for nervous system development. *EMBO J* 28, 3799-3807.
- Spradling, A.C., Stern, D., Beaton, A., Rhem, E.J., Lavery, T., Mozden, N., Misra, S., and Rubin, G.M. (1999). The Berkeley *Drosophila* Genome Project gene disruption project: Single P-element insertions mutating 25% of vital *Drosophila* genes. *Genetics* 153, 135-177.
- Staley, B.K., and Irvine, K.D. (2010). Warts and Yorkie mediate intestinal regeneration by influencing stem cell proliferation. *Curr Biol* 20, 1580-1587.
- Stark, A., Brennecke, J., Bushati, N., Russell, R.B., and Cohen, S.M. (2005). Animal MicroRNAs confer robustness to gene expression and have a significant impact on 3'UTR evolution. *Cell* 123, 1133-1146.
- Strand, M., and Micchelli, C.A. (2011). Quiescent gastric stem cells maintain the adult *Drosophila* stomach. *Proc Natl Acad Sci U S A* 108, 17696-17701.
- Streit, A., Bernasconi, L., Sergeev, P., Cruz, A., and Steinmann-Zwicky, M. (2002). mgm 1, the earliest sex-specific germline marker in *Drosophila*, reflects expression of the gene *esg* in male stem cells. *The International journal of developmental biology* 46, 159-166.
- Struhl, G., and Basler, K. (1993). Organizing activity of wingless protein in *Drosophila*. *Cell* 72, 527-540.
- Takashima, S., Gold, D., and Hartenstein, V. (2013). Stem cells and lineages of the intestine: a developmental and evolutionary perspective. *Dev Genes Evol* 223, 85-102.
- Takashima, S., and Hartenstein, V. (2012). Genetic control of intestinal stem cell specification and development: a comparative view. *Stem cell reviews* 8, 597-608.
- Takashima, S., Mkrtychyan, M., Younossi-Hartenstein, A., Merriam, J.R., and Hartenstein, V. (2008). The behaviour of *Drosophila* adult hindgut stem cells is controlled by Wnt and Hh signalling. *Nature* 454, 651-655.

- Takeishi, A., Kuranaga, E., Tonoki, A., Misaki, K., Yonemura, S., Kanuka, H., and Miura, M. (2013). Homeostatic epithelial renewal in the gut is required for dampening a fatal systemic wound response in *Drosophila*. *Cell Rep* 3, 919-930.
- Tanaka-Matakatsu, M., Uemura, T., Oda, H., Takeichi, M., and Hayashi, S. (1996). Cadherin-mediated cell adhesion and cell motility in *Drosophila* trachea regulated by the transcription factor Escargot. *Development* 122, 3697-3705.
- Thiery, J.P., Acloque, H., Huang, R.Y., and Nieto, M.A. (2009). Epithelial-mesenchymal transitions in development and disease. *Cell* 139, 871-890.
- Tumbar, T., Guasch, G., Greco, V., Blanpain, C., Lowry, W.E., Rendl, M., and Fuchs, E. (2004). Defining the epithelial stem cell niche in skin. *Science* 303, 359-363.
- Valencia-Sanchez, M.A., Liu, J., Hannon, G.J., and Parker, R. (2006). Control of translation and mRNA degradation by miRNAs and siRNAs. *Genes & development* 20, 515-524.
- Vallejo, D.M., Caparros, E., and Dominguez, M. (2011). Targeting Notch signalling by the conserved miR-8/200 microRNA family in development and cancer cells. *EMBO J* 30, 756-769.
- Vega, S., Morales, A.V., Ocana, O.H., Valdes, F., Fabregat, I., and Nieto, M.A. (2004). Snail blocks the cell cycle and confers resistance to cell death. *Genes & development* 18, 1131-1143.
- Venken, K.J., Schulze, K.L., Haelterman, N.A., Pan, H., He, Y., Evans-Holm, M., Carlson, J.W., Levis, R.W., Spradling, A.C., Hoskins, R.A., *et al.* (2011). MiMIC: a highly versatile transposon insertion resource for engineering *Drosophila melanogaster* genes. *Nature methods* 8, 737-743.
- Vetter, G., Saumet, A., Moes, M., Vallar, L., Le Bechec, A., Laurini, C., Sabbah, M., Arar, K., Theillet, C., Lecellier, C.H., *et al.* (2010). miR-661 expression in SNAI1-induced epithelial to mesenchymal transition contributes to breast cancer cell invasion by targeting Nectin-1 and StarD10 messengers. *Oncogene* 29, 4436-4448.
- Vidal, M., and Cagan, R.L. (2006). *Drosophila* models for cancer research. *Curr Opin Genet Dev* 16, 10-16.
- Wang, C., Zhao, R., Huang, P., Yang, F., Quan, Z., Xu, N., and Xi, R. (2013). APC loss-induced intestinal tumorigenesis in *Drosophila*: Roles of Ras in Wnt signaling activation and tumor progression. *Dev Biol* 378, 122-140.

Wang, M.C., Bohmann, D., and Jasper, H. (2005). JNK extends life span and limits growth by antagonizing cellular and organism-wide responses to insulin signaling. *Cell* 121, 115-125.

Wang, P., and Hou, S.X. (2010). Regulation of intestinal stem cells in mammals and *Drosophila*. *J Cell Physiol* 222, 33-37.

Wellner, U., Schubert, J., Burk, U.C., Schmalhofer, O., Zhu, F., Sonntag, A., Waldvogel, B., Vannier, C., Darling, D., zur Hausen, A., *et al.* (2009). The EMT-activator ZEB1 promotes tumorigenicity by repressing stemness-inhibiting microRNAs. *Nature cell biology* 11, 1487-1495.

Whiteley, M., Noguchi, P.D., Sensabaugh, S.M., Odenwald, W.F., and Kassis, J.A. (1992). The *Drosophila* gene escargot encodes a zinc finger motif found in snail-related genes. *Mechanisms of development* 36, 117-127.

Whittaker, A.J., Royzman, I., and Orr-Weaver, T.L. (2000). *Drosophila* double parked: a conserved, essential replication protein that colocalizes with the origin recognition complex and links DNA replication with mitosis and the down-regulation of S phase transcripts. *Genes & development* 14, 1765-1776.

Wilson, A., Laurenti, E., Oser, G., van der Wath, R.C., Blanco-Bose, W., Jaworski, M., Offner, S., Dunant, C.F., Eshkind, L., Bockamp, E., *et al.* (2008). Hematopoietic stem cells reversibly switch from dormancy to self-renewal during homeostasis and repair. *Cell* 135, 1118-1129.

Wilson, A.A., and Kotton, D.N. (2008). Another notch in stem cell biology: *Drosophila* intestinal stem cells and the specification of cell fates. *Bioessays* 30, 107-109.

Wu, J.S., and Luo, L. (2006). A protocol for mosaic analysis with a repressible cell marker (MARCM) in *Drosophila*. *Nat Protoc* 1, 2583-2589.

Wu, Y., Deng, J., Rychahou, P.G., Qiu, S., Evers, B.M., and Zhou, B.P. (2009). Stabilization of snail by NF-kappaB is required for inflammation-induced cell migration and invasion. *Cancer cell* 15, 416-428.

Xu, N., Wang, S.Q., Tan, D., Gao, Y., Lin, G., and Xi, R. (2011). EGFR, Wntless and JAK/STAT signaling cooperatively maintain *Drosophila* intestinal stem cells. *Dev Biol* 354, 31-43.

Yamada, S., Okumura, N., Wei, L., Fuchs, B.C., Fujii, T., Sugimoto, H., Nomoto, S., Takeda, S., Tanabe, K.K., and Kodera, Y. (2014). Epithelial to Mesenchymal Transition is Associated with Shorter Disease-Free Survival in Hepatocellular Carcinoma. *Annals of surgical oncology*.

Yamashita, S., Miyagi, C., Fukada, T., Kagara, N., Che, Y.S., and Hirano, T. (2004). Zinc transporter LIVI controls epithelial-mesenchymal transition in zebrafish gastrula organizer. *Nature* 429, 298-302.

Yang, J., Mani, S.A., Donaher, J.L., Ramaswamy, S., Itzykson, R.A., Come, C., Savagner, P., Gitelman, I., Richardson, A., and Weinberg, R.A. (2004). Twist, a master regulator of morphogenesis, plays an essential role in tumor metastasis. *Cell* 117, 927-939.

Yin, C., Knudson, C.M., Korsmeyer, S.J., and Van Dyke, T. (1997). Bax suppresses tumorigenesis and stimulates apoptosis in vivo. *Nature* 385, 637-640.

Zeng, X., Chauhan, C., and Hou, S.X. (2010). Characterization of midgut stem cell- and enteroblast-specific Gal4 lines in *Drosophila*. *Genesis* 48, 607-611.

Zeng, X., Chauhan, C., and Hou, S.X. (2013). Stem cells in the *Drosophila* digestive system. *Adv Exp Med Biol* 786, 63-78.

Zhang, J., Cheng, Q., Zhou, Y., Wang, Y., and Chen, X. (2013). Slug is a key mediator of hypoxia induced cadherin switch in HNSCC: correlations with poor prognosis. *Oral oncology* 49, 1043-1050.

Zhu, L., Gibson, P., Curre, D.S., Tong, Y., Richardson, R.J., Bayazitov, I.T., Poppleton, H., Zakharenko, S., Ellison, D.W., and Gilbertson, R.J. (2009). Prominin 1 marks intestinal stem cells that are susceptible to neoplastic transformation. *Nature* 457, 603-607.

Books

Ashburner, M. 1989. ***Drosophila. A laboratory handbook***. Cold Spring Harbor Laboratory Press, Cold Spring Harbor, NY.

Demerec M. 1950. ***Biology of Drosophila***. Cold Spring Harbor Laboratory Press, Cold Spring Harbor, NY.

Greenspan, R. J. 1997. ***Fly pushing: the theory and practice of Drosophila genetics***. New York University

Web pages

<http://www.flybase.org> – A Database of *Drosophila* Genes & Genomes.

<http://www.flyatlas.org> – **FlyAtlas**: the *Drosophila* gene expression atlas.

<http://flyatlas.gla.ac.uk/> – **FlyAtlas 2**: provides advanced features for exploring how genes are expressed in the tissues of *Drosophila melanogaster*.

<http://flytrap.med.yale.edu/> – **FlyTrap**: GFP protein trap database.

<http://flymove.uni-muenster.de/> – **FlyMove**: a new way to look at development of *Drosophila*. Trends Genet (2003) 19, 310.

<http://stockcenter.vdrc.at/> - **Vienna *Drosophila* RNAi Center**: the VDRC maintains and makes available a total of 31,920 *Drosophila* transgenic RNAi lines.

<http://www.shigen.nig.ac.jp/fly/nigfly> - **NIG, National Institute of Genetics** (Japan): maintains and distributes RNAi transgenic *Drosophila melanogaster* strains for research (11,380 stocks for 6085 genes).

<http://kyotofly.kit.jp/cgi-bin/stocks/index.cgi> - **DGRC, *Drosophila* Genetic Resource Center, Kyoto Institute of Technology**: maintains and distributes *Drosophila melanogaster* strains for research.

<http://flystocks.bio.indiana.edu/> - **Bloomington *Drosophila* Stock Center at Indiana University**: the BDSC collects, maintains and distributes *Drosophila melanogaster* strains for research.

<http://rsb.info.nih.gov/ij/> – **ImageJ**: Open source software for image processing and analysis in Java; Rasband, W.S., ImageJ, National Institutes of Health, Bethesda, Maryland, USA, 1997-2004;

<http://rsb.info.nih.gov/ij/plugins/mbf/index.html> – **MBF ImageJ**: "ImageJ for Microscopy" collection of ~200 plugins collated and organized by Tony Collins at the [McMaster Biophotonics Facility](#).

<http://fiji.sc/wiki/index.php/Fiji> – **FIJI ImageJ**: "FIJI is Just ImageJ" is an open source platform for biological image analysis derived from ImageJ. Nature Methods (2012) 9(7): 676-682.

<http://dshb.biology.uiowa.edu/> – **DSHB**: Developmental Studies Hybridoma Bank, University of Iowa, Department of Biology. Monoclonal antibodies for use in research.

Glossary





Acronyms and Abbreviations

a: antibody

bp: base pair

DNA: deoxyribonucleic acid

EB: enteroblast cells

EC: enterocyte

ee: enteorendocrine cells

EMT: epithelial to mesenchymal transition

F1: 1st filial generation

Esg: escargot

GFP: green fluorescent protein

GOF: gain of function

H2B: histone 2B

hs: heat shock

kb: kilobase

ISCs: intestinal stem cells

LOF: loss of function

MARCM: mosaic analysis with a repressible cell marker

MET: mesenchymal to epithelial transition

mRNA: messenger RNA

miRNA: micro-RNA

PCR: polymerase chain reaction

PH3: phosphor-histone 3

RNA: ribonucleic acid

RNAi: RNA interference

ReDDM: repressible dual differential marker

RFP: red fluorescent protein

RT: room temperature

TARGET: temporal and regional gene expression targeting

TUNEL : terminal deoxynucleotidyl transferase-mediated dUTP nick end labeling

UAS: upstream activating sequence

vs: versus

WT: wild type

Definitions

Adult stem cells: cells in developed adult tissues that generate new stem cells as well as daughters that will eventually differentiate

Apoptosis: a form of cell suicide characterized by specific morphological features, such as chromatin condensation and plasma membrane blebbing

Cancer: diseases in which abnormal cells divide without control and are able to invade other tissues. Cancer cells can spread to other parts of the body through the blood and lymph systems.

Cell turnover: a cycle of cell death and rebirth that contributes to an organ's normal tissue homeostasis

Enhancer trap: a transposable element containing a reporter gene, i.e. beta galactosidase gene or GFP, inserted randomly in the genome with the purpose of identifying regulatory sequences of genes.

Enteroblast: post-mitotic progenitor cell of *Drosophila* midgut which is marked by escargot – abbreviated as EB and also termed “precursor cell”

Epithelial to mesenchymal transition (EMT): genetic program that convert adherent epithelial cells into migratory cells that can invade the extracellular matrix

Gal4/UAS system: a method for controlling gene expression in *Drosophila*, *Xenopus* and Zebrafish. Is based on the GAL4 gene, encoding the yeast transcription activator protein Gal4, and the UAS (Upstream Activation Sequence), an enhancer to which Gal4 specifically binds to activate gene transcription.

Lineage labeling: a technique to follow the progeny of a dividing stem or progenitor cell. Can be based on mitotic dependent site-specific recombination (i.e. at a lox or an FRT site) to activates a marker gene (i.e. GFP) with constitutive expression. This gene will subsequently be inherited and expressed in future progeny cells, thereby indicating that they have descended by division from the initial cell

Mesenchymal to epithelial transition (MET): the inverse counterpart of EMT. Genetic program that convert migratory cells into adherent epithelial cells

Multipotency: the limited potential of adult stem cells or progenitors to give rise to certain differentiated cell type

Niche: cellular and/or extracellular microenvironments that provide cues governing stem cell behavior and maintenance

Pluripotency: see “multipotency”

Precursor cell: see “enteroblast”

Progenitor cell: see “enteroblast”

RNAi: a gene silencing phenomenon in which either endogenous or foreign double-stranded RNA molecules trigger the specific degradation of homologous mRNAs.

Somatic stem cells: see “adult stem cells”

Stem cells self-renewal: is the process by which stem cells divide to make identical siblings, perpetuating the stem cell pool throughout life

Tissue homeostasis: the maintenance of normal tissue morphology and function.

Tissue regeneration: the replacement of diseased or injured structures

Tissue or cell replenishment: the replacement of suboptimal cells, it occurs during homeostatic conditions

Tissue or cell turnover: synonym of tissue replenishment

Tissue plasticity: capacity of tissues to counterbalance environmental changes in an adaptative manner maintaining integrity during tissue homeostasis and tissue regeneration

Totipotency: the potential of a cell to give rise to all the differentiated cell types that constitute an adult organism.

Transient amplifying cells: progenitor cells undergoing divisions to expand the progenitors pool. They are typical of mammalian intestine but do not exist in adult *Drosophila* midgut.

Tumor: an abnormal benign or malignant new growth of tissue that possesses no physiological function and arises from uncontrolled usually rapid cellular proliferation —called also neoplasm

Wear and tear: damage or deterioration resulting from ordinary use.



Acknowledgments











